THE UNIVERSITY OF ALBERTA

RELEASE FORM

NAME OF AUTHOR: Richard Alan Dennis Wanko

TITLE OF THESIS: Measurements of the Temperature Dependence
of the Longitudinal Sound Velocity in
Single Crystals of Solid Helium

DEGREE FOR WHICH THESIS WAS PRESENTED: Ph.D.

YEAR THIS DEGREE GRANTED: 1973

Permission is hereby granted to THE UNIVERSITY OF ALBERTA LIBRARY to reproduce single copies of this thesis and to lend or sell such copies for

THE UNIVERSITY OF ALBERTA

RELEASE FORM

NAME OF AUTHOR: Richard Alex Dennis Hewko

TITLE OF THESIS: Measurements of the Temperature Dependence of the Longitudinal Sound Velocity in Single Crystals of Solid Helium

DEGREE FOR WHICH THESIS WAS PRESENTED: Ph.D.

YEAR THIS DEGREE GRANTED: 1973

THE UNIVERSITY OF ALBERTA

MEASUREMENTS OF THE TEMPERATURE DEPENDENCE OF THE LONGITUDINAL SOUND VELOCITY IN SINGLE CRYSTALS OF SOLID HELIUM

by

© RICHARD ALEX DENNIS HEWKO

A THESIS

SUBMITTED TO THE FACULTY OF GRADUATE STUDIES AND RESEARCH

IN PARTIAL FULFILMENT OF THE REQUIREMENTS FOR THE DEGREE

OF DOCTOR OF PHILOSOPHY

DEPARTMENT OF PHYSICS

EDMONTON, ALBERTA

FALL, 1973

UNIVERSITY OF ALBERTA

FACULTY OF GRADUATE STUDIES AND RESEARCH

The undersigned certify that they have read, and recommend to the Faculty of Graduate Studies and Research for acceptance, a thesis entitled "MEASUREMENTS OF THE TEMPERATURE DEPENDENCE OF THE LONGITUDINAL SOUND VELOCITY IN SINGLE CRYSTALS OF SOLID HELIUM", submitted by Richard Alex Dennis Hewko in partial fulfillment of the requirements for the degree of Doctor of Philosophy.

ABSTRACT

The temperature dependence of the longitudinal sound velocity in single crystals of hcp He^4 was measured from .75 K to the melting point at 86 bar and 120 bar with a 5 MHz longitudinally-cut quartz transducer. In the high temperature region the velocity obeys a simple power law. Its direction of change is contrary to that predicted by a reduced equation of state. At $\omega\tau_u \sim 1$ or $T \sim \theta_o/20$ a sharp anomaly or "knee" is observed. The resulting plateau (the velocity changes only slightly in this region) extends to lowest temperatures. We feel this plateau is evidence of the long sought coupling between first and second sound velocities.

ACKNOWLEDGEMENTS

I wish to express my gratitude to my supervisor, Professor J.P. Franck for his generous and active support. Thanks are also due to Dr. René Wanner for his active help as well as many other solid helium workers for discussions and preprints.

Allan O'Shea provided expert and dedicated technical assistance. The University of Alberta Computing Centre, and R. Teshima provided expert assistance with reference to computations. Thanks also to Mrs. Mary Yiu without whose valuable help this thesis would not have been completed.

The Award of a Bursary from the National Research Council of Canada is gratefully acknowledged.

I am especially thankful to my wife Melody for her understanding and co-operation.

TABLE OF CONTENTS

Page

LIST OF TABLES

LIST OF FIGURES

CHAPTER 1

INTRODUCTION

Solid helium was first studied in the hope of finding the simplest and most ideal of solids. These early experiments indicated that, in gross respects, helium was a solid like all other solids. However, detailed quantitative studies of the solid produced results remarkably different from the theories of the day.

The helium atom is quite light, and in the weak van-der-Waals potential well of its neighbors in the solid, has a large zero-point motion. This quantum-like behavior has led to investigations of helium and similar materials under the general name quantum solids. All modern theories of solid helium directly take into account the quantum nature of the solid and have explained many observed "anomalies", although many unanswered questions remain.

There are two stable isotopes of helium, He^3 and He^4. In the liquid state the two isotopes behave drastically different. This is due to the fact that He^4 has even spin (2 neutrons plus 2 protons plus 2 electrons) and thus obeys bose-einstein statistics, whereas He^3 has odd spin (1 neutron plus 2 protons plus 2 electrons) and thus obeys fermi-dirac statistics. These statistical effects come from overlap of the

individual wave functions. In the solid, the particles are highly localized with very little overlap. The overlap, however, is large enough to lead to some quantum effects such as spin exchange in He^3 and short range correlation in both isotopes.

All our experiments were performed on He^4 because chemical and isotopic purity can be obtained using simple and inexpensive techniques. Transport quantities, such as second sound and thermal conductivity are influenced dramatically by small concentrations of impurities. In solid helium, second sound can be propagated in a lightly damped mode while the thermal conductivity exhibits a large umpklapp maximum and a well defined phonon-Poiseuille flow region. This is experimental evidence that samples of He^4 low in impurities can be produced.

The experiments reported on here mark the second stage of work to determine the temperature, pressure, and frequency dependence of the attenuation of first sound in He^4. Although some qualitative observations were made, an accurate determination of the attenuation proved too difficult with the present state of technology.

However, measurements of the temperature dependence of the velocity showed anomalous behavior. This anomalous behavior appears to be evidence for coupling between first and second sound. The main

purpose of this work is to report on these findings. This anamalous behavior has been seen before in liquid He^4 (Whitney and Chase (1967)) and predicted as a coupling between first and second sound by many authors, including Niklasson (1968, 1970, 1971) and Gurevich and Efros (1966, 1967).

CHAPTER 2

THEORY

So much work has been done on the theory of solid helium on both lattice dynamics and sound velocity that I will mention here only some of the review articles recently published.

Classical lattice dynamics are treated extensively in several books. I have relied mainly on the paper by Musgrave (1954) and the series *Physical Acoustics* edited by Mason (1965). Lattice dynamics of solid helium are well covered in the review papers by Werthamer (1969) and Guyer (1969). The latest experimental data will be found in Wilk's book (1967), Keller's book (1969) and Trickey et al (1972). The temperature dependence theories were obtained with consultation to Bhatia's book (1967) and the series by Niklasson (1968, 1969, 1970, 1972).

2.1 Classical Lattice Dynamics

We shall present here a short introduction to classical lattice dynamics based on Ziman (1965). Although this formulation is not sufficient to solve the special problems of solid helium, the initial steps and broad treatment are identical.

If we have a lattice with identical atoms of mass m at equilibrium lattice sites $\vec{\ell}$ and where $\vec{u}_{\vec{\ell}}$ is the displacement of each atom from that site, then the kinetic energy of the crystal is T

$$T = \frac{1}{2} m \sum_{\vec{\ell}} \dot{\vec{u}}_{\vec{\ell}}^{2} \quad . \tag{2.1-1}$$

We will now write potential energy in a Taylor series expansion in terms of the $\vec{u}_{\vec{\ell}}$ so that

$$V = V_o + \sum_{\vec{\ell},j} u_{\vec{\ell}}^{j} \frac{\partial V}{\partial u_{\vec{\ell}}^{j}} + \sum_{\vec{\ell}\vec{\ell}',jj'} u_{\vec{\ell}}^{j} u_{\vec{\ell}'}^{j'} \frac{\partial^2 V}{\partial u_{\vec{\ell}}^{j} \partial u_{\vec{\ell}'}^{j'}} + \ldots . \tag{2.1-2}$$

where j represents the cartesian components of $\vec{u}_{\vec{\ell}}$. If we truncate the series after three terms (as above), we call this the harmonic approximation. Note that the first term is unimportant, and the second term vanishes for small oscillations about the equilibrium position in the bottom of the potential well.

If we use Lagrange's formulas we can write the equations of motion as

$$m \ddot{u}_{\vec{\ell}}^{j} = - \sum_{\vec{\ell}'j'} \left(\frac{\partial^2 V}{\partial u_{\vec{\ell}}^{j} \partial u_{\vec{\ell}'}^{j'}} \right) u_{\vec{\ell}}^{j'} \quad . \tag{2.1-3}$$

If now we let $G_{\vec{\ell}\vec{\ell}'}^{jj'}$ represent the elements of the dynamical matrix G, then

$$G^{jj'}_{\vec{\ell}\vec{\ell}'} = [\partial^2 V/\partial u^j_{\vec{\ell}}\ \partial u^{j'}_{\vec{\ell}'}]_o \tag{2.1-4}$$

Assuming translational invariance, we must have

$$G^{jj'}_{\vec{\ell}\vec{\ell}'} = G^{jj'}(\vec{h}) \quad \text{where} \quad \vec{h} = \vec{\ell}' - \vec{\ell} \tag{2.1-5}$$

hence

$$m\ \ddot{u}^j_{\vec{\ell}} = -\sum_{\vec{h}j'} G^{jj'}(\vec{h}) \cdot u^{j'}_{\vec{\ell}+\vec{h}} \ . \tag{2.1-6}$$

These several equations must satisfy the Bloch condition

$$u_{\vec{\ell}}(t) = e^{i\vec{q}.\vec{\ell}}\ u_o(t) = e^{i\vec{q}.\vec{\ell}}\ u_{\vec{q}}(t) \tag{2.1-7}$$

hence, with the origin as arbitrary

$$m\ \ddot{u}^j_{\vec{q}} = -\sum_{\vec{h}j'} G^{jj'}(\vec{h})\ e^{i\vec{q}.\vec{h}} \cdot u^{j'}_{\vec{q}}$$

$$= -\sum_{j'} G^{jj'}(\vec{q}) \cdot u^{j'}_{\vec{q}} \ . \tag{2.1-8}$$

We now assume a plane wave solution of the form

$$u_{\vec{q}} = u_o\ e^{i\omega t} \tag{2.1-9}$$

and we get in (2.1-8)

$$\sum_{j=1}^{3} (G^{jj'}(\vec{q}) - m\omega^2\delta_{jj'})u^{j'}_o(\vec{q}) = 0 \ . \tag{2.1-10}$$

The above equation has a solution if and only if the secular equation (the equation of the determinant of the set of equations' coefficients set to zero) has a solution. This secular equation has 3n solutions where the n represents the number of particles in a unit cell and the three represents the three modes or polarizations of vibration (two transverse and one longitudinal). The sound velocity $C^j(q)$ is given by

$$\vec{C}^j(\vec{q}) = \vec{\nabla}_q \, \omega_j(\vec{q}) \tag{2.1-11}$$

We usually only use the term 'sound' in the limit $\omega \to 0$. In this region

$$\omega_j(\vec{q}) = \vec{C}^j(\vec{q}) \cdot \vec{q}$$

where j represents the mode. The dispersion in $\omega_j(\vec{q})$ is negligible until one reaches frequencies of order 10^9 Hz.

We note, also, that the elements of the dynamical matrix are closely related to the elastic constants in the long wave length limit ($\omega \to 0$). This will be further dealt with in section 2.3.

2.2 Lattice Dynamics of Solid He^4

The classical theory of lattice dynamics fails dramatically for solid helium.

If one chooses the interaction potential between two helium atoms to be a Lennard-Jones of the type

$$V(r) = 4\varepsilon[(\sigma/r)^{12} - (\sigma/r)^{6}] \qquad (2.2\text{-}1)$$

and derives ε and σ from the virial coefficients of He^4 gas, the classical theory of lattice dynamics predicts a molar volume of 10 cm^3 (too small by a factor 2), a compressibility too small by a factor 30, and a sound velocity too large by a factor 4 when compared to hcp He^4 at 0 K and 26 bar the minimum pressure of solidification! Even worse, when De Wette and Nijkoer (1965) attempted to calculate the phonon frequencies and sound velocities using the aforementioned theory, they calculated imaginary frequencies for molar volumes greater than 12 cm^3/mole (even though the lattice is stable up to molar volumes of 21 cm^3/mole)!

On the other hand, thermal conductivity, elasticity and heat capacity measurements showed helium to behave quite normally.

The major cause of these deviations from classical behavior is the large zero-point motion of solid helium atoms. The attractive potential between helium atoms is the relatively weak Van der Waals interaction which produces a very narrow potential well. Estimating the zero-point motion from the indeterminacy

principle yields for its kinetic energy

$$E_z \sim \frac{(\Delta p)^2}{2m} \sim \frac{\hbar^2}{2ma^2} \qquad (2.2\text{-}2)$$

where a is the lattice spacing.

This large zero-point motion, combined with a narrow potential well, means that the mean position of the helium atom is not at the bottom of the well, but displaced to increase the lattice spacing. This means that the molar volume will be larger than expected as will the compressibility.

Figure 1 shows the position of a helium 4 atom in the well of its nearest neighbors. The cross-hatched area represents an approximate wave function for He^4. Notice that the He^4 atom sits at a relative maximum in the well which accounts for the imaginary frequencies obtained by any classical calculation. Thus, the wave function has two peaks corresponding to the minima of the well. One can think of the atom as moving in a spherical shell about its mean position.

The motion of any atom about its site will change the position of the potential well of its neighbor. Thus the neighbors motion will be correlated in such a way that the wave functions overlap as little as possible. We call correlations of this kind short range correlations.

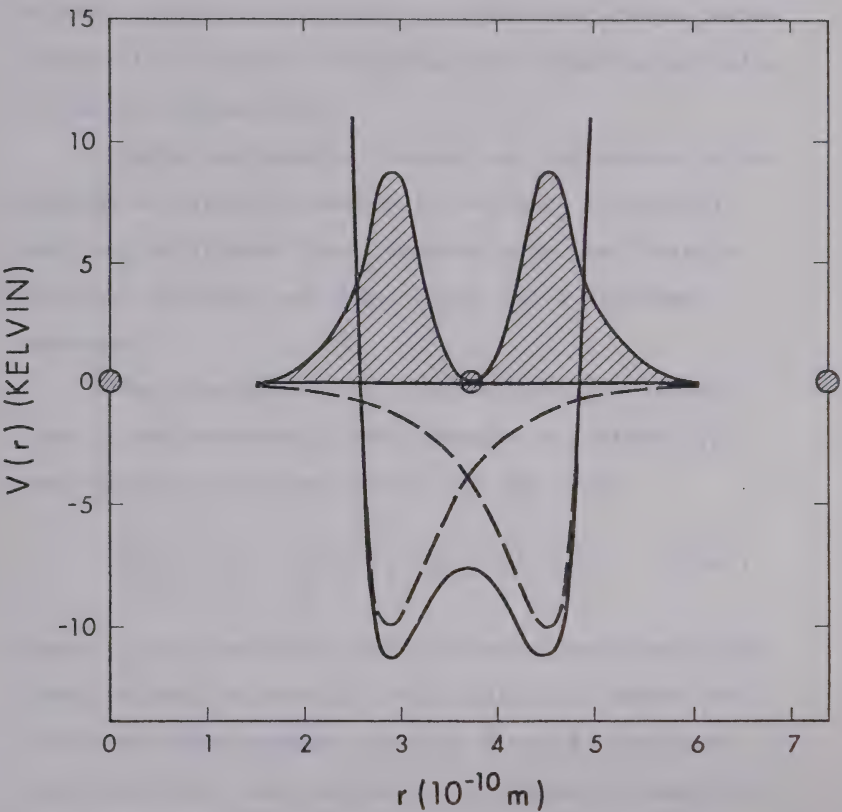

FIGURE 1 He^4 atom in potential well of nearest neighbors (Guyer (1969)).

If phonons exist in a solid, they are evidence of long range correlations in the solid. Any theory must therefore take into account the large zero-point motion, short range correlations and long range correlations if it expects to explain the behavior of solid helium to any accuracy.

There are several theoretical approaches to the problem of lattice dynamics in helium. In general they can be divided into theories that use a single particle approach and those which use a many-body approach.

The single particle picture (Nosanow (1964), Fredkin and Werthamer (1965)) assumes a Jastrow type wave function (Jastrow (1955) of the type

$$\psi(\vec{r}_1 \ldots \vec{r}_n) = \prod_i \phi_o(\vec{r}_i - \vec{\ell}_i)\ f(\vec{r}_i - \vec{r}_k) \qquad (2.2\text{-}3)$$

where ϕ_o are the single particle wave functions localized at lattice sites $\vec{\ell}_i$ while $f(\vec{r}_j - \vec{r}_k)$ describes the correlation between particle $\vec{j}$ and $\vec{k}$. We know something about the form of the correlation function $f(\vec{r})$. For example, at large $\vec{r}$ it must be unity while at $r = 0$ it must vanish because of the hard core. Also there should be a maximum in f about where the minimum in the Lennard-Jones potential V(r) occurs. A simple analytic form for f(r) is thus

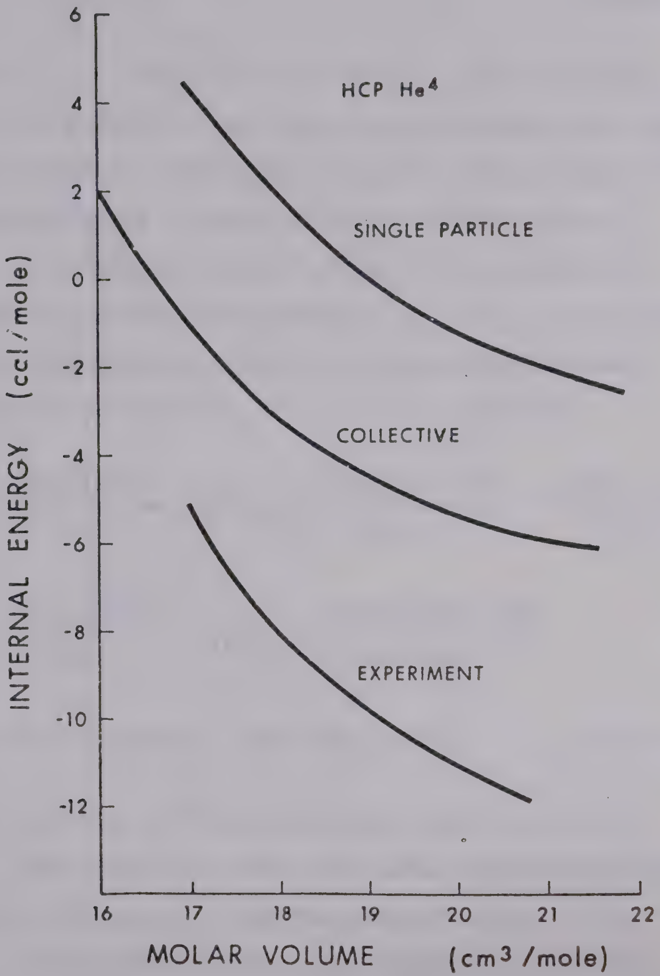

FIGURE 2 Internal energy as a function of molar volume comparing theory and experiment (single particle Nosanow (1966) and Hetherington et al (1967); collective - Gillis et al (1968).

$$f(r) = e^{-CV(r)} \tag{2.2-4}$$

where C is a variational parameter. Although there are many possible forms for f(r) consistent with the above criteria, they must be easily subject to variational analysis or they are too difficult to use.

Assuming an initial value for C, we can calculate the ground state energy E_o. If h_1 is the one particle hamiltonian and h_2 the two particle hamiltonian we can write E_o in a cluster expansion

$$E = \sum_j \frac{\langle j|h_1(j)|j\rangle}{\langle j|j\rangle} + \frac{1}{2!}\sum_{jk}\left(\frac{\langle jk|h_2(jk)|jk\rangle}{\langle jk|jk\rangle} - \frac{\langle j|h_1(j)|j\rangle}{\langle j|j\rangle} - \right.$$

$$\left. - \frac{\langle k|h_1(h)|k\rangle}{\langle k|k\rangle}\right) + \frac{1}{3!}\sum_{jk}\left(\frac{\langle jk\ell|h_3(jk\ell)|jk\ell\rangle}{\langle jk\ell|jk\ell\rangle} - \right.$$

$$\left. - \text{two body terms} + \text{one body terms}\right) \tag{2.2-5}$$

where j is the j^{th} particle wave function of ψ.

We truncate E after one term, minimize the equation for E to get E_o and then solve for $|j\rangle = \psi$.

It turns out that ϕ_o is roughly a spherical gaussian (as for the ground state of the simple harmonic oscillator)

$$\phi_o = e^{-A\frac{r^2}{2}} \tag{2.2-6}$$

where one minimizes E_o for a given C. One then self-consistently minimizes C and A to obtain the lowest E_o.

One can then take the cluster expansion to higher terms in E, although to my knowledge the expansion has not been carried past three terms.

Using many body techniques, Fredkin and Werthamer (1965) have shown how to calculate the phonon frequencies from these single particle wave functions.

$$m\omega^2 \cdot u(\vec{q}) = \sum_{\hbar} (1 - e^{i\vec{q}\cdot\vec{h}}) \frac{\partial^2}{\partial \vec{u}_{\vec{\ell}} \partial \vec{u}_{\vec{\ell}'}} \langle 0 | V_{eff}(r - r' + h) | 0 \rangle \vec{u}(\vec{q})$$

at T = 0, where V_{eff} is

$$V_{eff} = [V(r) + \frac{\hbar^2 k}{m} \cdot \nabla^2 V(r)] e^{-2kV(r)} \qquad (2.2\text{-}7)$$

and V(r) is the Lennard-Jones potential. This above calculation is the same as using V_{eff} in a Hartree calculation and taking no correlations into account. Many calculations have been done, but so far no calculations have been done for hcp He^4.

In the theories emphasizing collective phenomena, one usually examines the response of a crystal to an externally applied disturbance. These so-called self-consistent theories (Hooton (1958), Bernades (1960),

Boccara and Sarma (1965), Raninger (1965), Koehler (1966, 1967, 1968), Choquard (1967), Horner (1971)) consider the phonons as the basic co-ordinates of the solid. Essentially the result of these theories is that the spring constant between a pair of atoms is the second derivative of the interaction potential averaged over the motion of the atoms. Short range correlations must be added in later. These theories appear much better suited for numerical analysis.

If we say that the hamiltonian of our solid can be approximated by

$$\mathcal{H} = \sum_i T(i) + \sum_{i \neq j} V_{ij} \tag{2.2-8}$$

and further approximate $\mathcal{H}$ by H_h

$$\mathcal{H}_h = -\frac{\hbar^2}{2m} \sum_i \nabla_i^2 + V_o + \frac{1}{2} \sum_{\ell\ell'} \vec{u}^j_{\ell} G^{jj'}_{\ell\ell'} u^{j'}_{\ell}$$

where the G's are the spring constants and will be solved for variationally. The energy is minimized (Koehler (1968)) by

$$G^{jj}_{\ell\ell'} = \langle 0 | \nabla^j_{\ell} \nabla^j_{\ell'} | 0 \rangle \tag{2.2-9}$$

and the ground state eigenfunction is given by

$$|0\rangle = \exp\{-\frac{1}{2} u^{jj'}_{\ell} F^{jj'}_{\ell\ell'} u^j_{\ell'}\}$$

$$\left(F^{jj'}_{\ell\ell'}\right)^2 = \frac{m}{\hbar^2} \cdot G^{jj'}_{\ell\ell'} \quad . \tag{2.2-10}$$

Hence instead of averaging with respect to the single particle wave functions, we here are averaging with respect to the phonon ground state.

A third approach (Guyer (1969)) treats both short and long range interactions equally by using a Rayleigh-Schroedinger perturbation approach. This theory offers a fair description of He^4 in lowest order with a well defined method for going to higher orders.

Take the hamiltonian of the system to be

$$\mathcal{H} = \mathcal{H}_o + \frac{1}{2} \sum_{i \neq j} \tilde{v}(ij) = H_o + V$$

where $\tilde{v}(ij) = v(ij) - u_{ij}(ij)$ and $v(ij)$ is the pair interaction and $u_{ij}(ij)$ is the interaction between this pair and the rest of the particles. One is allowing a set of one, two, three or more particles to interact with each other in the Hartree field of the other particles

$$\mathcal{H}_o \ \phi_o(1 \ldots N) = E_o \ \phi_o(1 \ldots N) \tag{2.2-12}$$

where ϕ_o is the ground state wave function.

The Rayleigh-Schroedinger perturbation (Brueckner (1950)) expansion for the energy shift is

$$E - E_o = \langle V\rangle_o + \langle VG_oV\rangle_o + \langle VG_oVG_oV\rangle_o + \ldots \qquad (2.2\text{-}13)$$

$$G_o = [E_o - H_o]^{-1}$$

$$\langle V\rangle_o = \frac{\phi_o V\phi_o}{\phi_o\phi_o}$$

if we assume

$$\frac{\phi_o VG_oV\phi_o}{\phi_o\phi_o} = \left(\frac{1}{2!}\right)^2 \sum_{ij}{}' \sum_{ij}{}' \frac{\phi_o\tilde{v}(ij)G_o\tilde{v}(ij)\phi_o}{\phi_o\phi_o} \qquad (2.2\text{-}14)$$

$$\sim \frac{1}{2}\sum_{ij}{}' \frac{\phi_o\tilde{v}(ij)G_o\tilde{v}(ij)\phi_o}{\phi_o\phi_o}$$

which is identical to solving the equation

$$[H_o + \tilde{v}(ij)]\phi_{ij}(1\ldots N) = E_{ij}\phi_{ij}(1\ldots N) \quad . \qquad (2.2\text{-}15)$$

This is just our hamiltonian including two body terms only. To include three body terms

$$\langle VG_oV\rangle \cong \frac{1}{3!}\sum_{ijk}{}' [\langle v_3G_ov_3\rangle - \langle\tilde{v}(ij)G_ov(ij)\rangle$$

$$- \langle\tilde{v}(ik)G_o\tilde{v}(ik)\rangle - \langle\tilde{v}(jk)G_o\tilde{v}(jk)\rangle]$$

where $\tilde{v}_3 = \tilde{v}(ij + \tilde{v}(jk) + \tilde{v}(ik)$

and subtraction occurs because these three terms already appear in the two body term.

In essence, the one body term is the self-consistent phonon theory with no short range correlations. The two body term is the self-consistent phonon theory with two body correlations. This theory then is able to treat long and short range correlations in a coherent systematic manner.

2.3 Wave Propagation in Ideal Elastic Solids

The elastic constants $c_{ijk\ell}$ describe the stresses σ_{ij} in various directions in the crystal in terms of strains $\varepsilon_{k\ell}$ applied in various other directions

$$\sigma_{ij} = \sum_{k\ell} c_{ijk\ell} \cdot \varepsilon_{k} \quad . \tag{2.3-1}$$

σ_{ij} is the force acting on plane $\vec{i}$ in direction $\vec{j}$ and the strain $\varepsilon_{k\ell}$ is defined in terms of the displacement $\vec{u}$ as

$$\varepsilon_{k\ell} = \frac{1}{2}\left(\frac{du_k}{dx_\ell} + \frac{du_\ell}{dx_k}\right) \quad . \tag{2.3-2}$$

Equation (2.3-1) is simply Hook's law.

The equation of motion for an elementary cube is thus

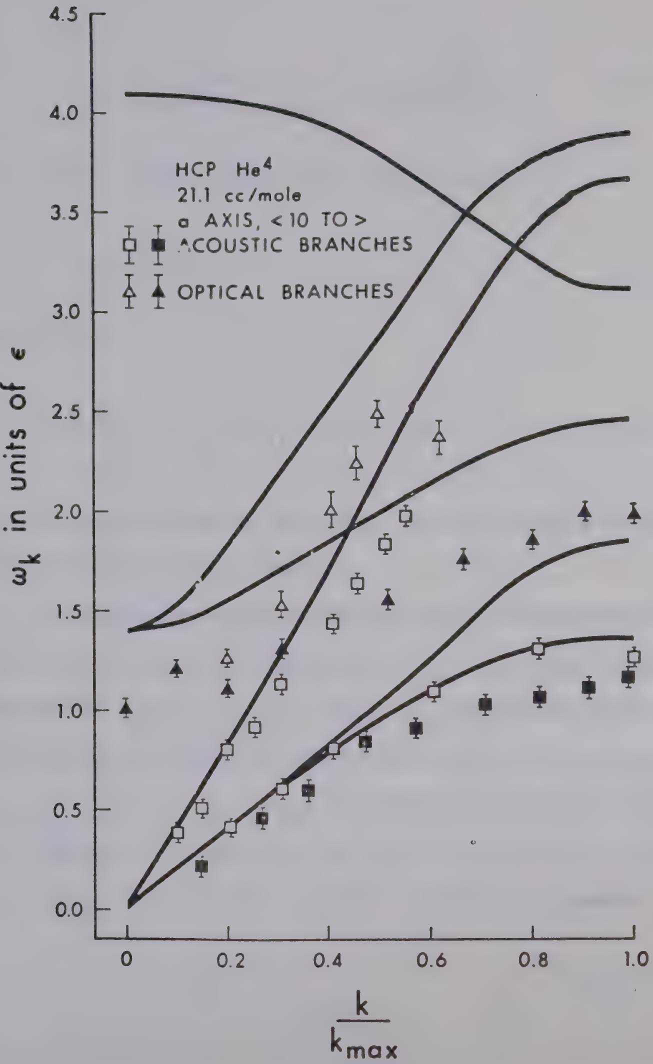

FIGURE 3 Phonon dispersion curves in the Basal plane for the collective picture as calculated by Gillis et al (1968) compared to experimental data of Lipshultz et al (1967).

$$\rho \ddot{u}_i = \sum_j \frac{d\sigma_{ij}}{dx_i} = \sum_{ik\ell} c_{ijk\ell} \frac{d^2 u_k}{dx_j dx_\ell} \quad . \qquad (2.3\text{-}3)$$

This has a plane wave solution of form

$$\vec{u}\; e^{i(\vec{q}.\vec{r}-\omega t)} \qquad (2.3\text{-}4)$$

from which

$$\rho\omega^2 u_i = \sum_{jk\ell} c_{ijk\ell}\, q_j q_k \cdot u_\ell \quad . \qquad (2.3\text{-}5)$$

We now may determine the sound velocities by solving the secular equation for $\vec{q}$.

If we now apply symmetry and thermodynamic arguments for hexagonal crystals, $c_{ijk\ell}$ has only 5 independent components c_{11}, c_{12}, c_{13}, c_{33}, c_{44}(where we have used the shortened notation of Voigt . $c_{1111}= c_{11}$, $c_{1122} = c_{12}$, $c_{1133} = c_{33}$, $c_{2323} = c_{44}$). Isotropic crystals have only two, namely, c_{11} and c_{12} as $c_{44} = \frac{1}{2}(c_{11}- c_{12})$, $c_{13}= c_{12}$, $c_{11} = c_{33}$. The matrix c_{ik} for hexagonal symmetry is

$$c_{ik} = \begin{pmatrix} c_{11} & c_{12} & c_{13} & 0 & 0 & 0 \\ c_{12} & c_{11} & c_{13} & 0 & 0 & 0 \\ c_{13} & c_{12} & c_{33} & 0 & 0 & 0 \\ 0 & 0 & 0 & c_{44} & 0 & 0 \\ 0 & 0 & 0 & 0 & c_{44} & 0 \\ 0 & 0 & 0 & 0 & 0 & \frac{1}{2}(c_{11}-c_{12}) \end{pmatrix} \qquad (2.3\text{-}6)$$

Several authors (Zener (1936), Gold (1950), Musgrave (1954)) have explicitly solved the secular equation for hexagonal symmetry. They find velocity surfaces (which are completely determined by the elastic constants and the density) have cylindrical symmetry about the "c" axis and hence the velocities can be expressed in terms of one angle "γ" the angle between propagation and the "c" axis. They find:

$$v_\ell = (c_\ell/\rho)^{\frac{1}{2}}$$

$$v_{t_1} = (c_{t_1}/\rho)^{\frac{1}{2}}$$

$$v_{t_2} = (c_{t_2}/\rho)^{\frac{1}{2}} \qquad (2.3\text{-}8)$$

where

$$c_\ell = \frac{1}{2}\{(c_{11}+c_{44})\sin^2\gamma + (c_{33}+c_{44})\cos^2\gamma + \phi(\gamma)\}$$

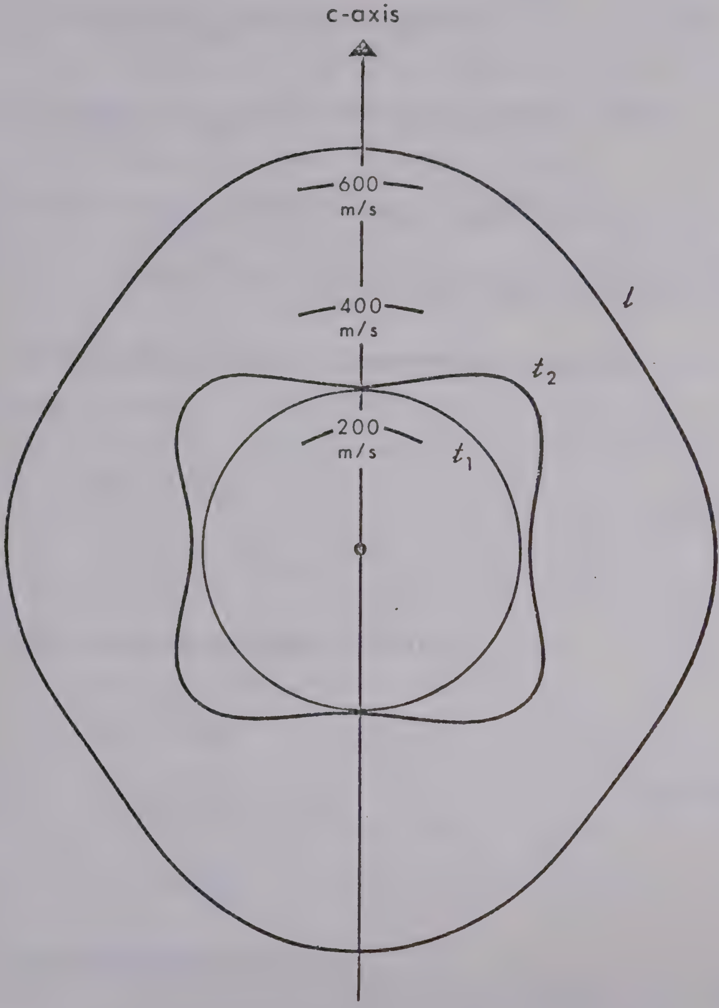

FIGURE 4 Velocity as a function of orientation according to a collective picture calculation by Gillis et al (1968) for hcp He^4 at 80 bar. The curves have cylindrical symmetry about the 'C'-axis.

$$c_{t_1} = \frac{1}{2}\{(c_{11}-c_{12})\sin^2\gamma\} + c_{44}\cos^2\gamma$$

$$c_{t_2} = \frac{1}{2}\{(c_{11}+c_{44})\sin^2\gamma + (c_{33}+c_{44})\cos^2\gamma - \phi(\gamma)\}$$

$$\phi^2(\gamma) = (c_{11}-c_{44})^2\sin^4\gamma + (c_{33}-c_{44})^2\cos^4\gamma +$$

$$+ 2\sin^2\gamma\ \cos^2\gamma[(c_{11}-c_{44})(c_{44}-c_{33})+2(c_{13}+c_{44})^2] \ .$$

For the special case of propagation along the "c" axis ($\gamma = 0$)

$$c_\ell = c_{33}$$
$$c_{t_1} = c_{t_2} = c_{44} \qquad (2.3\text{-}9)$$

and in the basal plane ($\gamma = 90°$)

$$c_\ell = c_{11}$$
$$c_{t_1} = \frac{1}{2}(c_{11} - c_{12}) \qquad (2.3\text{-}10)$$
$$c_{t_2} = c_{44} \ .$$

For an isotropic crystal

$$c_\ell = c_{11}$$
$$c_{t_1} = c_{t_2} = \frac{1}{2}(c_{11} - c_{12}) \ . \qquad (2.3\text{-}11)$$

Velocity surfaces are plotted in figure 4 according to Gilles et al (1968) for hcp He^4 at 80 bar.

Now, in general, sound velocities do not propagate perpendicular to the transducer, but may, in fact, deviate quite dramatically from a normal direction. Figure 5 shows the calculated deviation for the elastic constants calculation by Gillis et al (1968). The method of determining these deviations is given in an appendix in the form of a computer program.

For purely transverse waves, the disturbance must be perpendicular to the direction of propagation. For purely longitudinal waves, the disturbance must be along the direction of motion. For hexagonal crystals, only one of the transverse modes is a pure mode, the other two being mixed. That is,the disturbance moves at an angle to the direction of propagation that is a function of orientation. The two modes are always perpendicular to one another at any orientation and one is predominantly longitudinal while the other is predominantly transverse. We call these modes quasi-longitudinal and quasi-transverse respectively.

2.4 Related Quantities

If the elastic constants of a crystal are known, then several other quantities can be determined

Debye Temperature θ_D

The Debye temperature at 0k is (Alers (1965))

$$\theta_D = \frac{h}{k} \left\{\frac{3N}{4 V_m}\right\}^{1/3} V_D$$

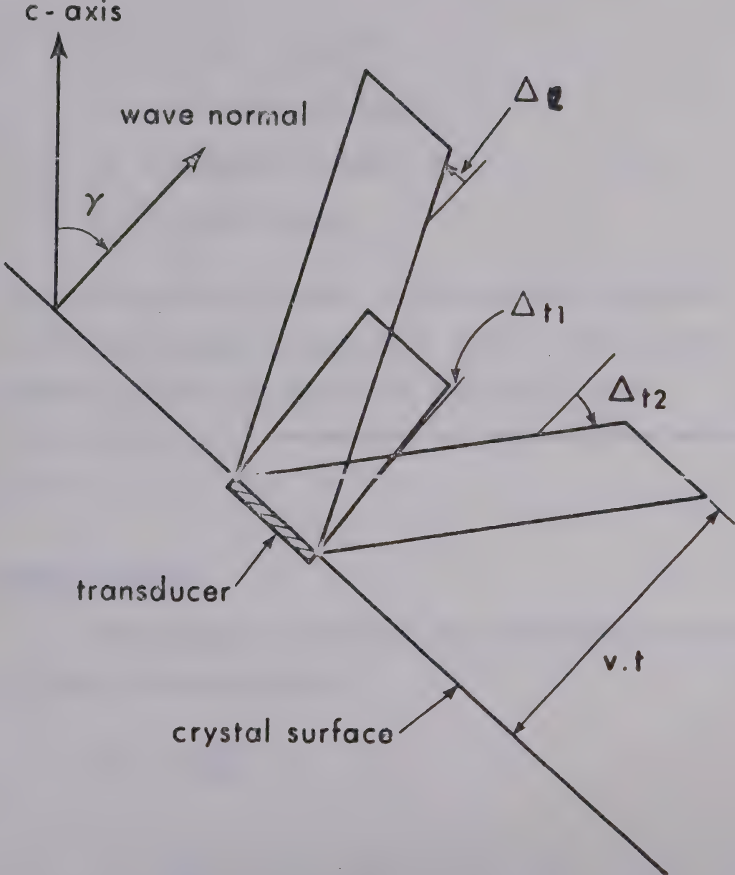

FIGURE 5 Propagation direction schematic.

where

$$v_D = \left(\int (v_\ell^{-3} + v_{t_1}^{-3} + v_{t_2}^{-3}) \frac{d\Omega}{12\pi} \right)^{1/3}$$

h = Planck constant

k = Boltzmann constant

N = Avogadros number

V_m = Molar volume

A computer program in the appendix for both cubic and hexagonal crystals is given. The Θ_D calculated in this way should be identical to the calorimetric Debye temperature at temperatures below $\Theta_D/50$.

Compressibility

For hexagonal crystals, the isothermal compressibility is (Nye (1964))

$$K_T = -\left(\frac{\partial V}{\partial P}\right)_T \cdot \frac{1}{V}$$

$$K_s = \frac{c_{11}^s + c_{12}^s - 4c_{13}^s + 2c_{33}^s}{c_{11}^s c_{33}^s + c_{12}^s c_{33}^s - 2c_{13}^s} \quad .$$

One must remember, however, that the compressibility calculated from elastic constants is adiabatic.

The difference between these two values is discussed thoroughly in sections 2.5 and 2.6, but is of order

$$\frac{c_{ik}^{S} - c_{ik}^{T}}{c_{ik}^{T}} = \frac{c_P}{c_V} - 1$$

where c_P and c_V are the heat capacities at constant pressure and volume.

Phonon Spectrum

In the long wave length limit ($\omega << 10^9$ hz), the sound velocity is equal to the phase velocity

$$v = \vec{\nabla}_q \, \omega(\vec{q}) \sim \frac{\omega(\vec{q})}{|\vec{q}|}$$

Second Sound

For an isotropic material, the velocity of second sound is (Niklasson (1970))

$$v_{II}^2 = \frac{1}{3} \frac{(v_\ell^{-3} + 2v_t^{-3})}{(v_\ell^{-5} + 2v_t^{-5})} \quad .$$

For hexagonal materials, the second sound velocity is not so easily obtained. Meuller et al (1973) have assumed

$$v_{II}^2(\theta) = \frac{1}{3} \frac{\sum_j v_j^{-3}(\theta)}{\sum_j v_j^{-5}(\theta)} \quad , \qquad j = \text{mode} \; .$$

which is an over-simplification.

The phase velocity of second sound in hexagonal crystals is given by a theory in Appendix A2.

The velocity $C_{II}(\theta)$ for this theory is

$$C_{II}(\theta) = \{\frac{1}{a_1}\sin^2\theta + \frac{1}{a_2}\cos^2\theta\}^{-\frac{1}{2}}$$

where

$$a_1 = \frac{B_z^2(\theta)}{Y_z\ A}$$

$$a_2 = \frac{B_x^2(\theta)}{Y_x\ A}$$

$$B_x(\theta) = \{\sum_j \int_o^{\Pi} \frac{\sin^3\theta' d\theta'}{c_j^3(\theta')} \cos\ \delta_j(\theta)\}$$

$$B_z(\theta) = \sum_j \{2 \int_o^{\Pi} \frac{\cos^2\theta' d\theta'}{c_j^3(\theta')} \sin\theta' \cos\ \delta_j(\theta)\}$$

$$Y_x = \sum_j \int_o^{\Pi} \frac{\sin^3\theta' d\theta'}{c_j^5(\theta')}$$

$$Y_z = \sum_j \int_o^{\Pi} \frac{\cos^2\theta' \sin\theta' d\theta'}{c_j^5(\theta')}$$

$$A = \sum_j 2 \int_o^{\Pi} \frac{\sin\theta' d\theta'}{c_j^3(\theta')}$$

where j is the mode (longitudinal, transverse), and θ is the orientation $\delta_j(\theta)$ is the deviation of the pulse from travel perpendicular to the tranducer.

These integrals have been arrived at assuming a harmonic solid with linear dispersion using a Debye approximation.

2.5 Sound Velocity as a Function of Temperature from Thermodynamic Arguments

Let us assume that it is possible to represent the temperature change in the sound velocity in terms of the adiabatic compressibility

$$v(T) = \left(\frac{1}{\rho K_s(T)}\right)^{\frac{1}{2}} \tag{2.5-1}$$

where ρ is the density and $K_s(T) \equiv -(\partial\ \ell n\ V/\partial P)_s$ the adiabatic compressibility. We can write

$$v^2(T) - v^2(0) = \frac{1}{\rho}\left[\frac{1}{K_s(T)} - \frac{1}{K_s(0)}\right] \tag{2.5-2}$$

or

$$\frac{K_T(T)}{K_s(T)} = \frac{(\partial P/\partial V)_s}{(\partial P/\partial V)_T} \quad . \tag{2.5-3}$$

Now

$$\left(\frac{\partial P}{\partial V}\right)_s = \frac{c_P}{c_V}\left(\frac{\partial P}{\partial V}\right)_T \tag{2.5-4}$$

so that

$$\frac{K_T}{K_s} = \frac{c_P}{c_V} = \frac{c_P - c_V}{c_V} + 1$$

$$c_P - c_V = T\left(\frac{\partial P}{\partial T}\right)_V \left(\frac{\partial V}{\partial T}\right)_P \tag{2.5-5}$$

the derivation of the above relation for c_P-c_V is given in the appendix, hence

$$K_T = K_s\left[1 + \frac{T}{c_V}\left(\frac{\partial P}{\partial T}\right)_V \left(\frac{\partial V}{\partial T}\right)_P\right] .$$

Now

$$\left(\frac{\partial V}{\partial T}\right)_P = -\left(\frac{\partial V}{\partial P}\right)_T \left(\frac{\partial P}{\partial T}\right)_V = VK_T\left(\frac{\partial P}{\partial T}\right)_V$$

or

$$K_T(T) = K_s(T)\left[1 + \frac{TVK_T(T)}{c_V}\left(\frac{\partial P}{\partial T}\right)_V^2\right] \qquad (2.5\text{-}6)$$

hence

$$K_T(T) \geq K_s(T) \quad \text{for all } T$$

equation (2.5-6) can also be written

$$\frac{1}{K_s(T)} = \frac{1}{K_T(T)} + \frac{TV}{c_V}\left(\frac{\partial P}{\partial T}\right)^2 . \qquad (2.5\text{-}6a)$$

Now we have experimental data at several volumes for the right hand side, so let us write the above as

$$v^2(T) - v^2(0) = \frac{1}{\rho}\left[\frac{1}{K_T(T)} - \frac{1}{K_T(0)} + \frac{TV}{c_V(T)}\left(\frac{\partial P}{\partial T}\right)_V^2\right]. \quad (2.5\text{-}7)$$

If we calculate this value we find $v^2(T)-v^2(0)$ is always negative and of the form

$$v^2(T) - v^2(0) = AT^n$$

where $n \sim 4$ and $A < 0$ (Jarvis et al (1968)).

One can also proceed from (2.5-1) assuming a reduced equation of state

$$S = S(T.\phi(V)) = S(x) \qquad (2.5\text{-}8)$$

where $\phi(V)$ is usually related to the Debye Theta by

$$\phi(V) = \frac{1}{\Theta_D}$$

but we will not specify this.

Now

$$\left(\frac{\partial P}{\partial T}\right)_V = \left(\frac{\partial S}{\partial V}\right)_T$$

which leads to

$$\frac{\partial}{\partial V}\left[\left(\frac{\partial P}{\partial T}\right)_V\right]_T = \left(\frac{\partial^2 S}{\partial V^2}\right)_T$$

or

$$\frac{\partial}{\partial T}\left[\left(\frac{\partial P}{\partial V}\right)_T\right]_V = \left(\frac{\partial^2 S}{\partial V^2}\right)_T$$

or

$$\frac{\partial}{\partial T}\left[\left(\frac{1}{K_T(T)}\right)\right]_V = -V\left(\frac{\partial^2 S}{\partial V^2}\right)_T \quad . \qquad (2.5\text{-}9)$$

Using (2.6-8) we have

$$dS = \frac{\partial S}{\partial x}\,dx = \frac{\partial S}{\partial x}\left[\left(\frac{\partial x}{\partial T}\right)_V dT + \left(\frac{\partial x}{\partial V}\right)_T dV\right] = \frac{\partial S}{\partial x}\left[\phi(V)\,dT + T\left(\frac{\partial \phi(V)}{\partial V}\right)_T dV\right]$$

$$dS = \left(\frac{\partial S}{\partial T}\right)_V dT + \left(\frac{\partial S}{\partial V}\right)_T dV \quad ,$$

hence

$$\left(\frac{\partial S}{\partial T}\right)_V = \frac{\partial S}{\partial x} \phi(V)$$

$$\left(\frac{\partial S}{\partial V}\right)_T = \frac{\partial S}{\partial x} T\left(\frac{\partial \phi(V)}{\partial V}\right)_T = \frac{T}{\phi(V)} \left(\frac{\partial S}{\partial T}\right)_V \left(\frac{\partial \phi(V)}{\partial V}\right)_T$$

$$\left(\frac{\partial S}{\partial V}\right)_T = c_V \left(\frac{\partial \ \ln \phi(V)}{\partial V}\right)_T \quad .$$

Now our assumption also makes

$$c_V = c_V(T \cdot \phi(V)) \quad ,$$

hence

$$\left(\frac{\partial^2 S}{\partial V^2}\right)_T = c_V \frac{\partial^2 \ln \phi(V)}{\partial V^2} + \left(\frac{\partial c_V}{\partial V}\right)_T \frac{\partial \ \ln \phi}{\partial V}$$

$$\left(\frac{\partial c_V}{\partial V}\right)_T = \frac{T}{\phi(V)} \left(\frac{\partial c_V}{\partial T}\right)_V \left(\frac{\partial \phi(V)}{\partial V}\right)_T$$

$$\left(\frac{\partial^2 S}{\partial V^2}\right)_T = c_V \frac{\partial^2 \ln \phi(V)}{\partial V^2} + T\left(\frac{\partial c_V}{\partial T}\right)_V \left(\frac{\partial \ \ln \phi(V)}{\partial V}\right)^2 \quad .$$

Now if we combine (2.5-9) and (2.5-10) and integrate over T at constant V and if we recall $\phi(V)$ and its derivatives are approximately temperature independent, then

$$-\frac{1}{V}\left(\frac{1}{K_T(T)}-\frac{1}{K_T(0)}\right)=\int_0^T\left(\frac{\partial^2 S}{\partial V^2}\right)_T dT$$

$$=\left(\frac{\partial^2 \ell n\ \phi}{\partial V^2}\right)_T\int_0^T c_V dT+\left(\frac{\partial\ \ell n\ \phi}{\partial V}\right)_T^2\int_0^T T\left(\frac{\partial c_V}{\partial T}\right) dT$$

and integrating by parts

$$-\frac{1}{V}\left(\frac{1}{K_T(T)}-\frac{1}{K_T(0)}\right)=\left(\frac{\partial^2 \ell n\ \phi}{\partial V^2}\right)_T\int_0^T c_V dT$$

$$+\left(\frac{\partial\ \ell n\ \phi}{\partial V}\right)\left(Tc_V-\int_0^T c_V dT\right)$$

let

$$\left(\frac{\partial\ \ell n\ \phi}{\ell n\ V}\right)_T=\gamma$$

$$\left(\frac{\partial\ \ell n\ \phi}{\partial V}\right)_T=\frac{\gamma}{V}$$

$$\left(\frac{\partial\ \ell n\ \phi}{\partial V^2}\right)_T=\frac{1}{V}\left(\frac{\partial\gamma}{\partial V}\right)-\frac{\gamma}{V^2}$$

and $\Delta u=\int_0^T c_V dT$ the change in internal energy

$$\left(\frac{1}{K_T(T)}-\frac{1}{K_T(0)}\right)=\Delta u\left(\frac{\gamma^2}{V}+\frac{\gamma}{V}-\frac{\partial\gamma}{\partial V}\right)-Tc_V\frac{\gamma^2}{V}\quad .\quad (2.5\text{-}11)$$

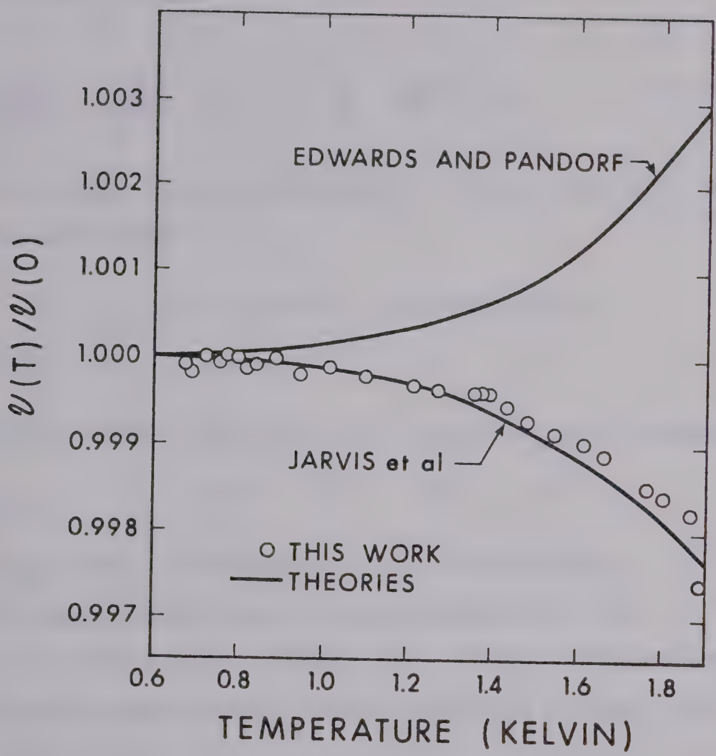

FIGURE 6 Comparison of the temperature dependence of the sound velocity using isothermal compressibilities as found by Edwards and Pandorf (1965) assuming a reduced equation of state, and by Jarvis et al from $(\partial P/\partial T)_V$ measurements (1968).

This is identical to a result obtained by Edwards and Pandorf (1965) if $\partial\gamma/\partial V = 0$

$$\frac{1}{K_s(T)} - \frac{1}{K_s(0)} = \Delta u \left[\frac{\gamma}{V} + \frac{\gamma^2}{V} - \frac{\partial\gamma}{\partial V}\right] = \alpha\Delta u \quad . \qquad (2.5\text{-}12)$$

If we make the association of $\phi = 1/\theta$, then γ is just the Gruneisen γ

$$\gamma \sim 1.01 + 0.083\ V \qquad \text{(Ahlers, 1970)} \ ,$$

hence

$$v^2(T) - v^2(0) = \frac{\alpha}{\rho}\ [\Delta u] > 0 \qquad \text{for} \quad V < 24.2\ \text{cc/mole}$$

$$\sim AT^4 \qquad \text{for} \quad A > 0 \quad .$$

This result contradicts (2.5-7) which says $A < 0$. Our experimental results agree quite well with (2.5-7) (see section 4.3-2, figure 6). Thus a reduced equation of state should only be used with extreme care for solid helium.

2.6 Temperature Dependence of the Sound Velocity from Elasticity and Thermodynamic Arguments

By definition, the adiabatic elastic constants are written

$$c^s_{mn} = \left(\frac{\partial\sigma_m}{\partial\varepsilon_n}\right)_S \qquad \text{(using Voight notation)} \qquad (2.6\text{-}1)$$

and the isothermals are

$$c_{mn}^{T} = \left(\frac{\partial \sigma_m}{\partial \varepsilon_n}\right)_T \quad . \tag{2.6-2}$$

The work W is given by

$$dW = -\sigma_m \; d\varepsilon_m \quad , \tag{2.6-3}$$

hence

$$dQ = TdS = dU - \sigma_m d\varepsilon_m$$

or

$$dU = TdS + \sigma_m d\varepsilon_m$$

and if

$$A = U - TS$$

then

$$dA = - SdT + \sigma_m d\varepsilon_m \tag{2.6-4}$$

$$dG = d(A - \sigma_m \varepsilon_m) = - SdT - \varepsilon_m d\sigma_m$$

hence

$$\sigma_m = \left(\frac{\partial A}{\partial \varepsilon_m}\right)$$

$$\varepsilon_m = \left(\frac{\partial G}{\partial \sigma_m}\right) \tag{2.6-5}$$

$$s = - \left(\frac{\partial A}{\partial T}\right)_\varepsilon = -\left(\frac{\partial G}{\partial T}\right)_\sigma \quad .$$

Here σ,ε as subscripts mean holding all σ,ε constant. Let

$$F_m = -\left(\frac{\partial \sigma_m}{\partial T}\right)_\varepsilon = \left(\frac{\partial S}{\partial \varepsilon_m}\right)_T \tag{2.6-6}$$

$$\beta_m = \left(\frac{\partial \varepsilon_m}{\partial T}\right)_\sigma = \left(\frac{\partial S}{\partial \sigma_m}\right)_T \tag{2.6-7}$$

where β_m is the thermal expansion tensor. Hence, if ε and T are independent and s and σ are dependent variables

$$d\sigma_m = c^T_{mn} d\varepsilon_n - F_m dT = \left(\frac{\partial \sigma_m}{\partial \varepsilon_n}\right)_T d\varepsilon_n + \left(\frac{\partial \sigma_m}{\partial T}\right)_{\varepsilon_n} dT \tag{2.6-8}$$

$$ds = \left(\frac{\partial S}{\partial \varepsilon_m}\right)_T d\varepsilon_m + \left(\frac{\partial S}{\partial T}\right)_\varepsilon dT = F_m d\varepsilon_m + (c_\varepsilon/T)dT \tag{2.6-9}$$

if $\quad c_\varepsilon = T\left(\frac{\partial S}{\partial T}\right)_\varepsilon$

for an isotropic crystal

$$F_1 = F_2 = F_3 = F \, , \quad F_4 = F_5 = F_6 = 0 \, ,$$

hence

$$d\sigma_m = c^T_{12} d\Delta + 2c^T_{44} d\varepsilon_m - FdT \qquad (m=1,2,3)$$

$$d\sigma_m = c^T_{44} d\varepsilon_m \qquad (m=4,5,6) \tag{2.6-10}$$

$$ds = Fd\Delta + \frac{c_V}{T} dT$$

where

$$\Delta = \sum_{i=1}^{3} \varepsilon_i$$

is the dilatation.

Now

$$\frac{dQ}{dt} = \frac{TdS}{dt} = \chi\nabla^2 T$$

where χ is the thermal conductivity, or

$$\chi\nabla^2 T = TF(\frac{\partial\Delta}{\partial t}) + c_V(\frac{\partial T}{\partial t}) \quad . \qquad (2.6\text{-}11)$$

Now in general the equation of motion is

$$\rho \frac{\partial^2 s_i}{\partial t^2} - \frac{\partial\sigma_{ji}}{\partial x_i} = 0 \qquad (2.6\text{-}12)$$

where $s_i(x)$ denotes the i^{th} component of the displacement of the particles at point x. By substituting the above into (2.7-12) we get:

$$\rho \frac{\partial^2 \vec{s}}{\partial t^2} = c_{44}^T \nabla^2 \vec{s} + (c_{12}^T + c_{44}^T)\text{grad } \Delta - F \text{ grad } T \ . \qquad (2.6\text{-}13)$$

Notice eqn. (2.7-11) already says that if $d\Delta = 0$, then there are no losses to heat - thus truly transverse waves will propagate without heat losses.

$$\rho_o V_s^2 = c_{44}^T = c_{44}^S \quad .$$

Lets try a plane wave solution to (2.7-10) of the form

$s_1 = s_o \exp\{i\omega t-kx_1\}$ $\quad s_2 = s_3 = 0 \quad$ $\Delta = -iks_i$

and $\quad T = T_o + T_1 \exp\{i(\omega t-kx_1)\}$, (2.6-14)

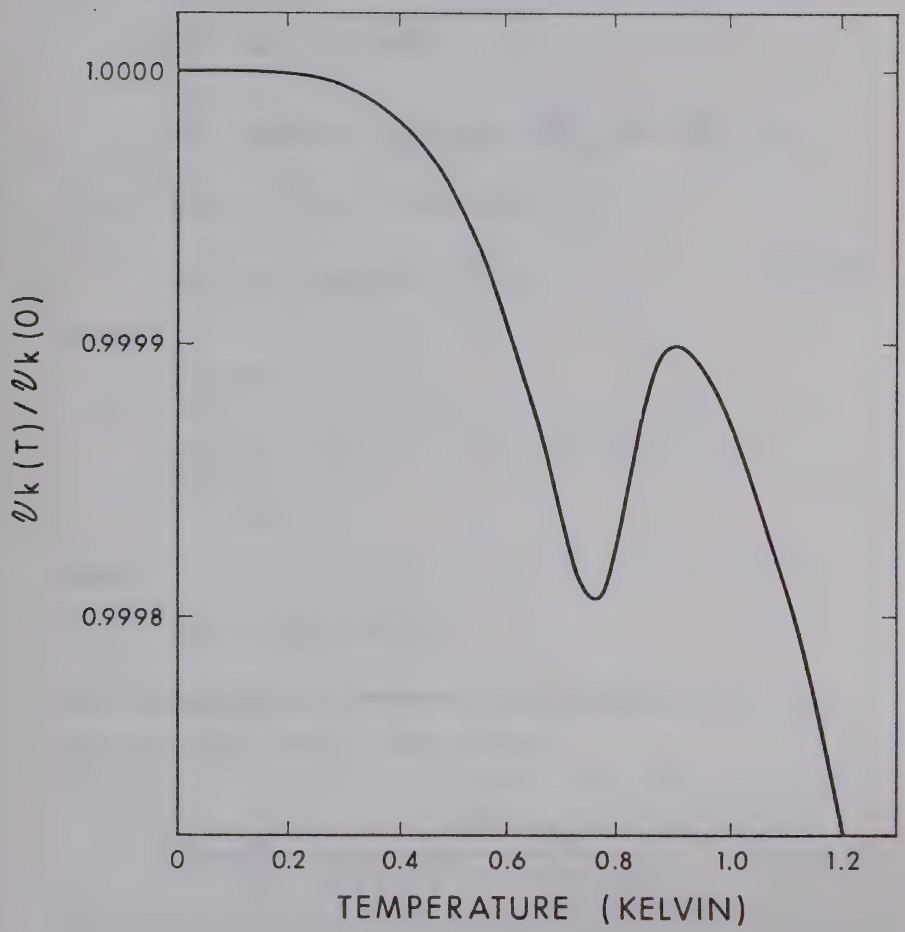

FIGURE 7 Variation of velocity with temperature calculated from Bhatia (1967).

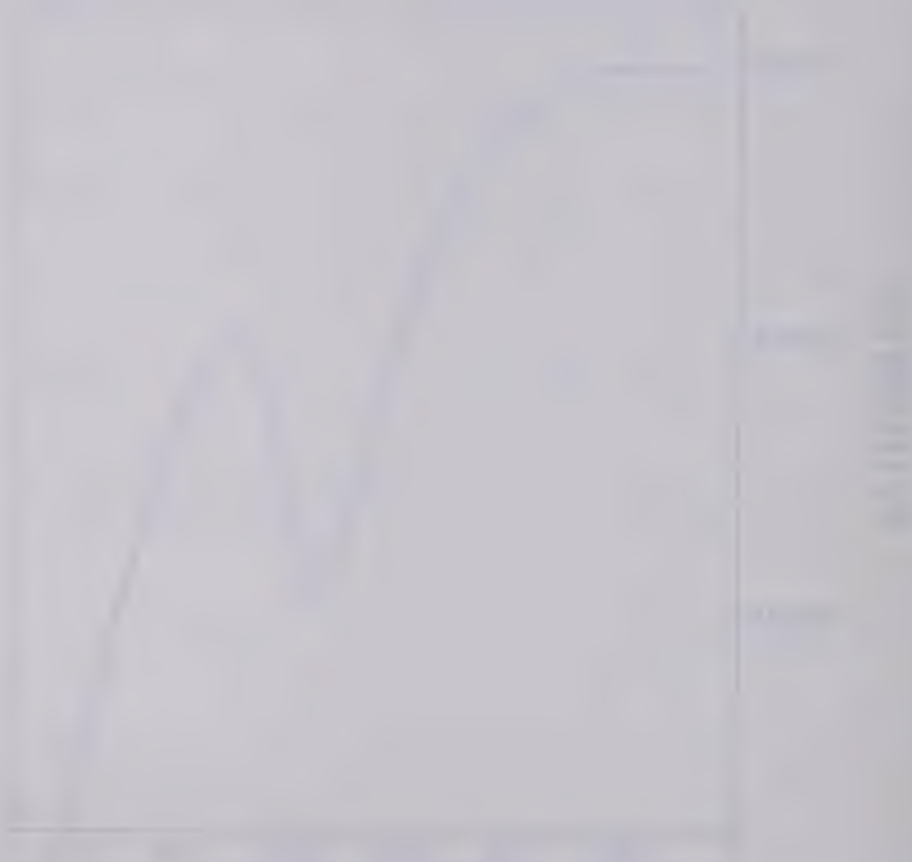

but first as

$$dS = Fd\Delta + (c_\varepsilon/T)dT$$

$$dS = (F/V)dV + (c_\varepsilon/T)dT = \left(\frac{\partial S}{\partial V}\right)_T dV + \left(\frac{\partial S}{\partial T}\right)_V dT$$

we see that $c_\varepsilon = c_V$, similarly $c_\sigma = c_P$

$$-c_\varepsilon + c_\sigma = c_P - c_V = T\beta^2 B_T \qquad (2.6\text{-}15)$$

where

$$\beta = 3\beta'$$

$$\beta_1 = \beta_2 = \beta_3 = \beta' \quad , \quad \beta_4 = \beta_5 = \beta_6 = 0$$

$$F = \beta B_T$$

where

$$B_T = \frac{1}{3}\,(c^T_{11} + 2c^T_{12})$$

the isothermal bulk modulus. Now plugging in (2.7-14) into (2.7-11) and (2.7-13) we have

$$k^2 = \frac{\rho\omega^2}{c^T_{11}} \left(\frac{1 - (ik^2\chi)/\omega c_V}{(c^S_{11}/c^T_{11}) - (ik^2\chi)/\omega c_V}\right) . \qquad (2.6\text{-}16)$$

Now let $k = k_1 - ik_2$, where $k_2 << k_1$, so that $k^2 = k_1^2 - 2ik_1k_2$, then we can write the velocity v and the attenuation α as

$$v^2 = \frac{c_{11}^S}{\rho}\left[\frac{f^2 + f_\chi^2}{(c_{11}^S/c_{11}^T)f^2 + f_\chi^2}\right]$$

$$\alpha = \pi\frac{v^2(f)}{v^2(0)}\left[\left(\frac{c_{11}^S - c_{11}^T}{c_{11}^T}\right)\frac{f\,f_\chi}{f^2 + f_\chi^2}\right] \qquad (2.6\text{-}17)$$

where

$$f_\chi = (2\pi)^{-1}\;\frac{c_V\;v^2}{\chi}\;\frac{c_{11}^S}{c_{11}^T} \quad .$$

Recall that the thermal conductivity is just

$$\chi = \frac{1}{3}\,c_V\;v^2\tau \qquad (2.6\text{-}18)$$

where τ is the relaxation time. Putting (2.7-18) into the expression for f_χ we get

$$f_\chi = (2\pi)^{-1}\;\frac{3}{\tau}\;\frac{c_{11}^S}{c_{11}^T} \sim \frac{1}{2\pi\tau} \quad .$$

Hence, f_χ is related to the thermal relaxation time. Thus at high T the velocity will be adiabatic and at low T isothermal, as $\tau_N \sim 2\times 10^{-12} \times (\theta/T)^3$. Or at high frequencies the velocity is isothermal and at low frequencies, adiabatic.

These formulas are easily made valid for cubic materials by replacing c_{11} with $c_{12} + 2c_{44}$, however to make it numerically valid for hcp materials is difficult because F and β are matrices.

2.7 Sound Velocity as a Function of Temperature When Coupled to the Localized Temperature Field

The following is a brief description of a series of papers by Niklasson and Sjölander (1968), and Niklasson (1970) giving a theory of transport quantities in anharmonic crystal using quantum statistical mechanics. Niklasson derives, and then solves a generalized transport equation (2.6-1) similar to the Boltzmann-Peierls equation

$$[2\omega\Omega - M_j(1) + M_j(1')]\frac{A_j(q,\omega)}{\omega}\, n(\omega)[1+n(\omega)]\gamma_j(q,\omega;Q,\Omega)$$

$$+\ i\mathcal{L}_j(q\Omega)\cdot\alpha_j = 2A_j(q,\omega)n(\omega)[1+n(\omega)]H^j(q\omega;Q\Omega)\langle u(Q,\Omega)\rangle \tag{2.7-1}$$

where ω is the energy of a phonon of momentum q;

Ω is the energy of a disturbance of wave vector Q;

j is the mode (longitudinal or transverse);

(1) and (1') stand for $(q+\frac{1}{2}Q;\omega+\frac{1}{2}\Omega)$ and $(q-\frac{1}{2}Q;\ \omega-\frac{1}{2}\Omega)$ respectively;

$A_j(q,\omega)$ is the generalized spectral function;

$n(\omega)$ is the equilibrium occupation number;

$\alpha_j(q\omega;Q\Omega)$ is the deviation from equilibrium occupation number;

$H_j(q\omega;Q\Omega)$ gives the coupling between thermal motions and lattice deformation;

$\mathcal{L}_j(Q,\Omega)$ is the generalized collision operator;

$\langle u(Q,\Omega)\rangle$ is the lattice deformation;

$M_j(1)$ is the diagonal part of the time-ordered equilibrium self energy.

We will only be solving this equation in the limit of low frequencies in the harmonic approximation. In the harmonic approximation, $\omega_j(q)$ are the harmonic phonon energies for mode j and momentum $\vec{q}$.

$$A_j(q,\omega) = \frac{1}{2}\{\delta(\omega+\omega_j(q)) + \delta(\omega-\omega_j(q))\} \tag{2.7-2}$$

$$n(\Omega) = [\exp\{\hbar\omega/kT\} - 1]^{-1}$$

and if we specify $\Omega \ll \tau^{-1} \ll \omega_a$ where τ is a typical phonon relaxation time and ω_a a typical phonon energy, then

$$M_j(1) = \omega_j^2(q) \tag{2.7-3}$$

$$\mathcal{L}_j(Q,\Omega) = \mathcal{L}_j(0,0) = \Gamma \quad \text{, the collision operator}$$

$$H_\alpha(q\omega;Q\Omega) = H^{oo}(q\omega;Q\Omega) = \frac{i\hbar}{kT}\frac{\omega_j^2(q)}{\omega}\,\Omega\sum_\beta \gamma_{\alpha\beta}^{jj}(q)\dot{Q}_\beta$$

where γ^{jj} is related to the generalized microscopic Gruneisen constant $\gamma_j(q)$ by

$$\gamma_j(q) = \sum_{\alpha\beta}\gamma_{\alpha\beta}^{jj}\frac{du_{\alpha\beta}}{d\,\ell n\,V} \tag{2.7-4}$$

where $u_{\alpha\beta}$ is the dilatation and V is the volume. For a pure expansion or compression

$$\gamma^j(q) = \frac{1}{3} \mathrm{Tr}\, \gamma^{jj}(q) \ .$$

Now define the inner product of f and g by

$$<f|g> = \sum_j \int \frac{d\vec{q}}{V} \int \frac{d\omega}{2\pi} A_j(q,\omega) n(\omega)(1+n(\omega)) f^* g \ . \qquad (2.7\text{-}5)$$

Finally we will separate a function into q, ω and j dependences by the projection operator onto q, ω as

$$P = \frac{|\omega><\omega|}{<\omega|\omega>} + \sum_\alpha \frac{|q\alpha><q\alpha|}{<q\alpha|q\alpha>} \qquad (2.7\text{-}6)$$

then we can write

$$\alpha_j = |\alpha> = |\omega> a_o + |\vec{q}>.\vec{a} + (1-P)|\alpha> \qquad (2.7\text{-}7)$$

and rewriting (2.6-1)

$$|\alpha> = (G + i\Gamma)^{-1} |H>\cdot u \qquad (2.7\text{-}1a)$$

where G is a flow term, Γ a collision term. Now in our approximation

$$G = G_o = \Omega - \frac{\omega_j(q)}{\omega} \vec{c}^j(\vec{q})\cdot\vec{Q}$$

where $\vec{c}^{\,j}(\vec{q}) = \vec{\nabla}_{\vec{q}}\, \omega_j(\vec{q})$ the phase velocity . (2.7-8)

If we now define

$$R = (1-P)(G+i\Gamma_o)(1-P)$$

and

$$R^{-1} = [(1-P)(G+i\Gamma_o)(1-P)]^{-1}$$

(note: R^{-1} does not exist when operating on $|q\rangle$ or $|\omega\rangle$ states; in fact $R^{-1}|\omega\rangle = R^{-1}|q\rangle = 0 = R|\omega\rangle = R|q\rangle$), then we can formally solve 2.71 by

$$a_o = \frac{F^o - N^{ol}.[N^{11}]^{-1}.F^1}{N^{oo} - N^{ol}.[N^{11}]^{-1}.N^{1o}} \cdot \vec{u}$$

(2.7-9)

$$\vec{a} = -[N^{11}]^{-1}.\, N^{1o} a_o + [N^{11}]^{-1}.F^1.\vec{u}$$

where

$$N^{oo} = \langle\omega|a(1-R^{-1}G)|\omega\rangle$$

$$N^{1o} = N^{ol} = \langle\omega|G(1-R^{-1}(G+i\Gamma_o^u))|\vec{q}\rangle$$

$$N^{11} = \langle q|(G+i\Gamma_o^u)[1-R^{-1}(G+i\Gamma_o^u))]|q\rangle$$

$$F_o = \langle\omega|\ 1 - GR^{-1}|H_o\rangle$$

$$F^1 = \langle q|\ 1 - (G+i\Gamma_o^u)R^{-1}|H_o\rangle$$

as

$$\Gamma_o = \Gamma_o^N + \Gamma_o^u$$

where

$$\Gamma_o|\omega> = 0$$

$$\Gamma_o^N|\vec{q}> = 0$$

thus Γ_o^u represents resistive (momentum non-conservation) scattering. If we further realize $\Gamma >> G_o$ in our region (collision dominated regime)

$$\tilde{R}^{-1} \sim [(1-P)\Gamma_o(1-P)]^{-1} \sim \Gamma_o^{-1} - \Gamma_o^{-1}P\Gamma_o^{-1}P\Gamma_o^{-1} \quad \text{if} \quad P\Gamma_oP << \Gamma_o$$

(2.7-10)

hence for cubic or isotropic crystals (hcp is dealt with in the appendix)

$$N^{oo} = [\Omega + ic_{II}^2 Q^2 \tau^{oo}] <\omega|\omega>$$

$$N^{o1} = N^{1o} = -c_{II}\vec{Q}(<\omega|\omega><q_x|q_x>)^{1/2} \qquad (2.7\text{-}11)$$

$$N^{11} = [(\Omega + \frac{i}{\tau_u})\delta_{\alpha\beta} + ic_{II}^2 \sum_{\gamma\delta} \tau''_{\alpha\beta;\gamma\delta} Q_\gamma Q_\delta] <q_x|q_x>$$

$$\bar{F}_o = \frac{i\hbar}{kT} \gamma\Omega\vec{Q}<\omega|\omega>$$

$$F'_{\alpha\beta} = \frac{\hbar}{kT} \gamma c_{II} \Omega \sum_{\gamma\delta} \tau'_{\alpha\beta;\gamma\delta} Q_\gamma Q_\delta (<\omega|\omega><q_x|q_x>)^{1/2}$$

where

$$<\omega|\omega> c_{II}^2 \tau^{\infty} = <c_x^j(q)\omega_j(q)|[(1-P)\Gamma_o(1-P)]^{-1}|\omega_j(q)c_x^j(q)>$$

$$<q_x|q_x>c_{II}^2\tau''_{\alpha\beta;\gamma\delta} = \frac{1}{2}\{<q_\alpha \frac{\omega_j}{\omega} c_\gamma^j|\tilde{R}^{-1}|c_\delta^j|q_\beta>+ <q_\alpha \frac{\omega_j}{\omega} c_\delta^j|\tilde{R}^{-1}|c_\gamma^j \frac{\omega_j}{\omega}|q_\beta>\}$$

$$(<q_x|q_x><\omega|\omega>)^{\frac{1}{2}}c_{II}\gamma\tau'_{\alpha\beta;\gamma\delta} = \frac{1}{2}\{<q_\alpha \frac{\omega_j}{\omega}c_\gamma|\tilde{R}^{-1}|\gamma_{\beta\delta}^{jj} \frac{\omega_j^2}{\omega}> + <q_\alpha \frac{\omega_j}{\omega} c_\delta^j|\tilde{R}^{-1}|\gamma_{\beta\gamma}^{jj} \frac{\omega_j^2}{\omega}> \}$$

$$<q_x|q_x>\frac{1}{\tau_u} = <q_x|\Gamma_o^u\{1 - \tilde{R}^{-1} \Gamma_o^u\}|q_x>$$

$$(<q_x|q_x><\omega|\omega>)^{\frac{1}{2}}c_{II} = <c_x^j(q)\omega_j(q)|\ 1 - \tilde{R}^{-1}\Gamma_o^u|q_x>$$

$$<\omega|\omega>\gamma = <\omega_j^2(q)|\gamma^j(q)> \quad .$$

Now τ^{oo}, $\tau''_{\alpha\beta;\gamma\delta}$, $\tau'_{\alpha\beta;\gamma\delta}$ are different averages over the inverse collision operator and are about the same magnitude as τ the total relaxation time. c_{II} is the velocity of second sound as usually measured and τ_u is the umklapp relaxation times. These constants are calculated for the isotropic and hcp cases for He^4 in the appendix.

If we define

$$\tau''(Q) = \frac{1}{Q^4} \sum_{\alpha\beta\gamma\delta} Q_\alpha Q_\beta Q_\gamma Q_\delta \tau''_{\alpha\beta;\gamma\delta}$$

and

$$\tau'(Q) = \frac{1}{Q^3} \sum_{\beta\gamma\delta} Q_\beta Q_\gamma Q_\delta \tau'_{\alpha\beta;\gamma\delta} \qquad (2.7\text{-}12)$$

then we can write to first order in $c_{II}^2 Q^2$ the generalized heat conductivity

$$\vec{Q}\cdot\chi(Q,\Omega)\cdot\vec{Q} = ic_V c_{II}^2 Q^2 \left[\frac{1 + \frac{\tau^{oo}}{\tau_u} - i\,\tau^{oo}\Omega}{\Omega + \frac{i}{\tau_u} + ic_{II}^2 Q^2 \tau''(Q)}\right] \tag{2.7-13}$$

which in the static case becomes

$$\kappa_o = c_V c_{II}^2 (\tau_u + \tau^{oo}) \quad . \tag{2.7-14}$$

Notice there is no Poiseuille Flow as we have ignored multiple scattering effects. The second sound velocity, if $\tau^{oo} << \tau_u$, is

$$c_{II} = \frac{\langle c_x^j(q)\,\omega_j(q)\,|\,q_x\rangle}{(\langle\omega|\omega\rangle\langle q_x|q_x\rangle)^{\frac{1}{2}}} = \frac{1}{3}\,\frac{\sum_j c_j^{-3}}{\sum_j c_j^{-5}} \quad \text{for isotropic case .} \tag{2.7-15}$$

Finally, the result we need, is the propagation of first sound with coupling to the localized temperature for the isotropic case.

$$\frac{[c_j^2(Q)]^2}{[c_j^{(is)}(Q)]^2} = 1 + \frac{K^{(is)}}{\rho[c_j^{(is)}(Q)]^2}\left(\frac{c_P}{c_V} - 1\right) \times N_j(Q,\Omega) \tag{2.7-16}$$

$$N_j(Q,\Omega) = \frac{(1-s^2)[c_j^{(is}(Q)]^2 Q_j^2 + 4\Gamma_2^o(Q)\Gamma_j^o(Q)}{(1-s^2)^2[c_j^{(is)}(Q)]^2 Q^2 + 4[\Gamma_2^o(Q)]^2}$$

This theory essentially presumes that around some localized distortion of the lattice, will appear a local distortion of the phonon spectrum. These phonons will be travelling in general with some group drift velocity v and decaying by various modes to equilibrium.

The drift velocity in general is characterized by the following equation

$$[-i\Omega + \frac{1}{\tau_u}] v_\alpha(Q,\Omega) + C_{II}^2 \sum_{\beta\gamma\delta} \tau''_{\alpha\beta\gamma\delta} Q_\gamma Q_\delta v_\beta(Q,\Omega)$$

$$= \left(\frac{\langle\omega|\omega\rangle}{\langle q_x|q_x\rangle}\right)^{\frac{1}{2}} [-\frac{i}{T} C_{II} Q_\alpha \bar{T}(Q,\Omega)$$

$$+ iC_{II}\gamma\Omega \sum_{\beta\gamma\delta} \tau'_{\alpha\beta\gamma\delta} Q_\gamma Q_\delta \langle u_\beta(Q,\Omega)\rangle]$$

where the term in $1/\tau_u$ is resistive losses, the term in τ'' is diffusive losses, the term in $\bar{T}$ is coherent heat flow losses, and the term in τ' is losses due to coupling between the drift velocity and the lattice deformation.

The generalized heat conductivity is

$$\vec{Q} \cdot \chi \cdot \vec{Q} = i\, C_v \{\Omega - \frac{N^{00} - N^{01} \cdot [N'']^{-1} \cdot N^{10}}{\langle\omega|\omega\rangle}\} .$$

If we use equations (2.7-12)

where

$$s = c_{II}/c_j^{(is)}(Q) \;;$$

Q_j is the part of the wave that is dilatational;

$\Gamma_2^o(Q) = \frac{1}{2}\{\frac{1}{\tau_u} + c_{II}^2 Q^2[\tau^{oo}+\tau''(Q)]\}$ the attenuation of second sound;

$$\Gamma_j^o(Q) = \frac{1}{2}\{\frac{1}{\tau_u} + c_{II}^2 Q^2 \tau''(Q)\}\frac{Q_j^2}{Q^2} - c_{II}^2 Q Q_j \tau_j'(Q) \;;$$

$K^{(is)} = \frac{1}{3}\,[c_{11}^{(is)} + 2c_{12}^{(is)}]$ where superscript (is) means isothermal;

$c_V = \frac{2\pi\rho h^2}{MkT^2}\langle\omega|\omega\rangle$ the heat capacity at constant volume.

If we assume $\Omega \sim Qc_j^{(is)}$, then $(1 - s^2) \sim \frac{2}{3}$

a) for $\Omega\tau$, $\Omega\tau_u \ll 1$

$$N_j \sim \frac{(1 - s^2)\Omega^2 + \frac{1}{\tau_u^2}}{(1 - s^2)^2\,\Omega^2 + \frac{1}{\tau_u^2}} \sim 1 \qquad (2.7\text{-}17)$$

hence propagation is adiabatic.

b) for $\Omega\tau \ll 1 \ll \Omega\tau_u$

$$N_j \sim \frac{(1 - s^2)\Omega^2}{(1 - s^2)\Omega^2} \sim \frac{3}{2} \qquad (2.7\text{-}18)$$

Hence propagation is enhanced due to coupling to second sound.

c) for $1 \ll \Omega\tau_u, \Omega\tau$

$$N_j \sim \frac{\{\frac{1}{2}\tau''(Q) - \tau'(Q)\}}{\{\tau^{oo} + \tau''(Q)\}} . \tag{2.7-19}$$

As $\tau''(Q) \sim \tau'(Q)$, then $N_j(Q)$ is usually negative. For $N_j = 0$; $\tau''(Q) = 2\tau'(Q)$ produces isothermal propagation (usually $N_j < 0$ and we never have isothermal propagation). (Note: for pure transverse modes $Q_j = 0$, hence $N_j = 0$ and propagation is always isothermal or always adiabatic as $c_{11}^S = c_{11}^T$).

2.8 Interference at the Transducer Due to Misalignment

When the mirror and tranducer are improperly aligned, the reflected pulse will strike the transducer at an angle. The arrival time of the pulse is, therefore, no longer sharp. Also, interference across the transducer will affect the amplitude of the received pulse.

Assume an input pulse $f(t)$ where

$$f(t) = A \sin \Omega t \qquad 0 < t < T$$
$$= 0 \quad \text{otherwise.}$$

Its fourier transform $F(\omega)$

$$F(\omega) = \int_{-\infty}^{\infty} f(t)e^{i\omega t}dt = \frac{-Ae^{i\omega T}}{\omega^2-\Omega^2}\{2\omega \sin \Omega T - \Omega \cos \Omega T\} \frac{-A\Omega}{\omega^2-\Omega^2} .$$

Now if our path length is $2d$ and the pulse

travels with velocity V, the arrival time of the n^{th} pulse is $\frac{2nd}{V}$, where ω is the frequency of the pulse. If our tranducer is a square of size z, we must modify our inverse transform to be

$$F_n(t) = \frac{1}{2\Pi z}\int_{-\infty}^{\infty}\int_{-z/2}^{z/2} F(\omega)e^{-i\omega(t-\frac{2nd}{V})(\frac{\sin 2n\theta x}{V})} dxd\omega \ .$$

if θ, the misalignment is small, $\sin 2n\theta \sim 2n\theta$.

Then

$$F_n(t) \ \frac{iVA}{2n\theta z}\{\frac{1}{2\Pi}\int_{\infty}^{\infty}[e^{-i\omega t^+} - e^{-i\omega t^-}]$$

$$\times\ [\frac{\Omega + e^{i\omega T}(i\omega \sin \Omega T - \Omega \cos \Omega T)}{\omega(\omega^2 - \Omega^2)}]d\omega\}$$

where
$$t^+ = t - \frac{n}{V}(2d + z\theta)$$

$$t^- = t - \frac{n}{V}(2d - z\theta)$$

$$I_1 = \frac{1}{2\Pi}\int_{-\infty}^{\infty}\frac{\Omega}{\omega(\omega^2-\Omega^2)} e^{-i\ t^+} d\omega$$

If $\omega \rightarrow \omega + i\varepsilon$, there are three poles at $-\Omega - i\varepsilon$, $\Omega - i\varepsilon$ and $-i\varepsilon$

$$I_1 = -\theta(t^+)\ \{\frac{-i}{\Omega} + \frac{i}{\Omega}\cos \Omega t^+\}$$

$$I_2 = -\frac{1}{2\Pi}\int_{-\infty}^{\infty}\frac{\Omega}{\omega(\omega^2-\Omega^2)} e^{i\omega t^-} d\omega = \frac{i}{\Omega}\theta(t^-)\ \{-1 + \cos \Omega t^-\}$$

$$I_3 = \frac{1}{2\Pi}\int_{-\infty}^{\infty}\frac{e^{-i\omega(t^+-T)}}{\omega(\omega^2-\Omega^2)}\{i\omega \sin\Omega T - \Omega\cos \Omega T\}d\omega$$

$$= \frac{-i\theta(t^+-T)}{\Omega}\{-\cos \Omega T - \cos \Omega t^+\}$$

$$I_4 = \frac{1}{2\Pi} \int_{\infty}^{\infty} \frac{e^{-i\omega(t^- - T)}}{\omega(\omega^2 - \Omega^2)} \{i\omega \sin \Omega t - \Omega \cos \Omega T\} d\omega$$

$$= + \frac{i\theta(t^+ - T)}{\Omega} \{-\cos \Omega T - \cos \Omega t^-\}$$

$$\text{where} \quad F_n(t) = \frac{iVA}{2n\theta z} \{I_1 + I_2 + I_3 + I_4\}$$

for

$$t < \frac{n}{V}(2d - z\theta) \quad \text{or} \quad t > T + \frac{n}{V}(2d + z\theta)$$

$$F_n(t) = 0$$

for

$$\frac{n}{V}(2d + z\theta) < t < T + \frac{n}{V}(2d - z\theta)$$

$$F_n(t) = \frac{VA}{2n\theta z} \{\cos \Omega t^+ - \cos \Omega t^-\}$$

$$F_n(t) = \frac{VA}{\Omega n\theta z} \sin \Omega (t - \frac{2nd}{V}) \sin \frac{n\theta z\Omega}{V}$$

hence the n^{th} pulse is similar to the first pulse, but delayed by $\frac{2nd}{V}$ and modified by an amplitude

$$\frac{\sin \frac{n\theta z\Omega}{V}}{\frac{n\theta z\Omega}{V}} .$$

Also note in the limit $n \to 0$, $\theta \to 0$ we get our original pulse.

However, the start of the pulse is not sharp but drawn out over a time $\frac{2nz\theta}{V}$. In this region

$$\frac{n}{V}(2d - z\theta) < t < \frac{n}{V}(2d + z\theta)$$

$$F_n(t) = \frac{VA}{2n\theta z}\{1 - \cos \Omega t^{-}\}$$

$$\text{at} \quad t = \frac{n}{V}(2d+z\theta), \quad F_n = \frac{VA}{2n\theta z}\{1 - \cos[\frac{n}{V}\, 2d+z\theta - \frac{n}{V}\, 2d-z\theta)]\}$$

$$F_n[\frac{n}{V}(2d+z\theta)] = \frac{VA}{2n\theta z}\{1 - \cos \frac{2nz\theta}{V}\} \frac{VA}{n\theta z} \sin^2 \frac{n\theta z}{V}$$

and thus there is a phase change during transition to the normal pulse motion.

The intensity of the n^{th} pulse at its maximum obeys the following

$$I_n = A^2 \sin^2 \Omega(t - \frac{2nd}{V}) \frac{\sin^2 \frac{n\theta z\Omega}{V}}{\frac{n^2\theta^2 z^2 \Omega^2}{V}} e^{-2\alpha t} \quad .$$

Thus our pulse shape is contained inside an envelope similar to that of double slit diffraction.

For $z = 1$ cm.

$\Omega = 5 \times 10^6$ Hz

$V = 700$ m/s

$\theta = \frac{1}{60}^{\circ}$

The first minimum appears at about the 23rd echo

This appears to say that my misalignment problem (first minimum at 15-20 echoes) is of the order of a minute of deviation. As the mirror curvature introduces deviations of only seconds of arc, it is felt at this time the misalignment is due to differential contraction.

This time change for the same parameters introduces an error in the direction of shortes times of $\frac{n}{26}\%$ or .04% for two consecutive pulses.

CHAPTER 3

EXPERIMENT

3.1 Low Temperature Apparatus

3.1-1 Cryostat

Helium is the only element which does not solidify under its own vapour pressure. The phase diagram (fig. 8) shows that a minimum pressure of 25 bar is needed to solidify He^4. As we wished to study hcp He^4 up to pressures of 150 bar, the cryostat was constructed to handle He^4 gas, liquid, and solid at pressures up to 250 bar (a safety margin of 100 bar).

Whereas growth at constant volume tends to produce polycrystalline samples, the crystals for this experiment were grown using a constant pressure technique. The bottom of the pressure cell was connected by a copper strip to the He^3 fluid container. The pressure cell was thus cooled from the bottom. The temperature at the top of the pressure cell was kept slightly above the melting temperature (20 to 50 mk) during crystal growth by a 32Ω/ft manganin wire automatically regulated heater running inside the pressure capillary. This heater ensured that no solid could form in the capillary and block it, ensuring constant pressure growth. A thermometer on the top outside of the pressure cell allowed manual and automatic monitoring of the temperature.

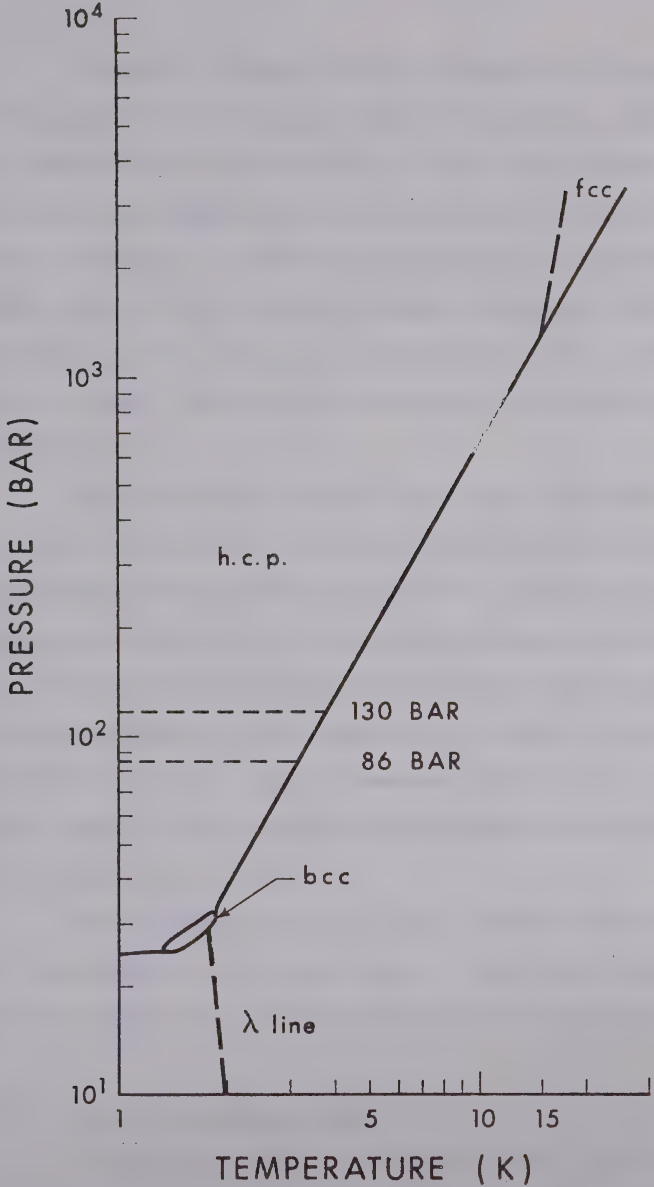

FIGURE 8 Phase diagram for He^4

Figure 9 illustrates the standard He^3 cryostat arrangement while figure 10 shows the pumping system. The pressure regulator on the He^4 pot line (Walker (1959)) maintains the temperature variations in the pot to a few mk between 1.4k and 4k. By placing a calibrated needle value on the ballast volume (Ackerman (1967)), one can cool the bottom of the pressure cell as slowly as one wishes, facilitating automatic regulation of crystat growth.

One filling of the He^4 pot lasts for about 16 hours at 2k. However, the growth period can be extended by refilling the pot through the fill needle valve while pumping on the He^4 pot. Although extreme care must be used, the growth period may be extended indefinitely. A rough estimate of the temperature in the pot can be obtained by using a vapor pressure reading on a bourdon gauge (model FA 145, Wallace and Tierman, Belleville, N.J.) in the pump line.

One filling of the He^3 pot lasted from 30-60 min. depending on the heat input. The lowest temperature achievable when the ultrasonics were on was about 0.7k.

3.1-2 The High Pressure Cell

Originally, these experiments were aimed at determining the temperature dependence of the ultrasonic attenuation. This consideration affected the design of

FIGURE 9

CRYOSTAT

1. Copper Can (22" × 3" diameter)
2. Needle Value
3. Thermometer-Heater (100Ω Allen-Bradley)
4. High Pressure Capillary (3/32" OD × 1/32" ID)
5. He^4 Pot (4 1/2" × 2 3/4" diameter)
6. He^4 Pot (1" × 1" diameter)
7. High Pressure Cell (see figure 11)
8. Thermometer (cryocal 2443,
   type CR 250 - 1.5 - 40 - He^3)
9. Vapor Pressure Capillary (1/32" OD)
10. Capillary is Anchored to He^4 Pot
11. He^4 Liquid
12. He^3 Liquid
13. Thermometer (100Ω Allen-Bradley)
14. Copper Bar (6" × 1 1/4" × 1/4")
15. Vapor Pressure Bulb (2" × 1/2" × 3/8")

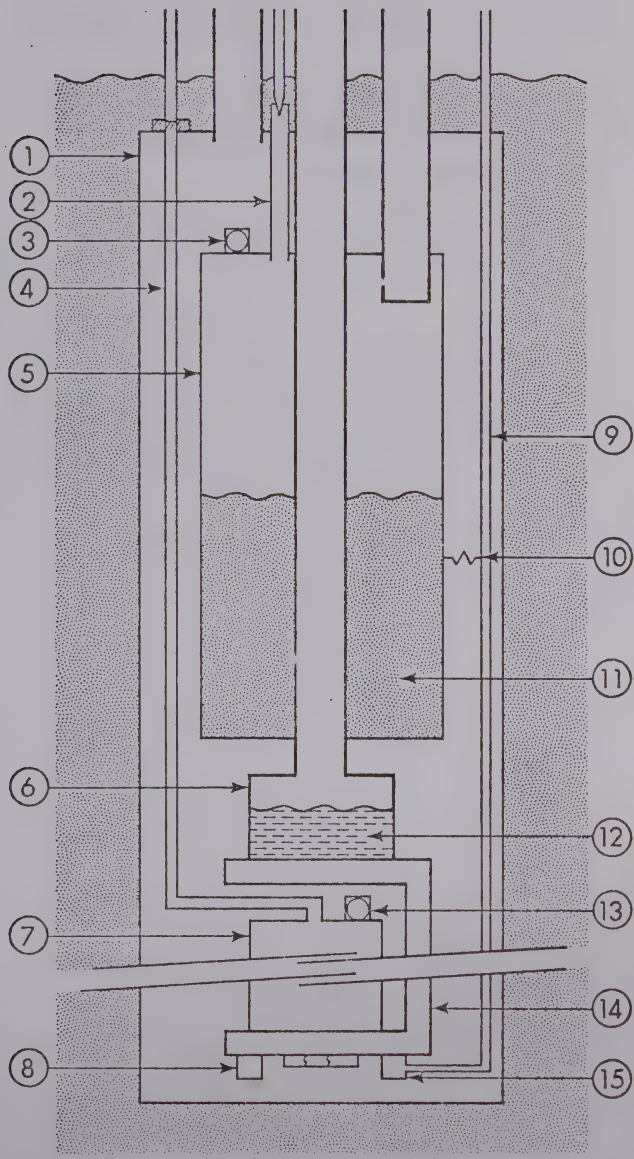
1
2
3
4
5
6
7
8
9
10
11
12
13
14
15

FIGURE 10

PUMPING AND PRESSURE STABILIZATION SYSTEM

1. He^3 Storage
2. Walker Pressure Regulator
3. Ballast Volume
4. Needle Value
5. Cold Cathode Guage (H.S. Martin & Sons, Evanston, Ill.)
6. Diffusion Pump (Edwards High Vacuum, 350 Watts)
7. Exchange Gas Storage (He^4)
8. He^3 Rotary Pump (sealed)
9. He^4 Pot Rotary Pump
10. He^4 Exchange and Backing Pump

R to recovery system

V Vent to atmosphere

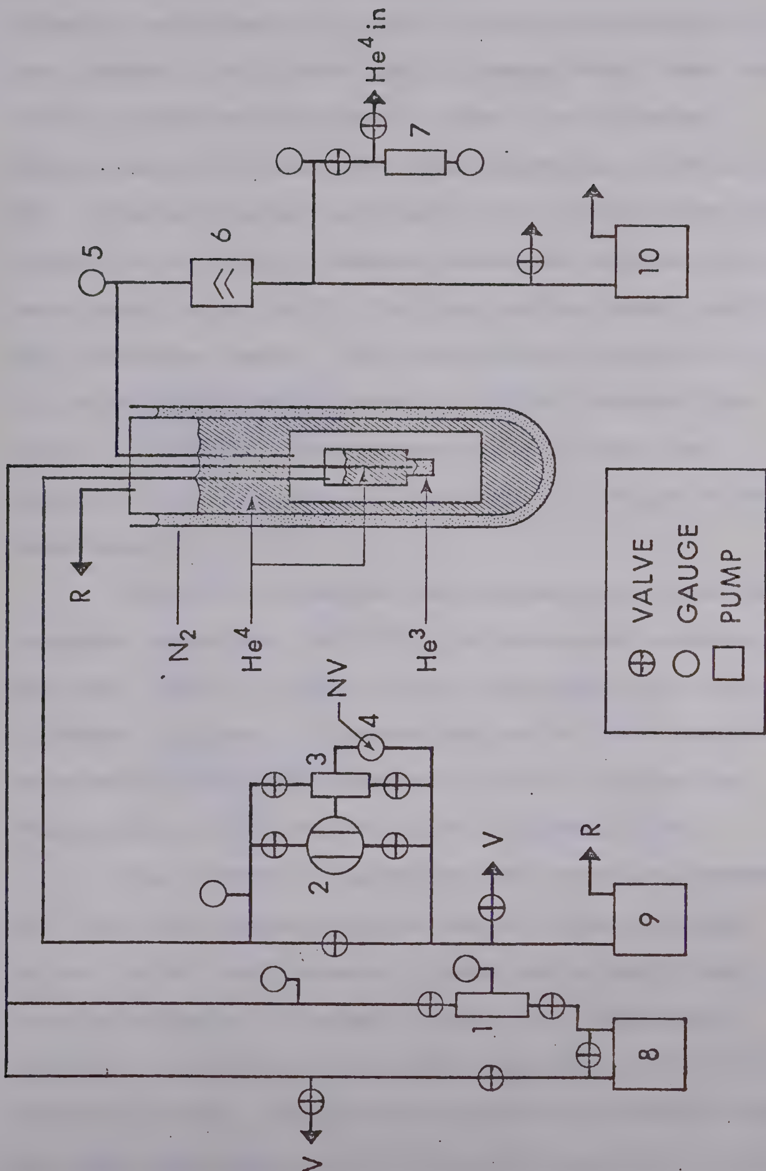

VALVE
GAUGE
PUMP
He^4 in
N_2
He^4
He^3
R
V
NV
1
2
3
4
5
6
7
8
9
10

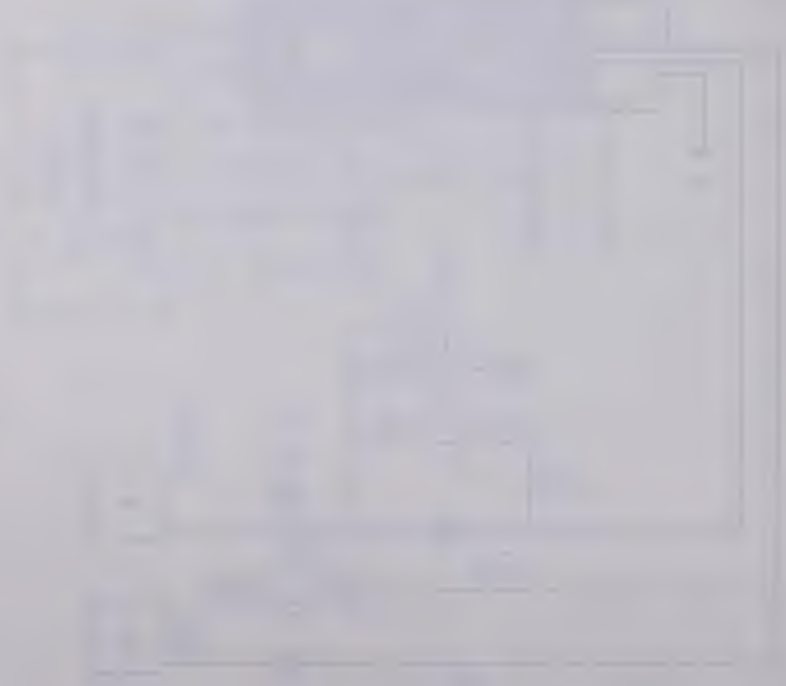

the pressure cell. A single transducer and mirror symmetry were chosen in that it allows observation of many echoes. The mirror had a diameter three times the mirror transducer distance of about 1 cm allowing deviations of the beam path from perpendicular of up to 45°. Typical elastic constants (for example those of Crepeau et al (1970)) predict deviations between ray and wave normal of up to 20° for longitudinal waves and 35° for transverse waves. Thus velocities in crystals of all orientations were observable. The distance from mirror to transducer was chosen to be as small as possible while minimizing the effect of ringing by the transducer.

Figure 11 shows the high pressure cell and the tranducer mounting. At first the transducer assembly was hung freely by three 2-inch long brass bolts from a thread in plate. Alignment was set at room temperature by examining the echo pattern in xylene and acetone. This system did not maintain the alignment to 4k.

The system of suspension was therefore changed so that the suspending plate was no longer threaded in but rather held between a ledge and a split ring circlip tightly by six set screws. The transducer assembly was suspended from this plate by a set of six push-pull bolts. Three bolts pulled the assembly toward the suspension plate while three bolts pressed it away from the suspension plate. This system maintained align-

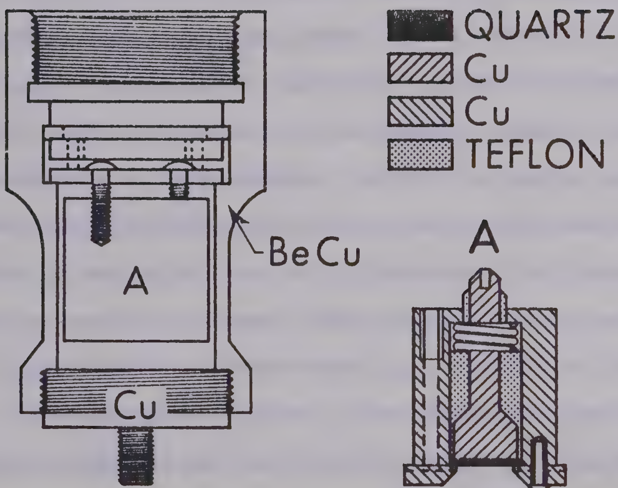

FIGURE 11 High Pressure Cell

ment well to 4k, however, repeated cyclings to 4k and room temperature gradually brought the transducer and mirror out of alignment.

It is interesting to point out that extreme tightening of the push-pull bolts caused distortion in the holding plate which gave rise to interference patterns in the ultrasonic echo pattern.

The mirror was a copper plate 3cm in diameter (although only 2.8 cm was usable by the transducer) and one-quarter inch thick, polished flat to within 3 fringes of Na light. A range of polishing powders was used including various grades of grit papers, alumdum powder, emery powder and rouge powder. After the mirror was threaded into the bottom of the pressure cell and soft soldered it was only flat to 10 fringes of Na light across its usable surface. This corresponds to roughly 3% of a wavelength of 5 MHz sound in a crystal at 120 bar.

The bottom of the cell (the copper mirror) was attached by thread and nut to a 12" × 2" × ¼" copper bar bent into a "U" and fastened to the base of the He^3 pot.

To the top of the pressure cell was attached the pressure capillary. The 32Ω/ft wire was grounded inside the top of the pressure cell.

The success rate for quality crystals in this cell was one in four at 120 bar and two in three at 85 bar.

3.1-3 Crystal Growth

My experience with single crystal growth at 120 bar and 85 bar appears to be slightly different than growth at lower pressures (for example Crepeau et al (1970), Wanner and Franck (1970) and Vignos and Fairbank (1966)). Growth from the superfluid phase is only possible at pressures in the neighbourhood of 25 bar.

The growth procedure I have followed is outlined below. The pressure cell was brought to temperature equilibrium by letting it stabilize for about two hours with the sound system operating at a temperature about 20 mk above the melting point. The automatic heater was then set to maintain this temperature while the low flow calibrated needle valve (Ackerman (1967)) in conjunction with the pressure regulator (Walker (1959)) lowered the temperature of the He^4 pot. This pot was connected by He^3 fluid and the copper "U" bar to the bottom of the pressure cell. Thus the bottom of the cell was slowly cooled while the top of the cell was kept above the melting temperature for a period of 12-24 hours. The longer the growth time, in general, the better quality the crystal. This final temperature gradient was then held for another 24 hours to allow crystal defects not in thermal equilibrium (dislocations, for example) to move to the surface outside the portion of the crystal used for ultrasonic measurements. The temperature at the top of the cell was then lowered by

slowly changing the setting on the automatic heater until the whole cell was filled with solid. If the crystal was still low in echoes further annealing would be done (a further 24 hours) followed by cycling down to 1.3k and then back close to the melting point. If the crystal was still of insufficient quality, it was melted. Crystals of over 50 echoes were kept. Only one crystal with less than 50 echoes was studied, 'D3', as it had 20 echoes of very good pulse shape. This crystal however, showed a knee at very high temperatures (2.6k) which may be due to the fact it was not good quality (see sections 4 and 5).

The rejection rate at 120 bar was three crystals out of four, while at 85 bar was one out of three. From my experience it was easier to grow crystals at lower pressures.

Although no direct evidence was available to determine whether the crystals were single or not, there was indirect evidence available. At 85 bar we measured sound velocities that varied up to 15%. This high anisotropy is identical to that predicted by Gilles et al (1968) and found experimentally at lower pressures by Creapeau et al (1970), Wanner and Franck (1970) and Greywall (1970). Also it is unlikely that crystals with low angle grain boundaries or small crystallites could produce over 50 ultrasonic echoes (attenuations of the order of .1 cm^{-1}). For these reasons we believe that

our crystals were single.

The ultrasonics were left running during growth to facilitate monitoring. One observes a decay in amplitude of liquid echoes until they almost completely disappear. At this stage, probably, large numbers of crystallites have formed and covered the mirror giving random reflection. Then, slowly, solid echoes begin to grow (displaced to shorter times). Annealing improves both echoe quantity and quality.

3.2 Temperature Measurement and Control

The temperature at the bottom of the pressure cell was determined by an Allan Bradley resistor (100 Ω) whose resistance was measured by an Oxford instrument resistance thermometer bridge which was rigged for two and three terminal resistance measurements. This allows one to compute the four terminals resistance assuming the resistance to all four leads is identical. The resistor was prepared by grinding the outer coating down to the carbon centre and then covering with a thin coat of GE varnish (#7031) and baked at 90°C for two hours. The resistor was then inserted into a tightly fitted machined hole in a copper block. The lead wires were wound several times around the end of the block, then wound around the copper "U" bar, then wound several times around the He^4 pot. Finally the leads were anchored at 4k and then taken through a vacuum feed - through to

room temperature at the top of the cryostat and connected to the bridge.

The new resistor at the top of the cell was also a 100 Ω Allen-Bradley prepared in the same way and attached to the top outside of the pressure cell by bolt and grease. It was not anchored at the copper "U" bar as it was used during crystal growth, but was anchored at the He^4 pot and at 4k.

The thermometry was later changed at the bottom of the pressure cell using a cryocal, Inc. calibrated resistor CR 250-1.5-40-He^3 S/N 2443 Germanium. This resistor was coated with a mixture of vacuum grease and copper filings and inserted into the "U" bar at the bottom of the pressure cell. The resistors were calibrated against the 1962 He^3 scale and the 1958 He^4 scale of temperatures by a vapour pressure cell bolted to the bottom of the "U" bar.

At the top of the He^4 pot two resistors were used. One was a roughly calibrated two terminal thermometer (calibrated using the boiling point of He^4 and the λ point) and one was a simple 100 Ω heater.

A 30Ω/ft manganin wire was placed inside the high pressure capillary and grounded to the top inside of the pressure cell. This heater was used in conjunction with the thermometer at the top outside of the pressure cell in the following manner. A resistance R corresponding to the desired temperature is set in the temperature

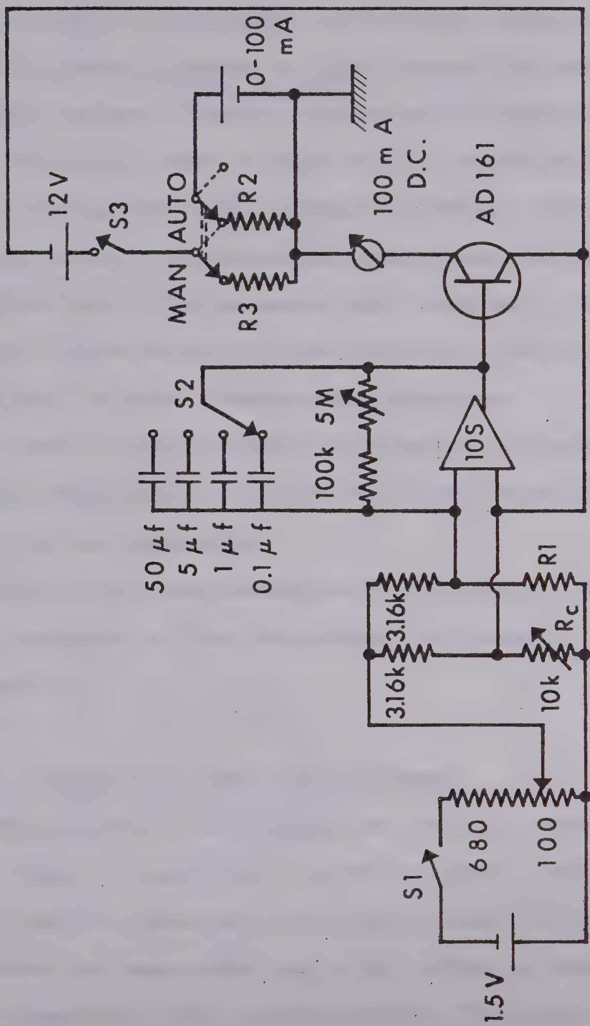

FIGURE 12   Temperature regulator schematic

regulator (figure 12). If the cell is too cold, an e.m.f. is set up across the amplifier (105) which turns on the transistor allowing current to flow through the manganin wire. When the top of the cell reaches the desired temperature the e.m.f. goes to zero and the transistor shuts off. By choosing the time constant properly, the cell can be continuously cooled while maintaining the temperature at the top of the pressure cell constant. The "Manual-auto" mode switch allows the proper settings to be worked out, without damaging the crystals.

I would like to thank Len Vienneau for helpful discussions which led to the use of large temperature gradients during annealing.

The calibration technique for the lower thermometer is accurate to 10 mk throughout the range of measurements.

3.3 High Pressure Gas Handling Equipment

The purity of the helium gas used is important for many types of measurement on He^4 systems. Purifying by super-leak is undoubtedly the best method, although second sound has been observed in He^4 crystals prepared from gas evaporated from liquid helium. For measuring sound velocities, such high purity is probably unnecessary.

Figure 13 illustrates our gas handling procedure. The system was first evacuated, then commercial grade He^4 is fed into an activated charcoal trap cooled by

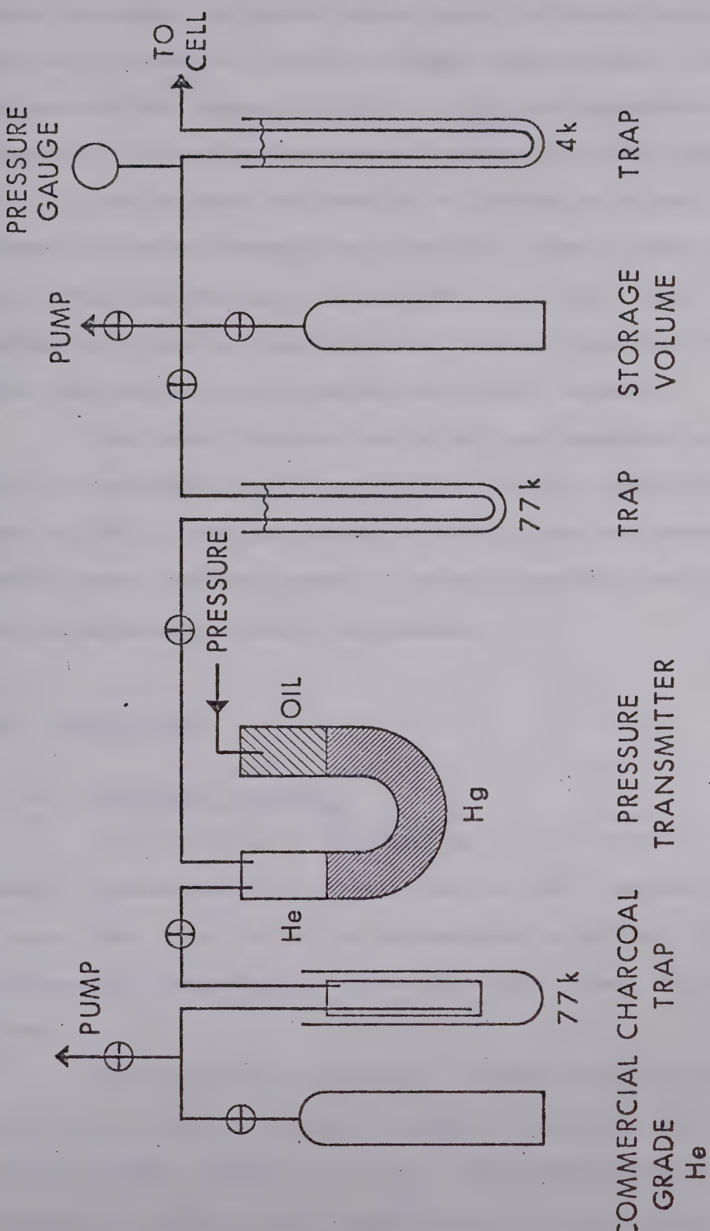

FIGURE 13 Gas handling and purification

liquid nitrogen to remove water vapor and other materials that will freeze at liquid nitrogen temperatures. The helium was then passed through a pressure trasmitter (necessary to achieve pressures greater than 180 bar).

The gas was then fed to a nitrogen trap and allowed to reach thermal equilibrium. Finally the gas was slowly fed through a liquid He^4 trap till again thermal equilibrium was reached. The gas was then stored with the residue being pumped away after warming.

The ideal limit of purity of gas prepared in this way is the natural abundance of He^3 in He^4 (about one part in 10^6). The gas prepared in this way was found satisfactory for the growth of single crystals and for the measurement of sound velocities.

3.4 Ultrasonics

3.4-1 Transducer Assembly

The etalon is a longitudinally cut (X-cut) quartz transducer flat to one part in 10^{+6} coated with a thin film (100-1000 A°) of evaporated aluminum. The fundamental frequency for the etalon was chosen to be 5 MHz.

The etalon was backed by a brass piston polished flat by hand to ½ a fringe of sodium light over its entire backing surface (1.2 cm). The backing piston is about 2.5 cm long and is inserted in a teflon sleeve.

The diameter of the piston and sleeve is the same as that of the etalon (1.2 cm). The piston is spring loaded into a large brass cylinder (2.5 cm in diameter). The brass cylinder and piston were hand polished in a special assembly over 5 cm in diameter, so that both pieces could be polished simultaneously without rounding at the edges. The two assemblies were made flat to about 2 fringes of Na light by polishing with various alumdun, emery and rouge powders.

The assembly was fronted with a disc flange 2.5 cm in diameter and 1 cm interior hole, 2 mm thick. This brass flange was placed against the transducer to hold it against the spring. It was bolted by three bolts to the outer cylinder. This flange was also polished, however, it was difficult to get it flat near the inner edge. Thus, it was flat to one fringe of Na light except near the inner circle where five closely spaced fringes could be seen. Next the inside, polished part of the flange was slotted six times with a file to produce radial slots about 0.01 cm in depth. The purpose of the slots was to prevent liquid helium from being trapped close to the transducer. If this happens the liquid may freeze later than the rest of the crystal introducing possible defects close to the transducer, or even not freezing at all.

This assembly was then mounted by push-pull screws to another assembly described in section 3.1-2 and is

illustrated in figure 11.

3.4.-2 Electronics

A block diagram of the electronics is illustrated in figure 14. The pulse originates in an Arenberg pulse generator (Model PG-650C mod IJD ADD5D SN704) which is pulsed by a Hewlett Packard (222A) pulse generator. The radio frequency signal was then matched by a stub matching network through a tee. One branch of the tee travels through the high pressure capillary and connects to the back of the piston in the etalon assembly (section 3.4-1). The other branch of the tee takes the pulse through an Arenberg tunable preamplifies (PA 620 SN 312B) and then through an Arenberg Wide Band Amplifier (WA 600-D SN 298). The final result is displayed on a Tektronix oscilloscope (R 556) or on a chart recorder (Hewlett Packard Mosely 580M).

The initial pulse was from 20 to 200 Vpp, at 5MHz with a pulse width from 0.5 to 5 μs and a repetition rate of 100 per second. The pulse generator and the main trigger of the scope were triggered by the the same pulse from a Tektronisc Time Mark Generator (type 184 SN 5655). The time mark generator also produces a second trigger pulse coherent to the first pulse to one part in 10^7. It was found that the internal delay trigger and the internal normal trigger had variable drift of ± 3 μs an hour. External triggering eliminates this source of error.

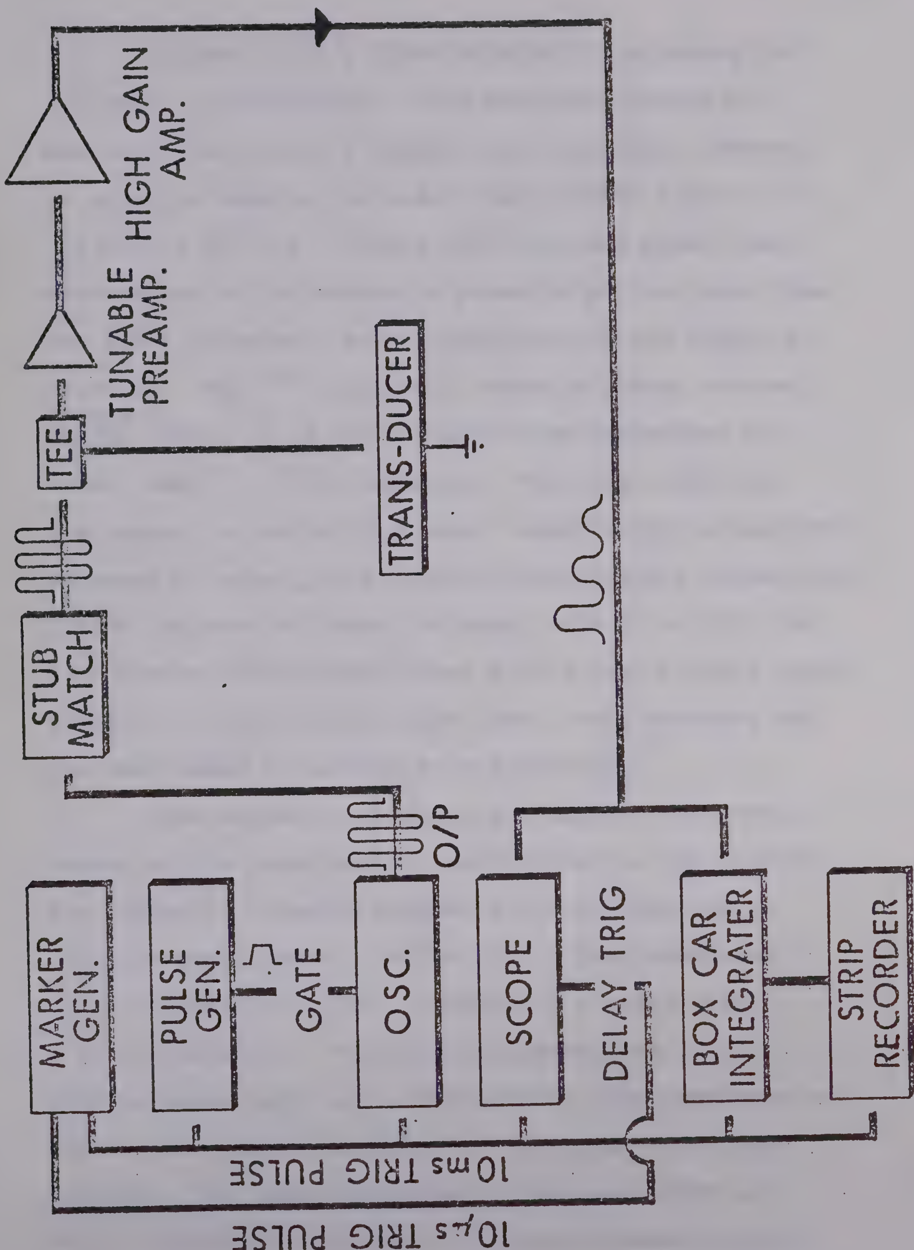

FIGURE 14 Block diagram of electronics

Figure 14 is a block diagram illustrating the electronic configuration. The coherence method of measuring the velocity employs the fact that a change in velocity changes the start time of each pulse. As the pulses are all starting with the same phase, the measurement of the change in phase at a given time from the first pulse will be an indication of the change in velocity. The n^{th} pulse will record a change in time of $\frac{2nd}{V}$ where d is the distance from transducer to mirror and V is the velocity. The larger the n, the larger the velocity change. Sensitivity is therefore enhanced by using later echoes, unfortunately attenuation limits the echo so chosen to about $n = 15$ to 25. The time chosen for watching phase shifts must be very stable relative to the initial pulse time. This accounts for the care taken to provide this stability.

One wishes to transfer the maximum electronic energy at the generator to sound motion in the crystal. The acoustic mismatch between solid He^4 and quartz is quite high (about a factor 100). The transducer is equivalent to a 1 MΩ resistor in a series with a 20 pf capacitor. The high frequency line in the high pressure tube has a transmission line impedance of 100 Ω. The output impedance of the pulse oscillator is 50 Ω. The input impedance of the amplifiers is 90 Ω. To match the cable in the high pressure tube to the transducer directly would be very difficult as well

as only being exact at one frequency. The method which gives good matching without being terribly sensitive to frequency is the stub matching network being composed of three lengths of cable like the letter Π with input and output at the two vertices. The theory needs the length of cable between source and receiver to be comparable to the wavelength of the cable. For our case the wavelength was about 40 m and the cable length about 10 m. Each of the two hanging cables were terminated with a variable inductor in parallel with a variable capacitor. This allowed the network to be matched without cutting the cable. The solution for the input impedance z_i of the network for a load z_i and cable length 'a' and wave vector k is

$$z_i = z_o(1 - \frac{z_o - z_i}{z_o + z_i} e^{-2ika})/(1 + \frac{z_o - z_i}{z_o + z_i} e^{-2ika})$$

where z_o is the impedance of the cable. Single stub matching is a 'T' type network, while double stub matching is a 'Π' type network. Although the values can be worked out in theory, the various impedances are not well enough known to be calculated in practice. Thus we used a double stub matching network terminated in variable capacitors and inductors.

It was found that the matching giving the largest echoes would change with temperature. Although the velocity measurements were not affected by this, the

attenuation measurements were made more difficult.

3.4-3 Method

The first step in measuring velocities was to calibrate the distance travelled. This was done by finding the time of flight in our pressure cell at various pressures in equilibrium with exchange gas to the He^4 bath (4.15 k). This result was then compared at several pressures to known velocities in the liquid. The results are discussed in 4.1.

The pulse echo method was used to calibrate the distance as well as to establish the absolute value of the velocity in the solid. The transducer was excited with a pulse from the pulse generator (20 to 200 Vpp for 5 to 5 μs with a repetition rate of 100 pulses per second). The transducer then mechanically vibrates at 5MHz and sends a sound pulse through the crystal which is reflected at the mirror and returned to the transducer. Part of this pulse was then reflected and part transmitted to the recording equipment. If one then rectifies and integrates the signal using a gate of about 1 μs, one gets a series of pulses out as in figure 16. The time delay between each pulse was measured. To calculate the average time of flight, a least squares fit to 10 or 20 echoes yielded most accurate results (this method tends to nullify some systematic errors compared to a simple mean, for example). Ringing of the transducer can

cause distortion in the first few echoes. For this reason, it is better to take measurements on later echoes. We chose echoes around the twentieth for almost all measurements.

Once the absolute velocity has been determined, the phase comparison method can be used to determine the change in velocity. For this method a pulse with good shape was chosen and one with which the radio frequency signal was undistorted. The amplifier was adjusted to transmit a non-recfified signal and then part of the echo maximum was chosen to be centred on the scope. Because of the external triggering on the scope (every 10 μs), only one part of each peak is accessible. Our appropriate scale was now chosen to ensure linearity of the scope over the measurement region, as well as convenience for measurement. It was found that an 'A' scale setting of 100μs/cm and a 'B' scale reading of (0.05 - 0.1μs/cm) gave best results. Normally, the delay was in the 500 μs region (the twentieth echo). At our frequency a period was 2×10^{-7} seconds or two to four cm. on our scale. It was found that the signal could be read to 1/50 of a wave length. As the temperature was changed, the pulse would move to lower time of flights and the change in phase was recorded. As the change in phase is proportional to echo number, this had to be taken into account in the calculations. The appendix contains computer programs used in the numerical

analysis.

3.4-4 Error Evaluation

Errors in the pulse-echo technique came mainly from two sources: variation in pulse shape and the linearity in the delay trigger. The 'A' scale was maintained on one scale to prevent errors by scale changes. A typical time of flight was 25 μs, so to see 40 pulses one had to be on the 100μs/cm scale. The linearity in the delay trigger is quoted as 0.5%. Errors in the pulse shape were much more difficult to analyse. That part of the pulse shape error that is systematic can be removed by taking a least squares fit to several pulses. However, random contributions, as well as systematic errors of frequency of the order of the sampling time are more difficult to evaluate. Hopefully ringing effects were small as we were taking our pulses at least 15 or so from the original pulse. There is a possibility of the 2nd transverse branch being propagated along with the original longitudinal pulse. This is very difficult to remove. Random scatter from the sides of the bomb as well as the effects of misalignment and diffraction also will contribute to error. The best indication of error, is therefore, the standard deviation of the least square fit to the echoes - normally about 3%. As the error in the distance calibration is approximately 1%, the total errors were probably about 3.5%.

The limitations of the phase detection technique were the flutter time of the oscilloscope triggers, the period of the radio frequency oscillation and the distortion to the signal.

For a frequency of 5 MHz, the period is only 2×10^{-7} seconds. If one can read the change in phase to 1/50 of a wave length, one can achieve a precision of 4×10^{-9} seconds. Compared to our mean flight time of 2.5×10^{-5} seconds we have an accuracy of 1.6×10^{-4}. The flutter of the delay trigger is 2×10^{-5} which gives an error of 1.7×10^{-4}. At low amplitudes (at low temperatures the attenuation was high) the signal would be slightly distorted, perhaps doubling the quoted error. Some systematic errors are not important here, as we are measuring only the relative change (for example, the error in distance calibration does not contribute to this error). Greater accuracy could be obtained by using higher frequencies, but this would still be limited by scope flutter (5×10^{-5}). The phase superposition technique is even better, allowing accuracies of 10^{-5} to 10^{-6} (McSkimin (1961)). This method can be extended by integrating over the spectrum and using two pulses, one slightly delayed (R. Wanner - private communication). Using more pulses is possible also. J. Holder (1970) has devised a method using a large number of pulses properly delayed and integrated

to accuracy of 10^{-8}. All these methods are presently being investigated, although the latter would cause overheating in the sample.

CHAPTER 4

RESULTS

4.1 Sound Velocity in Fluid He^4 as a Function of Pressure

In order to calibrate the distance between the transducer and the mirror, the sound velocity was measured from 25 bar to 135 bar in the fluid at 4.15k. This velocity was then compared to the corrected values of Vignos and Fairbank (1966) from 1 bar to 50 bar in the region of overlap.

The pulse echo method was used to measure these velocities. A sound pulse was sent out from the transducer to the mirror which was reflected back. The electronics detected the echo as well as any further echoes and the echo train was then displayed on an oscilloscope (Tektronix R 556). For a more detailed description of the technique see section 3.4-3.

The high pressure cell was maintained at constant temperature by thermal contact via He^4 exchange gas to a liquid helium bath at 4.15k. The data of Vignos and Fairbank (1966) was extrapolated to 4.15k using a quadratic fit to their data at from .5k to 4k. Then a correction of + 1% was added to account for a systematic error noted by Wanner (thesis, 1970) and Abraham et al (1970). Using these values in the region of overlap, a value for the distance was determined.

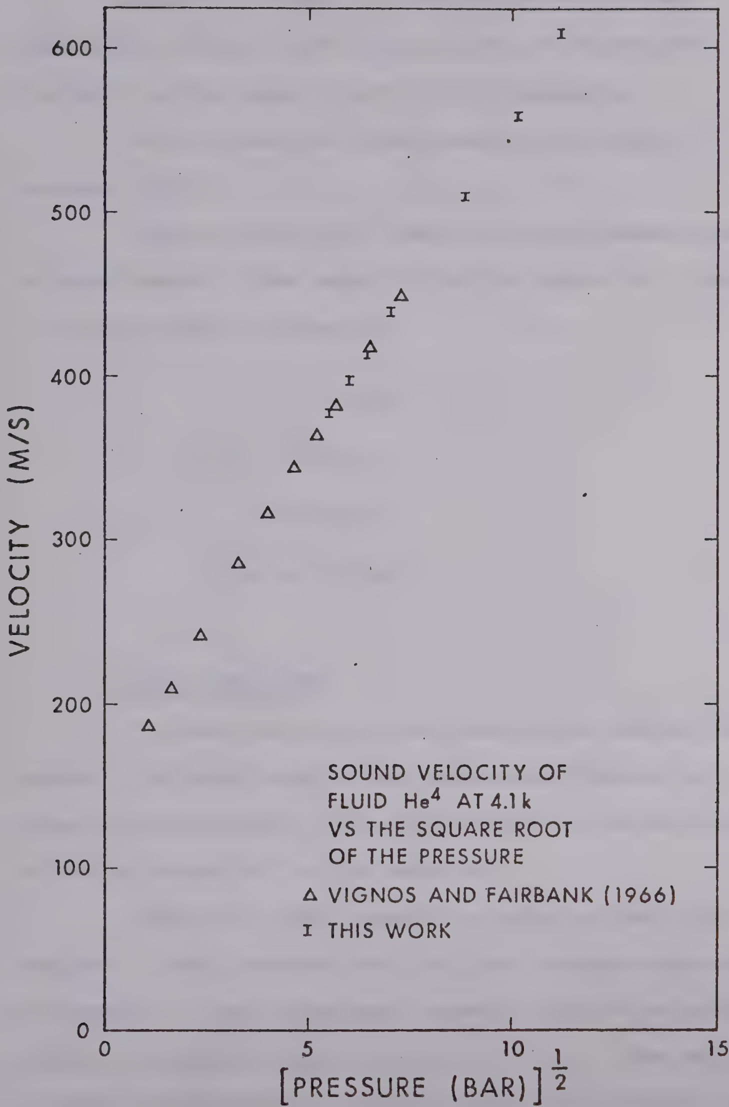

FIGURE 15 Velocity versus the square root of the pressure in fluid He^4.

Figure 15 shows the resulting calculated velocities plotted with the results of Vignos and Fairbank vs the square root of the pressure.

Notice that the relationship is roughly a straight line.

Table 1 lists the results of the present series of experiments. The best fit of the velocity V(m/s) to the pressure P (bar) is

$$V = A_0 + A_1 P^{\frac{1}{2}} + A_2 P$$

$$A_0 = 138.663$$

$$A_1 = 47.2186$$

$$A_2 = -0.472669$$

4.2 The Echo Envelope

The echo pattern in an absorptive medium with properly adjusted mirror and transducer should be decaying exponential. The decay rate is an indication of the attenuation in the material.

Figure 16 (top) shows the echo pattern for acetone in our pressure cell at room temperature after alignment at one atmosphere pressure with a separation between transducer and mirror of 1.46 cm. The velocity at these temperatures is about 1200 m/s and the pulse can be seen for about 3ms.

TABLE 1

Pressure (Bar)	Velocity (m/s) ± 1%
130.6	615.25
100.0	561.37
99.7	559.35
77.1	511.67
47.6	439.74
47.2	439.58
39.7	415.39
39.6	413.97
34.1	397.11
34.0	396.97
28.8	377.72

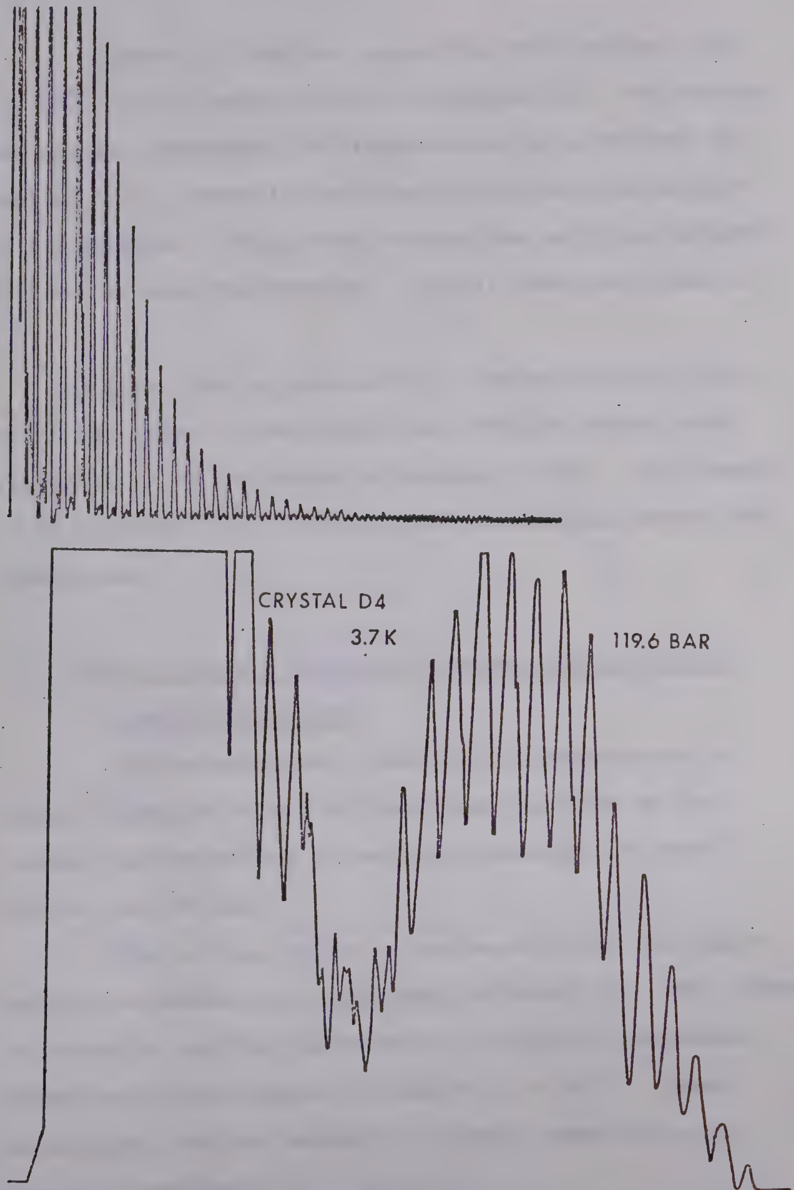

FIGURE 16 Echo Evelope: at upper for acetone at room temperature, and below for He^4 solid at 3.7k.

Figure 16 (bottom) shows the echo pattern for hcp He^4 at 3.7k and 120 bar for crystal D4. The maxima and minima correspond to interference as predicted in section 2.8. There is not complete extinction because of attenuation. Thus, even though the cell was properly aligned at room temperature, the cell was unaligned at 3.7k.

Error due to curvature of the mirror will only be of the order of seconds of arc whereas actual misalignment is of the order of minutes of arc. At present it is presumed that differential contraction causes the misalignment.

4.3 Velocity as a Function of Temperature in Single Crystals of hcp He^4

The velocity as a function of temperature in single crystals of hcp He^4 has been measured at two volumes corresponding to melting pressures of about 120 bar and 86 bar.

The initial velocity was measured by the pulse reflection method to an accuracy of about 3%. The change in velocity was then measured by the phase comparison technique to an accuracy of about 2×10^{-4}. These techniques, and the method of crystal growth are outlined in sections 3.4-3 and 3.1-3.

Figures 17 to 26 are graphs on 10 of the 12 crystals measured. The relative velocity is plotted

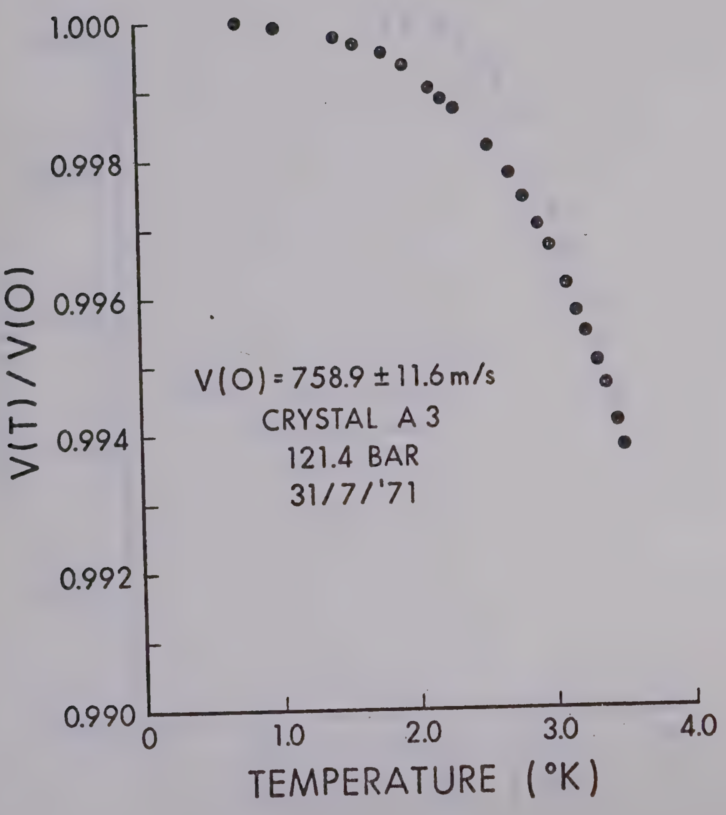

FIGURE 17 Relative velocity change versus temperature

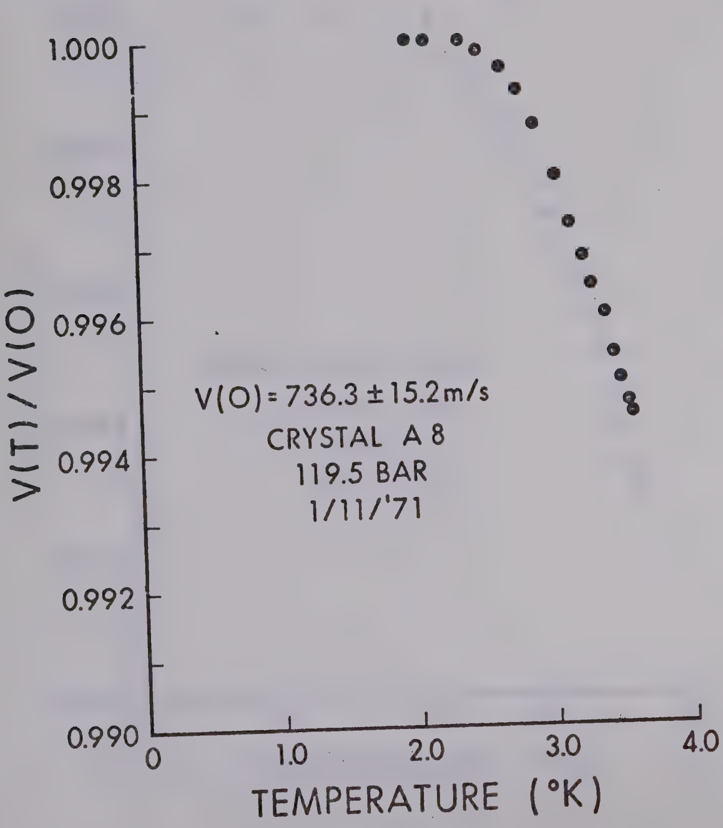

FIGURE 18 Relative velocity change versus temperature

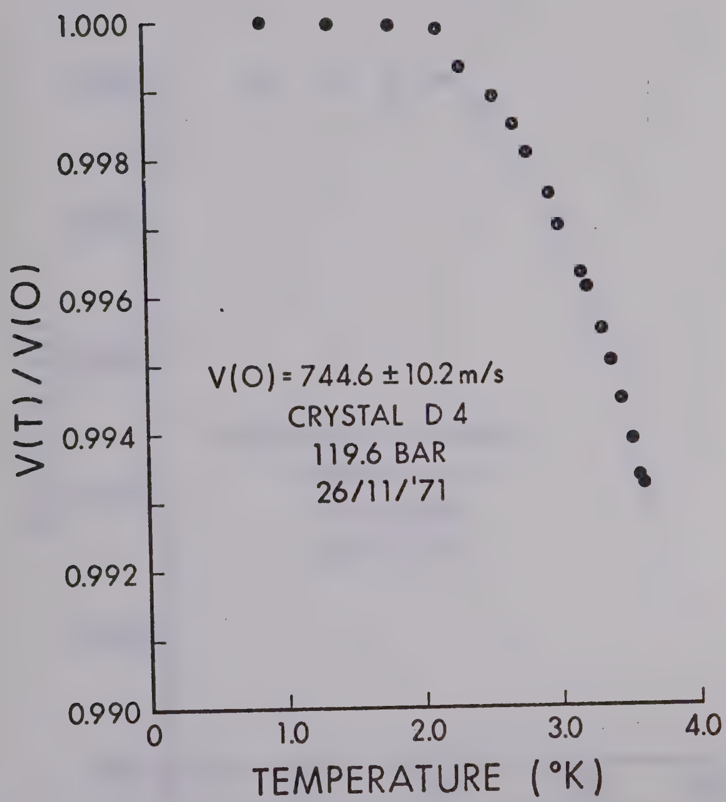

FIGURE 19 Relative velocity change versus temperature

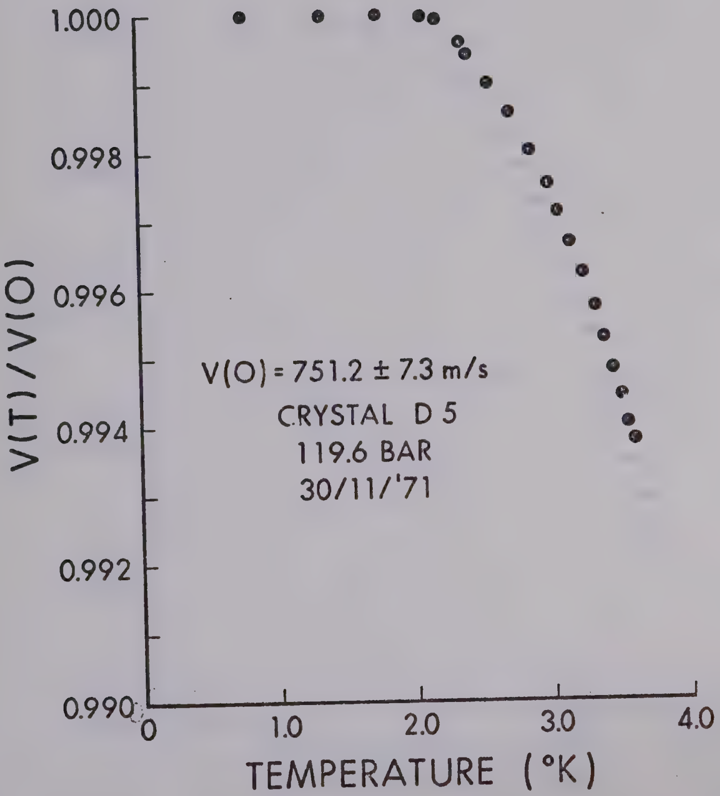

FIGURE 20 Relative velocity change versus temperature

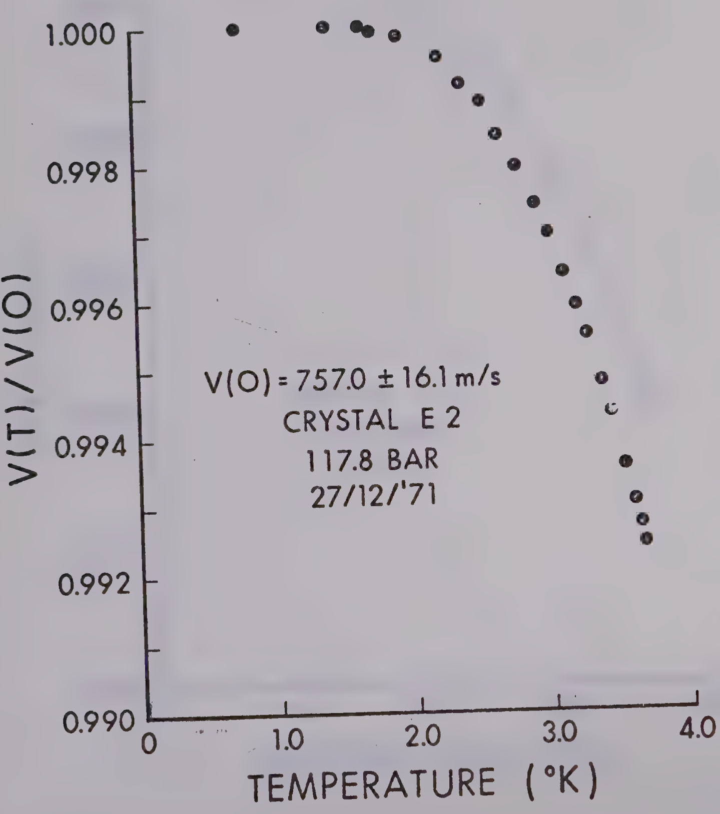

FIGURE 21 Relative velocity change versus temperature

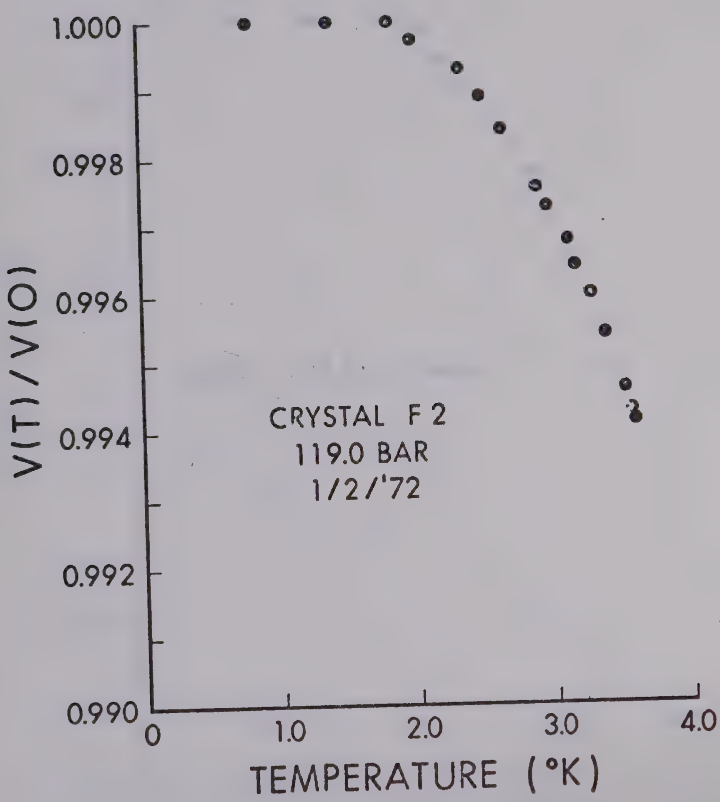

FIGURE 22 Relative velocity change versus temperature

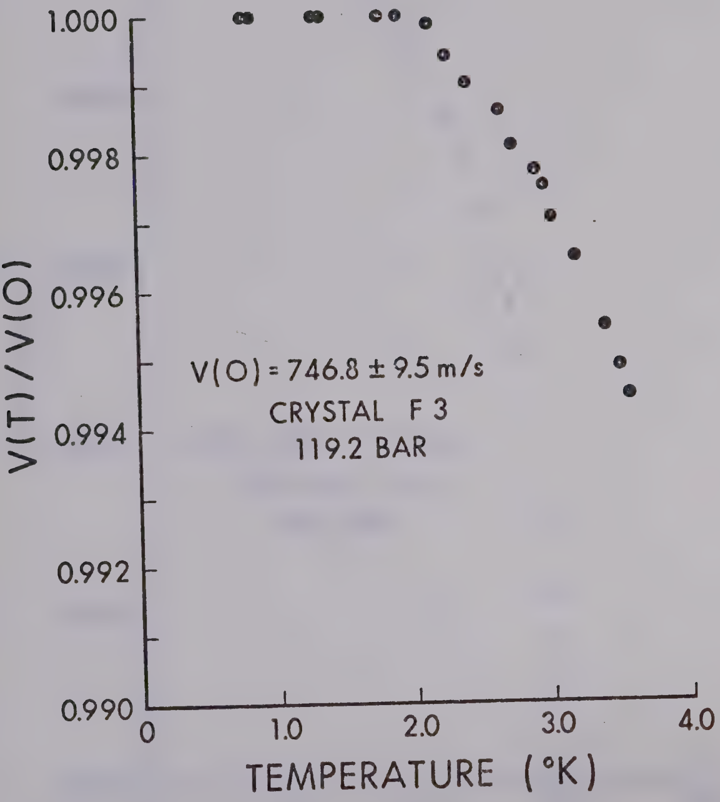

FIGURE 23 Relative velocity change versus temperature

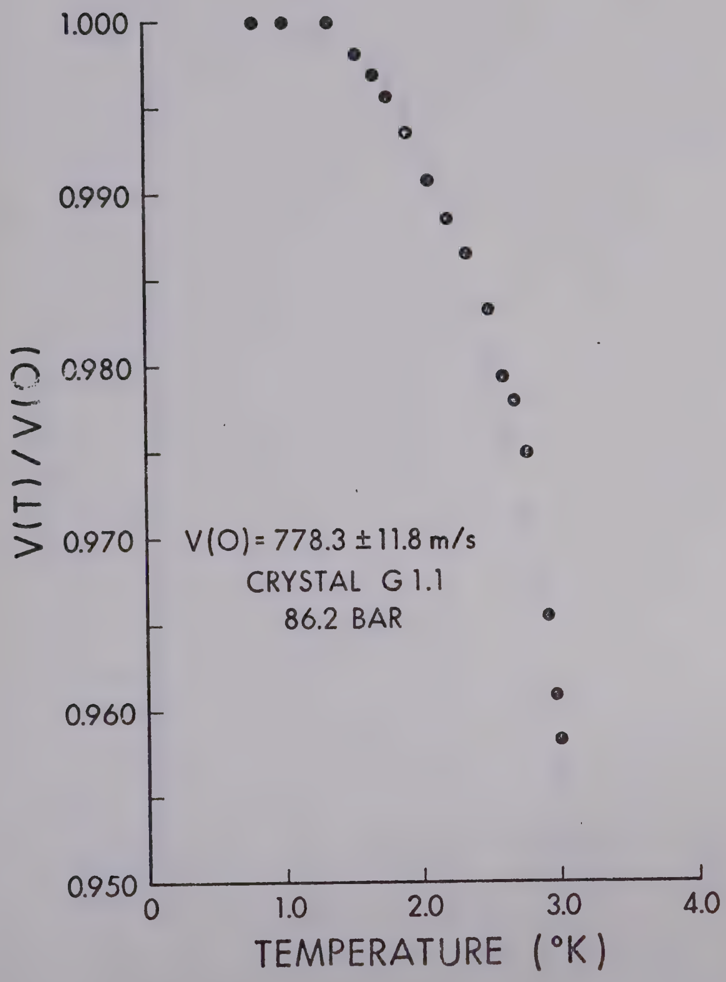

FIGURE 24 Relative velocity change versus temperature

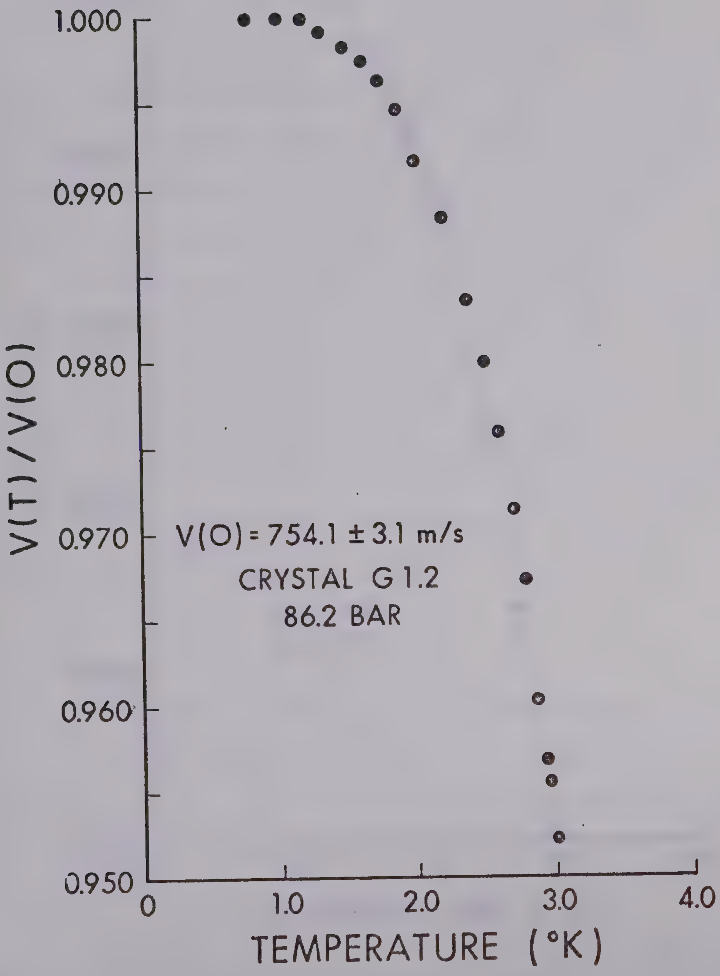

FIGURE 25 Relative velocity change versus temperature

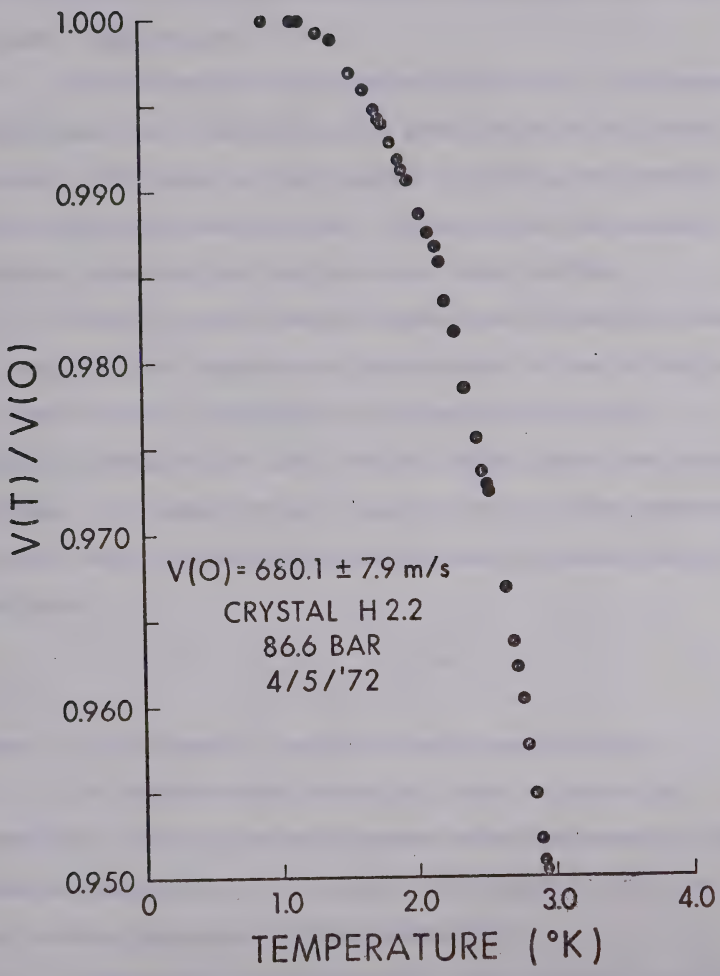

FIGURE 26 Relative velocity change versus temperature

against the absolute temperature. The relative velocity is the actual velocity divided by the velocity at the coldest temperature.

The crystals are numbered such that a different letter implies a recyclying to room temperature. Thus crystal E2 would be the second crystal grown during a specific cool down period. F2 would be the second crystal grown during the next cool down period.

Most of the crystals grown show an abrupt change in slope in the temperature dependence of the velocity at about 2k for crystals at 120 bar and at 1k for crystals grown at 86 bar. We call this point the anomaly or knee. At temperatures higher than T_c (the temperature of the knee) the velocity roughly obeys a power law of the form

$$V = V(0) - AT^n$$

where n is about 4 (as predicted classically).

At temperatures below T_c the velocity is constant. Not all crystals grown show the anomaly (for example, crystal A3). However, the crystals with the most echoes appeared to have anomalies.

Comparison of our results with various theories will be given in the next section. Complete data on our crystals are tabulated in the appendix.

It was a possibility that the knee was caused by some defect in the measuring apparatus. That is, the

reason the velocity remained constant was because the temperature of the crystal was not changing.

Firstly, it should be noted that the pulse height (that is, the attenuation) did not reach an extrema until .1k or .2k lower than the anomaly. This is evidence of the temperature changing after the anomaly. Secondly, the crystals grown at lower pressures have the anomaly shifted to about 1k. It thus appears that the cryostat does achieve temperatures in the crystal lower than the anomaly.

It was also possible that our sound beam was heating the crystal to the point of making the temperature roughly constant. This heating, in general, would depend on the conductivity of the crystal and thus might be in a different spot for different melting pressures.

The sound beam was 140 V_{rms} for 300 μs per second and at a steady current of about 2 mA for a duty cycle of 80 μ watts. At 120 bar the thermal conductivity at 1k is about 10 watts/cm°k and at 2k is about 0.1 watts/cm°k. In our cell there would be created a temperature gradient of about 1 mk at 2k and 10^{-2} mk at 1k.

To make sure heating from the ultrasonics was not a problem, an experiment was done with the duty cycle reduced by 100 (figure 27). The two curves are essentially identical.

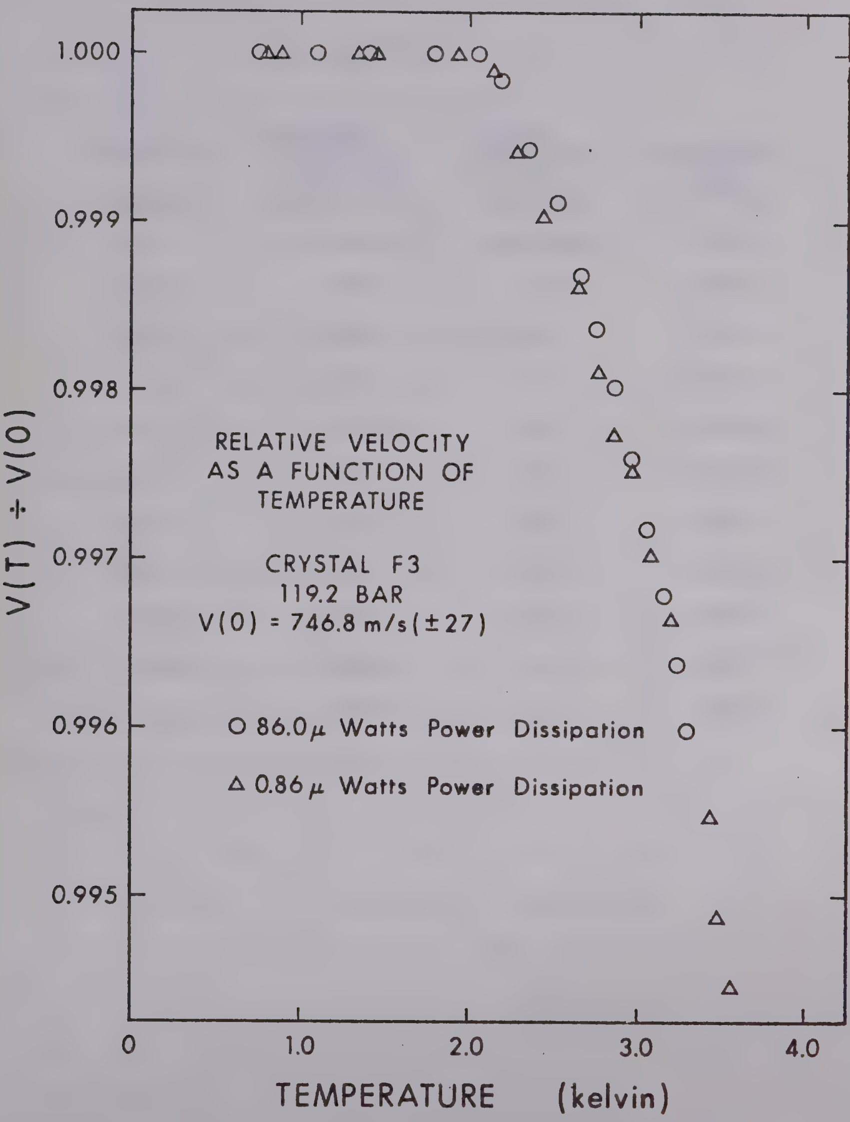

FIGURE 27 Relative velocity as a function of temperature for crystal F3 at two different ultrasonic input powers.

TABLE 2

Crystal	Absolute Velocity (m/s ± 3%)	Knee Position (± .1k)	Pressure (Bar)
A3	758.9	no knee	121.4
A8	736.3	2.3	119.5
D3	755.0	2.8	119.2
D4	745.0	2.1	119.6
D5	751.0	2.3	119.6
E2	757.0	1.9	119.8
F2	717.0	1.8	119.0
F3	747.0	2.1	119.2
G1.2	778.0	1.2	86.2
H2.2	680.0	1.1	86.6
I2	669.0	1.1	86.4

This experiment was done on crystal F3 about 5 days apart. Annealing might account for the slight difference between the two crystals at $T \geq T_c$.

A factor in favour of the effect being real is that A3 does not show the knee. Further there is large variation in the knee position as illustrated in table 2.

4.4 Observations of the Attenuation

To my knowledge, there is only one mention of the attenuation in an ultrasonic experiment (Vignos and Fairbank (1966)) in which an upper limit was placed on the attenuation of order .3 to .7 cm^{-1} at 10 MHz over their measurements in the solid from 1 to 150 bar.

No accurate measurements of the attenuation could be made on our system due to several factors. The fact that the transducer and mirror were slightly misaligned caused disruptions in the echo envelope. It was also observed that two neighboring echoes would vary in size making the second larger than the first (or vice-versa) as a function of temperature. Also, a general deterioration of pulse shape consistently occurred at low temperatures (but pulse shape was recoverable when the crystal was returned to higher temperatures).

One of our crystals (crystal A8) had very small misalignment as well as a large number of echoes (140). If we blindly apply a least square fit of the

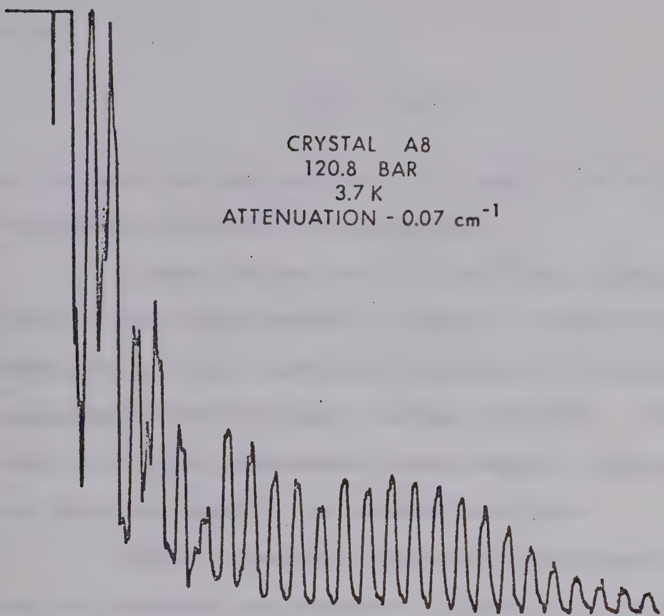

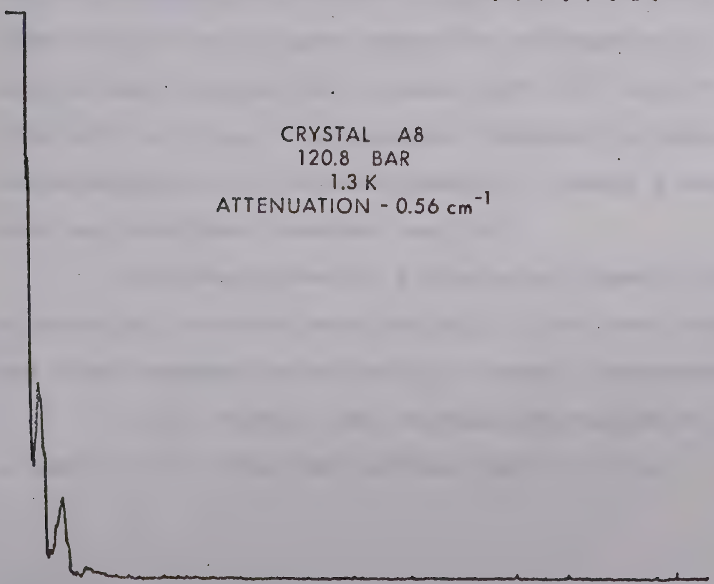

FIGURE 28 Echo Pattern for crystal A8 at two temperatures.

form

$$f(x) = Be^{-Ax}$$

to the echo pattern we can get a rough idea of the attenuation and how it is changing.

Crystal A8 was one of the first crystals in which a knee was observed. However, as this result was unexpected, proper care was not taken in the velocity measurement and systematic errors occurred. There was left a fine integrated pulse record, fortunately, and that was used in the present analysis.

Table 3 shows the values of the attenuation at the two temperatures measured (figure 27). If we view these figures as an upper bound, the attenuation at 5 MHz and 120 bar in solid He^4 is about 0.07 cm^{-1} at 3.7k and 0.56 cm^{-1} at 1.3k. This apparent increase in attenuation was observed in all crystals except D5 (where a small peak may have been observed near 1k).

In crystals showing a pronounced anomaly, the attenuation increased very rapidly in the knee region, and then increased more slowly to lowest temperatures.

In all crystals the attenuation changed by about a factor of 3-7 from the melting point to .75k.

TABLE 3

T	Crystal	Attenuation	Echoes
3.7k	A8	.068	23
1.3k	A8	.56	4

CHAPTER 5

COMPARISON OF RESULTS TO THEORIES

5.1 Sound Velocity in the Fluid

In section 4.1 we showed experimental results giving a pressure "P" dependence for the velocity "W" of

$$W \propto P^{\frac{1}{2}} \quad . \qquad (5.1\text{-}1)$$

In a corresponding states treatment we can write for He^4

$$W^2 = \gamma_o \frac{RT}{M} \{1+F^*P^*+G^*P^{*2}+H^*P^{*3}+\ldots\} \quad . \qquad (5.1\text{-}2)$$

where $P^* = \frac{P}{P_o} = \sigma^3 P/\varepsilon$ for Lennard-Jones Potential of type

$$V^{(r)} = 4\varepsilon[(\sigma/r)^{12} - (\sigma/r)^6] \qquad (5.1\text{-}3)$$

For He^4 it has been determined from second virial coefficient data (Hirschfelder et al (1954)) that

$$P_o = 87.4 \frac{kg}{cm^2} = 89.1 \text{ BAR} \quad .$$

In the limit of $P^* = 0$ we should get a value for γ_o that is about $\frac{5}{3}$ (normal for monotonic gases).

$$\gamma_o = \frac{MW^2(0)}{RT} = \frac{(147)^2 4}{83 \times 4} = 2.6 \quad .$$

This particular treatment also assumes that P^* is small. In our case $P^* \sim 1$ and as the value of γ_o is not correct, this simple picture must be abandoned. De Boes and Lunbeck (1948) introduced corrections for quantum behavior by introducing an extra expansion in the quantum parameter $\Lambda^* = \frac{h}{\sigma\sqrt{m\varepsilon}} = 2.64$ for He^4. Because Λ^* is greater than one, this expansion is invalid in our case.

In a similar fashion, all the simple theories which I have examined dealing with dense fluids, including the above and the solid sphere available volume theories, give bad results in either the PVT relation or in the pressure dependence of the velocities. The theories in general predict higher powers in the 'P' dependence of the velocity (like P^3 in the Carnevale and Litovity (1955) theory) as well as much smaller changes in velocity with P than observed.

From the above, I conclude that a proper understanding of the velocity dependence in fluid He^4 under pressure will depend on the development of a more exact theoretical treatment which takes into account quantum effects including short and long range correlations.

5.2 Theoretical Treatment of Velocity Results

5.2.1 Introduction

Figures 17 through 26 show the typical behavior

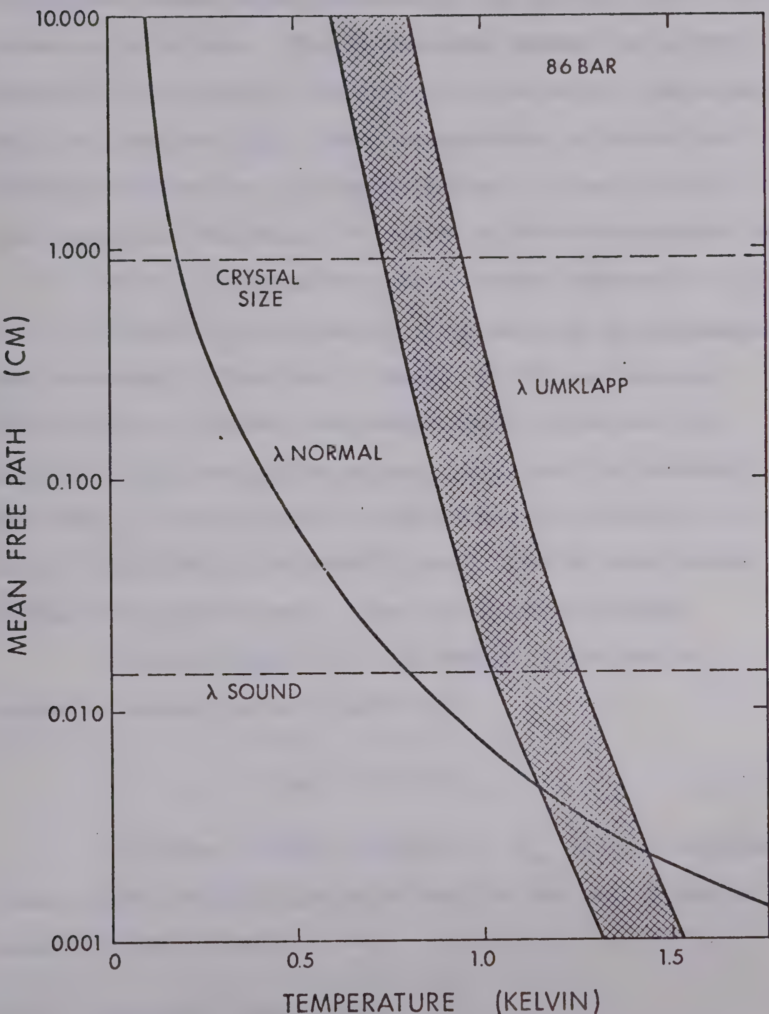

FIGURE 29 Mean free paths at 86 bar from Hogan et al (1969).

of the relative change in velocity. We will first try to explain those crystals showing the anomaly and then those which do not. The temperature where the abrupt change in the rate of change of the velocity (the knee) will be labelled T_c. This temperature, although not clearly defined due to discrepancies in the velocity in the region of the knee, is called T_c for convenience only.

We will examine the data in two regions $T > T_c$ and $T < T_c$. Above T_c, the velocity appears to be adiabatic and reasonably classical. Where $T \lesssim T_c$ we believe that coupling between the temperature field and the lattice field are taking place. One could alternately say that, in this region, temperature differences are being equalized by coherent propagation of heat waves, rather than diffusively, that is by second sound.

Notice figure 29. The second sound region normally occurs for a T such that

$$\Omega\tau_N << 1 << \Omega\tau_u \; .$$

The knee occurs roughly at $\Omega\tau_u \simeq 1$ an indication that second sound propagation may be the key to understanding the anomaly.

5.2.2 <u>Velocity Change When</u> $T > T_c$

Sections 2.5 and 2.6 give detailed theories for classical behavior of a solid. Briefly, I will mention their basic conclusions.

Classical theories all state that at high enough temperatures (or low enough frequencies) all sound motion will be adiabatic. Whenever a longitudinal wave is excited it produces compressions and rarefactions which in turn produce temperature gradients along the path of propagation.

For example, a fluid with cross-section A to the normal of wave propagation, has, say, created a temperature gradient ΔT. Then the amount of heat Q_1 flowing across a cross-section in the time the wave travels $\lambda/2$ is

$$Q_1 = \kappa \times \frac{2\Delta T}{\lambda} \times A \times \frac{\lambda}{2V} \approx \frac{A\kappa\Delta T}{V}$$

Now the amount of heat required to equalize the temperature is Q_2

$$Q_2 = \frac{A\lambda}{2} \times \frac{c_p}{V_m} \times \frac{1}{2}\,\Delta T \approx \frac{A\,c_p\lambda\Delta T}{4V_m} \qquad (5.2\text{-}2)$$

where κ is the thermal conductivity;

c_p is the heat capacity at constant pressure;

V_m is the molar volume;

V_D is the Debye velocity.

Thus if $\omega << \frac{1}{4}\,\frac{c_p V^2}{V_m \kappa}$ the propagation will be adiabatic as opposed to isothermal.

Now

$$\kappa \approx \frac{1}{3}\,\frac{V_D^2\,\tau_u c_V}{V_m} \qquad (5.2.3)$$

or

$$\omega\tau_u << \frac{3}{4}\frac{V^2}{V_D^2}\ \frac{c_P}{c_V} \sim 1 \quad . \tag{5.2-4}$$

From thermal conductivity data we know that

$\omega\tau_u = 1$ at 1.1k to 1.5k for 5MHz at 86 bar

and 1.3k to 1.7k for 5MHz at 120 bar.

Figure 28 shows mean free paths at 86 bar. Thus for $T > 1.7k$ we should have adiabatic propagation.

$$V^2(T) = V_T^2(T) + \alpha(T)\left(\frac{c_P}{c_V} - 1\right) N(T) \quad . \tag{5.2-5}$$

Writing the velocity in the form discussed in section 2 we recall that V(T) is adiabatic for N(T) = 1 for all theories. To get an idea of the form of V(T) lets recall equation (2.5-12)

$$\frac{1}{K_S(T)} - \frac{1}{K_S(0)} = [U-U_o]\left\{\frac{\gamma}{V} + \frac{\gamma^2}{V} - \frac{\partial\gamma}{\partial V}\right\}$$

all velocity measurements are made at constant volume so that

$$U-U_o = \int_o^T C_v dT \;\alpha\; T^4 \quad \text{for a Debye solid} .$$

If we assume that γ is roughly constant in temperature we can write the adiabatic velocity as

$$v_a^2 \cong A + BT^4 \quad .$$

Further, for a Debye solid, the isothermal velocity

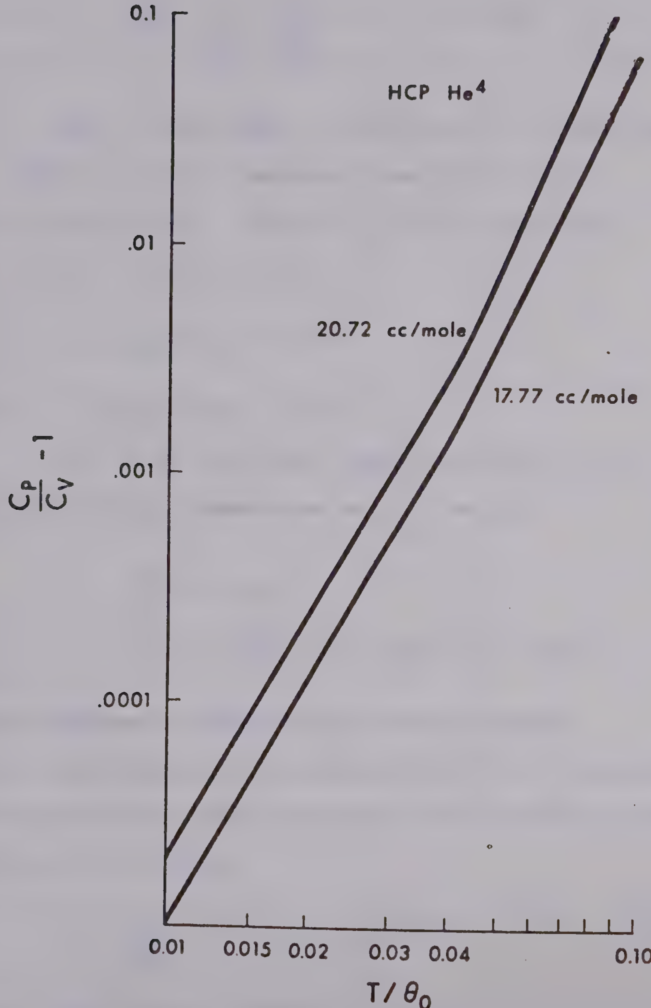

FIGURE 30 Experimental for $(c_p/c_v - 1)$ according to Jarvis et al (1968) from $(\partial P/\partial T)_v$ measurements.

$$v_T^2 \cong \frac{v_a}{\text{const} \times (\frac{c_p}{c_V} - 1)} \approx A + BT^4 \; .$$

Now, as was shown in section 2.5, helium does not appear to obey a reduced equation of state for the velocities. However, it was determined that in the region $T > T_c$,

$$v_T(T) \propto A + BT^n$$

where n varies from 3.5 to 4.5.

If, as in the Debye model, we give v_T, v_a, the same temperature dependence as $\frac{c_p}{c_V}$ we get

$$v_T^2 = A + BT^n$$

$$v_a^2 = v_T^2 \; (\frac{c_p}{c_V} - 1) \text{ const} = c + DT^n$$

as the temperature dependent terms are small.

Now figure 30 illustrates $(\frac{c_p}{c_V} - 1)$ according to Jarvis et al (1968). One can fit these data to an equation of the form

$$(\frac{c_p}{c_V} - 1) = B(\theta) \; T^{n(\theta)} \tag{5.3-8}$$

where $n(\theta) = 5.56 - .0467 \; \theta_D$

and θ_D is the Debye Theta

$n = 3.8$ at 86 bar

$n = 3.6$ at 120 bar.

Figure 31 shows a fit with the theory of Niklasson to crystal I2 using the value of n from equation (5.3-8). Although this is a three parameter fit - two parameters to fit v and one to fit the knee - the relaxation τ' is of significant importance in the region of the knee only. All the other parameters, except A and B in the adiabatic velocity, are experimentally determined. The parameter A is essentially normalized to unity by dividing by the isothermal velocity. Thus, we have, in reality, a one parameter fit. It is interesting to note that $N(T)$ is within 1% of unity for the region $T > 1.5k$. I think this is sufficient evidence to state that the velocity above the knee is adiabatic.

It is interesting to note that the $(\partial P/\partial T)_v$ data of Jarvis et al (1968) shows a change in the power of the temperature change at about $T/\theta \sim .04$. This change in power is reflected in their $(c_p/c_v - 1)$ results giving rise to a small kink in the curves. The reason for this behavior is not known at present.

5.2.3 Velocity Change in the Region $T \sim T_c$ - Classical Theory

The velocity change relative to the isothermal velocity in a classical model can be put in the form

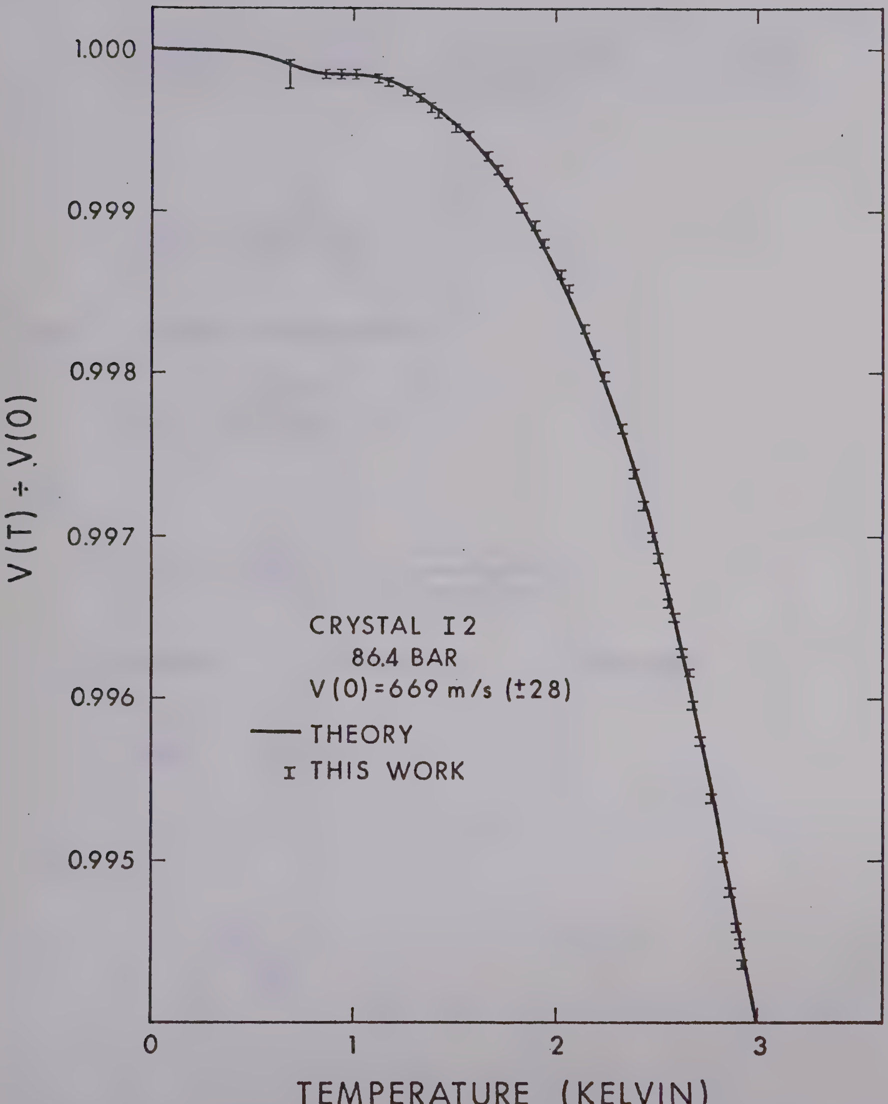

FIGURE 31 Relative velocity change as a function of temperature for crystal I2 illustrating accuracy of fit for $T > T_c$.

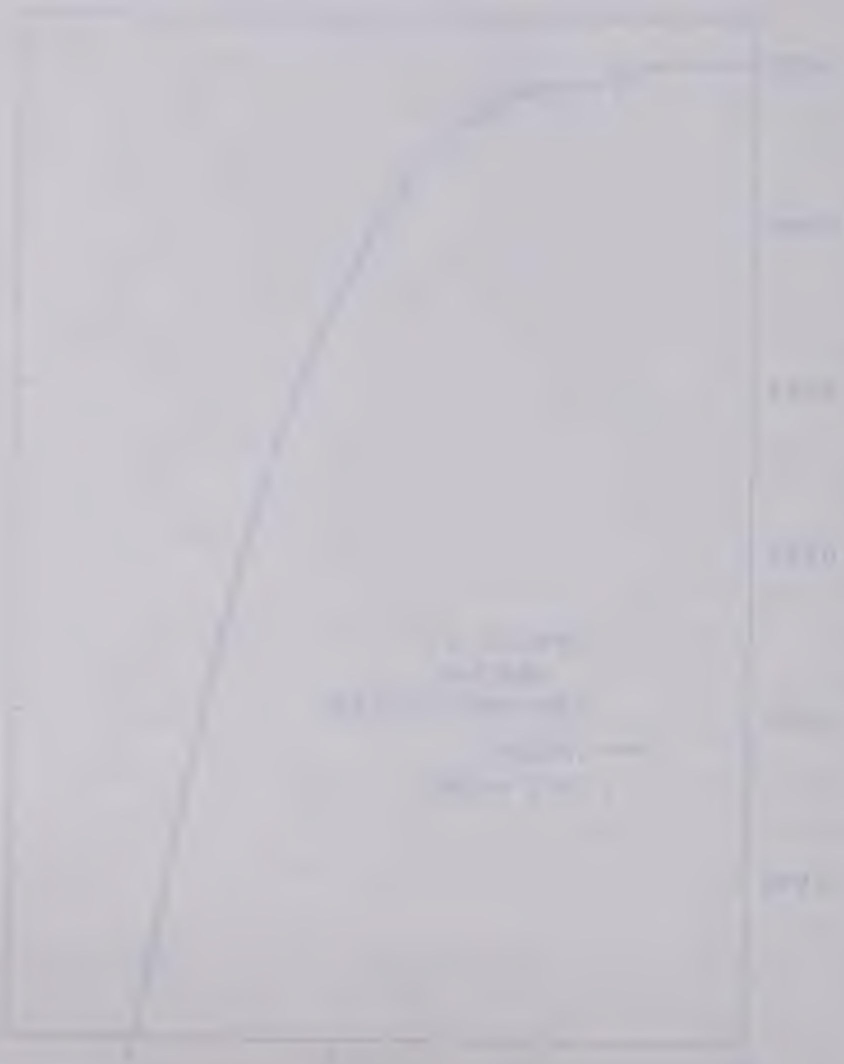

$$\frac{V^2(T)}{V_T^2(T)} = 1 + (\frac{c_P}{c_V} - 1) \frac{1}{K_T \rho V_T(T)^2} N(T) \qquad (5.2\text{-}9)$$

where

$$N(T) = \frac{\alpha f_\kappa^2}{f^2 + \alpha f_\kappa^2}$$

and f is the frequency and

$$f = \frac{c_V V^2(T)}{2\pi \kappa V_m}$$

and

$$\alpha = 1 + (\frac{c_P}{c_V} - 1) \frac{1}{K_T(T) \rho V_T^2(T)} .$$

To first order α in $N(T)$ is $\alpha \sim 1$ and hence

$$N(T) \sim \frac{f_\kappa^2}{f^2 + f^2} .$$

Now for $T > T_c$

$$\kappa \sim \frac{1}{3} \frac{V_D^2 \, u c_V}{V_m}$$

or

$$f_\kappa = \frac{1}{6\pi} \frac{V^2}{V_D^2} \tau_u^{-1}$$

For $T < T_c$, $\tau_u \to \tau_B$ the boundary scattering relaxation time. For our case τ_B is, of course a constant, roughly 10^{-5} sec.

f_κ in this region is

$$\frac{1}{6\pi}\frac{V^2}{V_D^2}\tau_B^{-1} .$$

Let

$$\tau_R = \frac{\tau_u\tau_B}{\tau_u + \tau_B} ;$$

thus

$$N(T) = \frac{\left(\frac{1}{\tau_R 2\pi}\right)^2}{f^2 + \left(\frac{1}{2\pi\tau_R}\right)^2}$$

as

$$\left(\frac{1}{3}\frac{V^2}{V_D^2}\right) \sim 1 .$$

Thus for $T \to 0$, $N(T) \to (1/\tau_R 2\pi)^2 \approx 10^{-22}$ for our case

$T \to \infty$, $N(T) \to 1$ as $\tau_R, \tau_u \to 0$.

A rapid change should occur in N(T) about at

$$f \sim \frac{1}{2\pi\tau_u} \quad \text{or} \quad \omega\tau_u \sim 1 .$$

Figure 32 shows crystal D4 fit to the above classical equations. Although one sees a small plateau

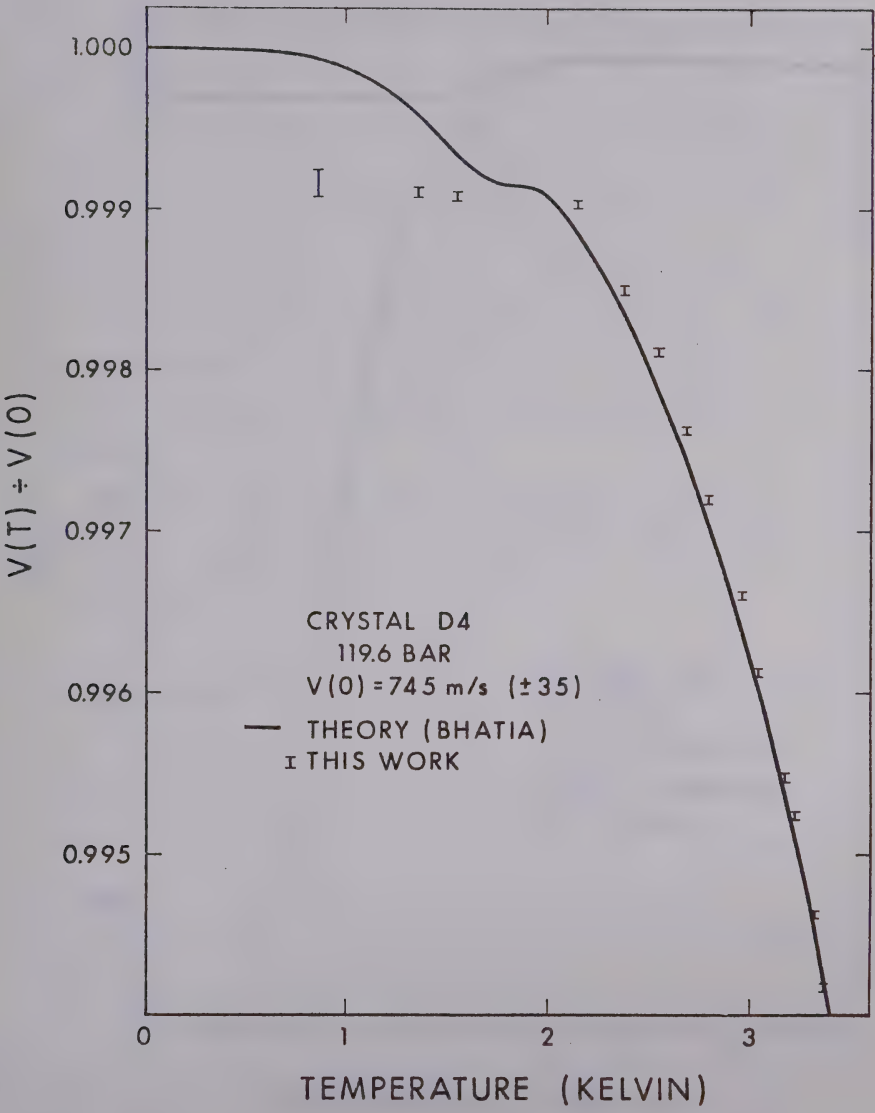

FIGURE 32 Relative change in velocity compared to classical theory (Bhatia (1967)).

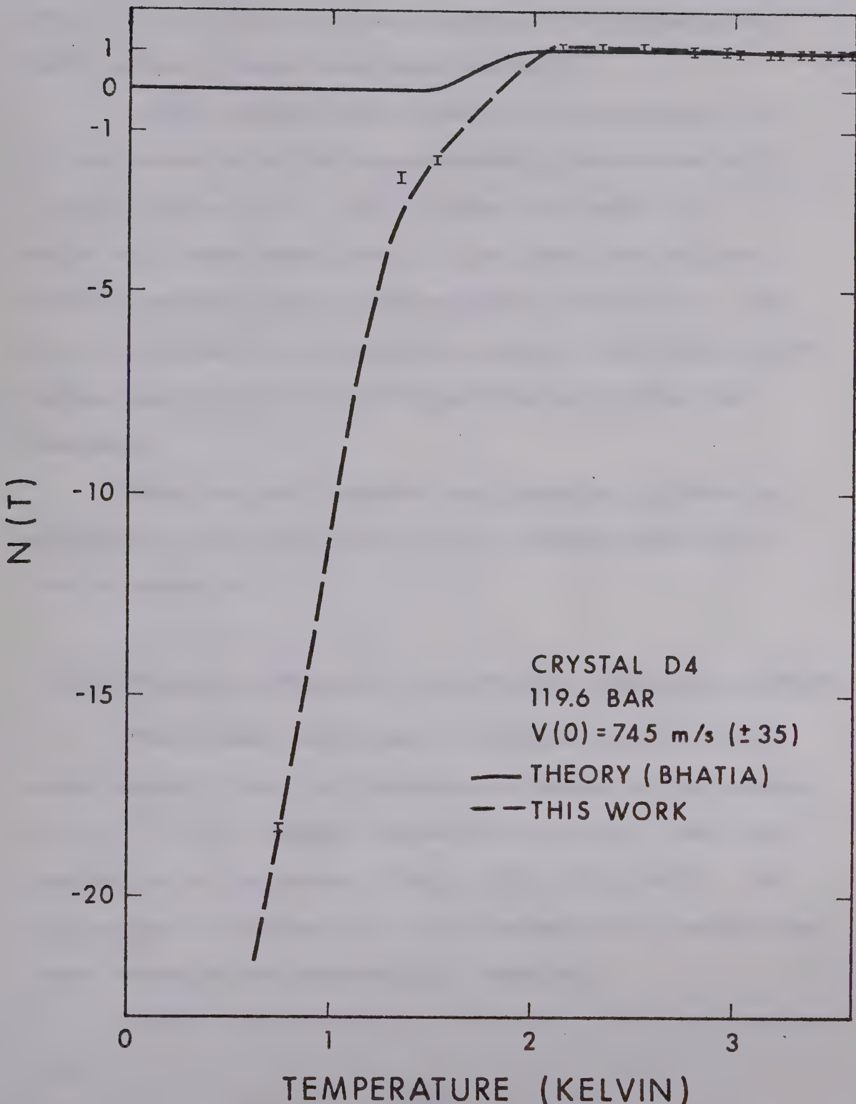

FIGURE 33 Factor N(T) for crystal D4 compared to classical theory (Bhatia (1967)).

at 1.7 K to 1.9 K, this is inadequate to explain the much larger plateau seen experimentally.

A more severe test would be to compare the N(T) of the theory with the experimentally determined $N_x(T)$ from the above fit. This is shown in figure 33. While N(T) goes from 0 to 1, $N_x(T)$ goes from -18 to 1. This is another sign of the weakness of the fit. This fit is typical of all crystals although the lowest $N_x(T)$ values vary from -36 to -8 depending on crystal and pressure.

Thus, we must abandon the classical picture in explaining our results and go to a theory where N(T) can go negative.

5.2.4 Velocity Change in the Isotropic Niklasson Picture

There have been several theories dealing with sound velocity and its temperature change in the region ($\omega\tau \ll 1 \ll \omega\tau_u$) notably (Gurevich and Efros, 1967) and the series by Niklasson (1968, 1969, 1970, 1971). In the region of interest for our frequencies of excitation, these theories are essentially identical.

Using the notation of Niklasson (1970) we have for N(T)

$$N(T) = \frac{(1-s^2)\omega^2 + 4\Gamma_2^o(Q)\Gamma_j^o(Q)}{(1-s^2)^2\omega^2 + 4[\Gamma_2^o(Q)]^2}$$

where s is the ratio of second sound to first sound.

$$s = \frac{c_{II}}{c_L}$$

Γ_2^o is the attenuation of second sound (with no coupling to lattice)

$$\Gamma_2^o = \frac{1}{2} \{\frac{1}{\tau_u} + s^2\omega^2[\tau^{oo} + \tau^{11}(Q)\}$$

$$\Gamma_j^o = \frac{1}{2} \{\frac{1}{\tau_u} + s^2\omega^2\tau^{11}(Q)\} - s^2\omega^2\tau^1(Q)$$

where τ^{oo}, τ'', and τ' are all relaxation times of the order of the total relaxation time τ

$$\tau = \left(\frac{1}{\tau_u} + \frac{1}{\tau_B} + \frac{1}{\tau_N}\right)^{-1}$$

For an isotropic crystal, Γ_j^o becomes

$$\Gamma_j^o = \frac{1}{2} \{\frac{1}{\tau_u} - s^2\omega^2\tau^{11}(Q)\}$$

as $|\vec{\tau}'(Q)| = \tau''(Q) = \tau''$ independent of Q, hence for

$$T \to \infty, \quad N(T) \to 1$$

$$T \to 0, \quad N(T) \to -\frac{\tau''}{\tau^{oo} + \tau''} \quad .$$

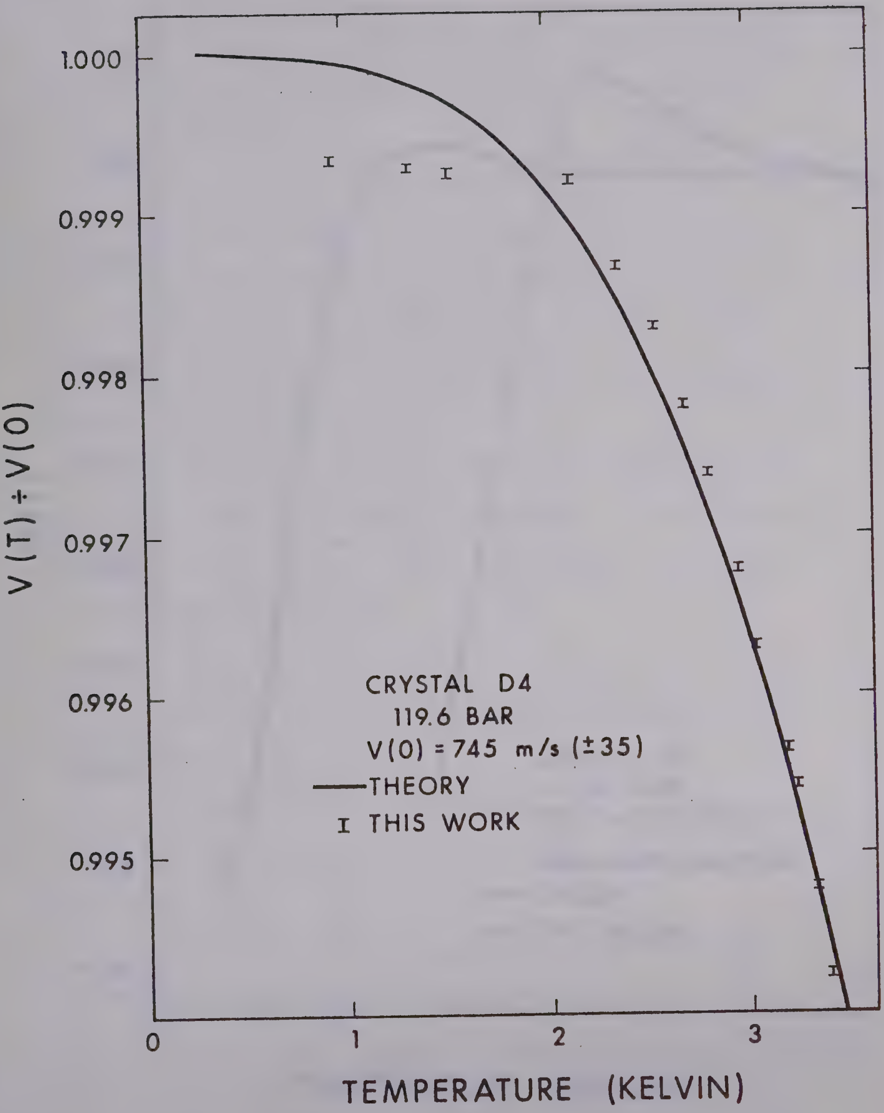

FIGURE 34 Relative change in velocity for crystal D4 compared to the isotropic theory of Niklasson (1970).

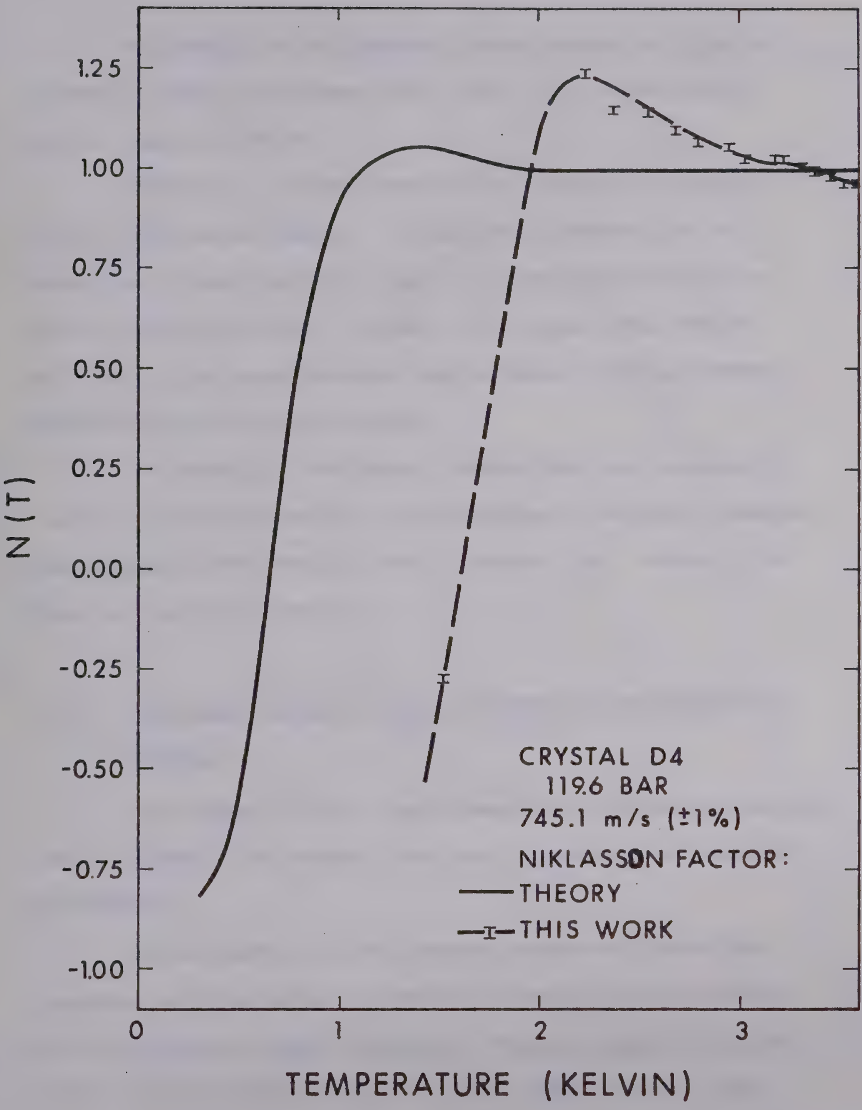

FIGURE 35 Factor N(T) compared to the isotropic theory of Niklasson (1970).

Although the Niklasson theory seems to give a slightly better agreement for N(T), it is obviously still unsatisfactory.

Figure 34 shows crystal D4 fitted to the isotropic Niklasson theory. A slightly better fit is possible if one varies τ_u and τ_N, however the fit is only slightly better. Figure 35 shows the factor N(T) with its experimental equivalent. The agreement here is qualitatively better.

In general, Niklasson theory for the isotropic case is insufficient for our purposes. We can, however, parameterize the theory for a better fit. We will do this in the next section.

5.2.5 Velocity Change with a Parameterized Niklasson Theory

Niklasson (1971) has attempted a parameterization of his theory for Argon, but our approach is somewhat different.

As we need N(T) to become large and negative, varying 's' the ratio of second sound to first sound, will only have a small effect. We must vary $\vec{\tau}'(Q)$ and $\tau''(Q)$. If we make $\vec{\tau}'(Q)$ 20 to 40 times larger than $\tau''(Q)$ we can get much better fits. Figure 36 shows

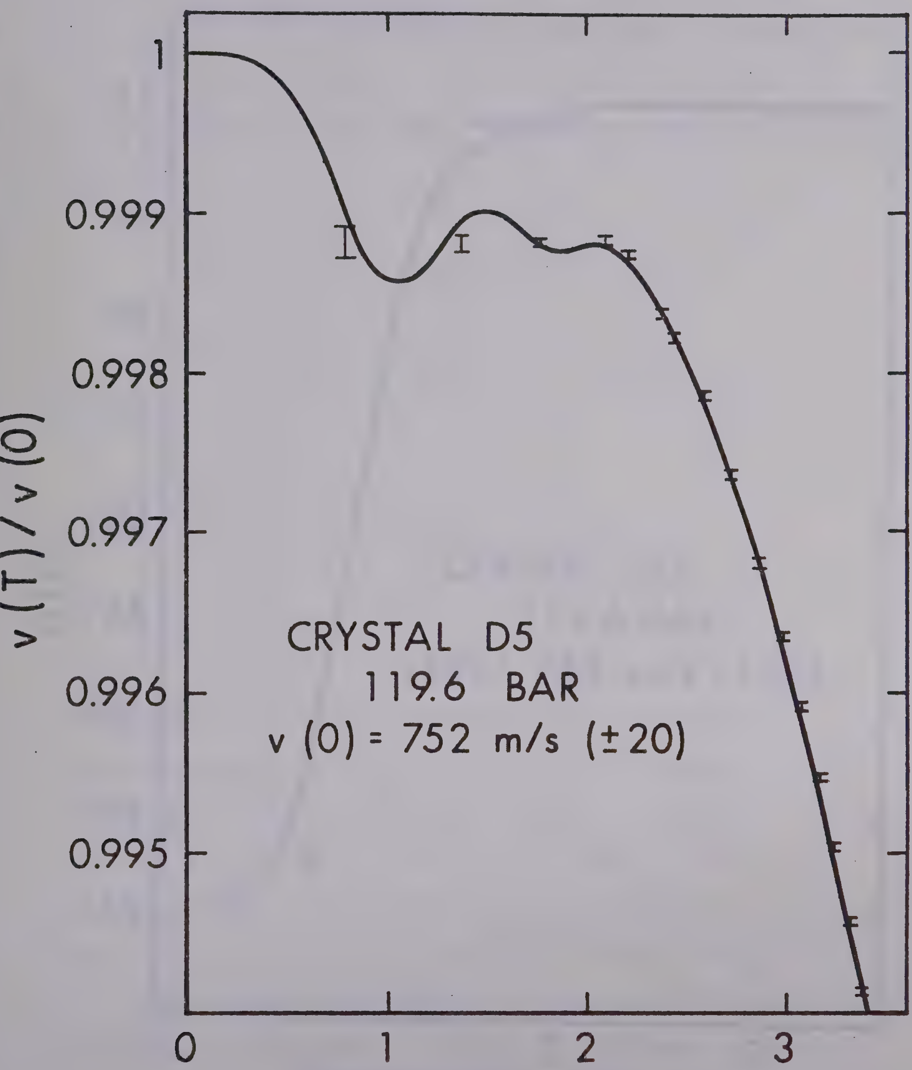

FIGURE 36 Relative velocity change for crystal D5 compared to the parameterized theory of Niklasson (1970).

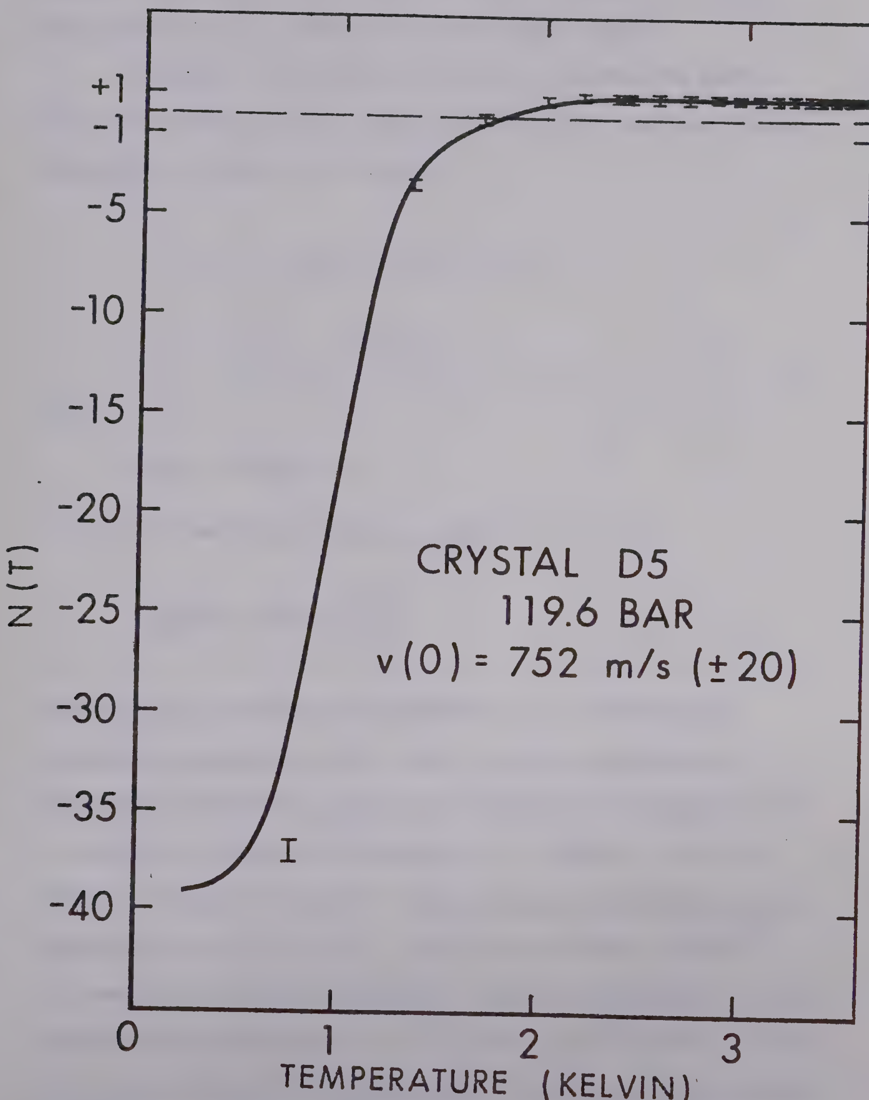

FIGURE 37 Factor N(T) for crystal D5 compared to the parameterized theory of Niklasson (1970).

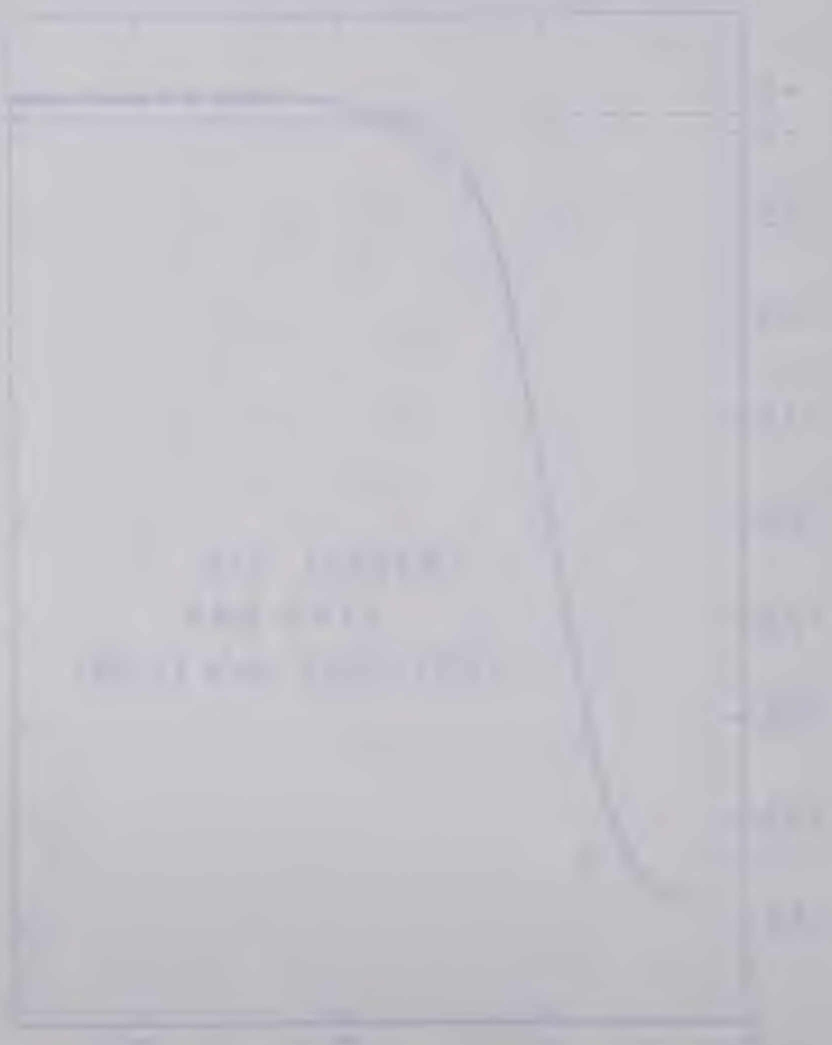

crystal D5 with $\vec{\tau}'(Q) = 23 \times \tau''(Q)$. Figure 37 shows the factor N(T). These fits are quite good.

However, is there a physical reason for such a wide variation in $\tau'(Q)$ and $\tau''(Q)$? Lets examine these relaxation times more closely.

$$\tau''(Q) = \frac{1}{Q^4} \sum_{\alpha\beta\gamma\delta} Q_\alpha Q_\beta Q_\gamma Q_\delta \tau''_{\alpha\beta\gamma\delta}$$

$$\tau'(Q) = \frac{1}{Q^3} \sum_{\beta\gamma\delta} Q_\beta Q_\gamma Q_\delta \tau'_{\alpha\beta\gamma\delta}$$

where

$$\tau''_{\alpha\beta\gamma\delta} = \tau'_{\alpha\beta\gamma\delta}$$

as long as we have a hcp or cubic crystal and

$$\gamma^{jj}_{\alpha\beta}(q) = 3\gamma(q) \frac{q_\alpha q_\beta}{q^2}$$

where $\gamma^{jj}_{\alpha\beta}$ is the branch dependent (j) microscopic gruneisen parameter and $\gamma(q)$ is the maroscopic gruneisen parameter. Now the temperature dependence of γ varies as much as 6%(Jarvis et al (1968)) and in a rather intricate fashion - thus there is probably some dependence on $|\vec{q}|$ of $\gamma^{jj}_{\alpha\beta}$. As the c/a ratio for He^4 is constant at most pressures, there is probably little orientation dependence in γ^{jj} (Franck and Wanner (1970)). The vector nature of $\tau'_\alpha(Q)$ will contribute to the variation in this parameter. Whereas $\tau''(Q)$ will be proportional

to some average τ - say $\tau_{isotropic}$, $\tau'_\alpha(Q)$ will be proportional to τ_α. Although τ_N is roughly isotropic in hcp He^4, τ_u varies by about 50 depending on orientation. There will also be an effect due to anisotropy of $\tau'_{\alpha\beta\gamma\delta}$ of the order of the variation in velocity - about 20%

$$\tau_\alpha = \frac{1}{Q^3} \sum_{\alpha\gamma\beta} Q_\beta Q_\gamma Q_\delta \tau^u_{\alpha\beta\gamma\delta} \quad .$$

As crystal D_4 was about 40° to the c-axis, and as τ_u is .5 τ_u^{iso} at this point, and as our weighting favors modes perpendicular to α,

$$\tau_u^\alpha \sim 2 \text{ to } 4 \text{ times } \tau_u^{iso} \quad .$$

These considerations seem to say that $\tau_\alpha^{11}(Q)$ will probably only be 5 times $\tau''(Q)$ at these orientations at the most.

Hence we must look elsewhere for this variation. If we examine the equation for the drift velocity

$$[-i\Omega + \frac{1}{\tau_u}]\, v_\alpha(Q,\Omega) + C_\Pi^2 \sum_{\beta\gamma\delta} \tau''_{\alpha\beta\gamma\delta} Q_\gamma Q_\delta V_\beta(Q,\Omega)$$

$$= \left(\frac{\langle\omega|\omega\rangle}{\langle q_x|q_x\rangle}\right)^{\frac{1}{2}} [\frac{-i}{T} C_\Pi Q_\alpha \bar{T}(Q,\Omega) + iC_\Pi \gamma\Omega \sum_{\beta\gamma\delta} \tau_{\alpha\beta\gamma\delta} Q_\gamma Q_\delta \langle u_\beta(Q,\Omega)\rangle].$$

It can be seen that τ'' represents the relaxation in the phonon drift velocity due to diffusion like processes, whereas τ' represents the relaxation due to coupling to the

lattice deformation.

Now, recall that helium is a quantum crystal. Small changes in the local lattice will produce changes in the local lattice constants which in turn will affect the phonon spectrum. These changes in the phonon spectrum, in general, will mean quite long range effects in the lattice due to the consequences of the self-consistent nature of the phonon field. One can thus view $C_{II}\tau'$ as a mean free path or coherence length which essentially gives the spatial dimensions of the effects of the local lattice deformation. It is not unreasonable to expect $C_{II}\tau'$ to be larger in quantum crystals than in ordinary crystals, which is what is observed.

We, therefore, believe that the large value of τ' necessary to fit our data is direct evidence of the quantum nature of the solid. Notice that the variation of no other parameter could possibly fit our data.

5.3 A Qualitative Description of the Attenuation

During measurements, the attenuation was indirectly observed through the change in amplitude of the pulse being observed. The following gives a qualitative description of our observations, and a comparison to the various theories.

At $T >> T_c$ we observed little attenuation (after seeing over 100 echoes), however when one neared T_c, a rapid increase in attenuation occurred. This peak in the

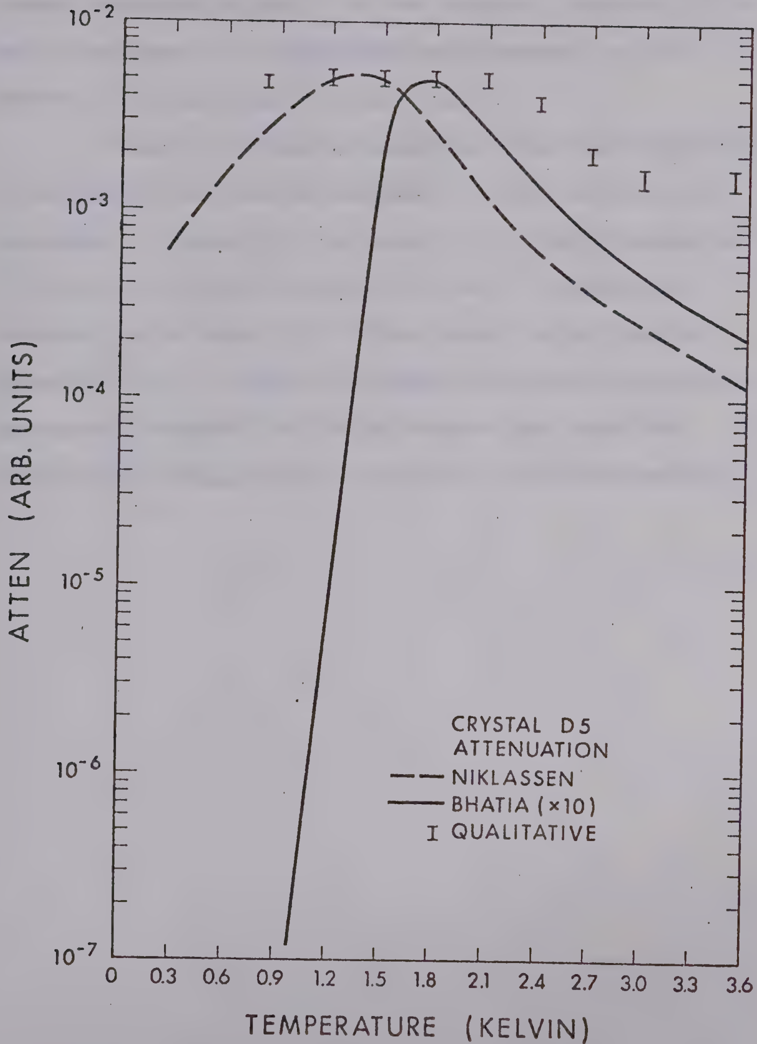

FIGURE 38 Qualitative comparison of experiment to theories of Niklasson (1970) and Bhatia (1967).

attenuation was very broad and increased steadily to our lowest measured values. On one crystal (crystal D5) a small decrease in attenuation was observed at 0.8k, however, the decrease was very small.

Figure 38 shows attenuation from the theories of Niklasson and Bhatia compared to our qualitative appraisal. Crystal D5 had about 70 visible echoes at 3.6k, and 20 visible echoes at 0.8k - a change in attenuation of about 3.5. The theory of Niklasson appears to be in better agreement with our qualitative estimates, however, our measurements are much too primitive at this point to make any firm statements.

CHAPTER 6

CONCLUSIONS

In single crystals of hcp He^4, the velocity change in temperature has a sharp "knee" or anomaly at $\frac{T}{\theta} \sim \frac{1}{20}$. This knee occurs where $\omega\tau_u \sim 1$. It can be explained in terms of a parameterized Niklasson theory if we assume the second sound resonance predicted by Niklasson is much broader than the theory predicts.

The high temperature region gives a good fit to the adiabatic velocity derived by Niklasson. The direction of change of velocity in this region ($T > T_c$) is decreasing for increasing temperature, lending support to the compressibilities calculated by Jarvis et al. (1968) over those calculated by Edwards et al (1965) calculated assuming a reduced equation of state.

The attenuation shows qualitative agreement with Niklassson's parameterized theory, however, only rough qualitative data are available for analysis.

Further work is necessary to determine the fine structure in the velocity plateau, as well as low temperature measurements to determine the value of the velocity in the zero sound limit. Measurements of the attenuation is necessary to determine which of several theories is more accurate.

BIBLIOGRAPHY

Abraham, B.M., Eckstein, Y., Ketterson, J.B., Kuchnir, M., Roach, P.R., Phys. Rev. A1, 250 (1970).

Ackerman, C.C., Thesis, Duke University (1967).

Ahlers, G., Phys. Rev. A2, (1970).

Alers, G.A., Physical Acoustics, W.P. Mason edit., Vol. IIIB, p.1, Academic Press, N.Y. (1965).

Bernades, N., Phys. Rev. 120, 1927 (1960).

Bhatia, A.B., Ultrasonic Absorption, Clarendon Press, Oxford (1967).

Blinick, J.S., Maris, H.J., Phys. Rev. B2, 2139 (1970).

Boccara, N. and Sarma, G., Physics 1, 219 (1965).

Brueckner, K.A., The Many Body Problem, Wiley, N.Y. (1959).

Carnevale, E.H. Litovitz, T.A., 1955, J. Acoust. Soc. Am. 27, 547.

Choquard, P., The Anharmonic Crystal, Benjamin, N.Y. (1967).

Crepeau, R.H., Heybey, O., Lee, D.M., Strauss, S.A., Phys. Rev. A3, 1162 (1971).

de Boer, J. and Lunbeck, R.J., (1948), Physica, 14, 520.

de Wette, R.W. and Nijboer, B.R.A., Physics Letters 18, 19 (1965).

Edwards, D.O., and Pandorf, R.C., Phys. Rev. 140A, 816 (1965).

Franck, J.P., Wanner, R., Phys. Rev. Lett. 25, 345 (1970).

Fredkin, D.R. and Werthamer, N.R., Phys. Rev. 167, 607 (1965).

Gillis, N.S., Koehler, T.R., Werthamer, N.R., Phys. Rev. 175, 1110 (1968).

Gold, L., Phys. Rev. 77, 390 (1950).

Gurevich, V.L., and Efros, A.L., Zh. Exps. Teor. Fiz. 51 (1966): Engl. Tr. Phys. JETP 24, 1146 (1967).

Guyer, R.A., Solid State Physics 23, 413 (1969).

Hetherington, J.H., Mull n, W.J., Nosanow, L.H., Phys. Rev. 154, 175 (1967).

Hirschfelder, J.O., Curtiss, C.F. and Bird, R.B., (1954) Molecular Theory of Gases and Liquids, John Wiley and Sons, N.Y.).

Hogan, E.M., Guyer, R.A., Fairbank, H.A., Phys. Rev. 185, 356 (1969).

Holder, J., (1970) The Review of Scientific Instruments, 41, 1355-56.

Hooton, D.I., Phil. Mag., 3, 49 (1958).

Horner, H., Z. Physik 205, 72 (1967).

Jarvis, J.F., Ramm, D., Meyer, H., Phys. Rev. 170, 320 (1968).

Jastrow, R., Phys. Rev. 98, 1479 (1955).

Keller, W., Helium 3 and Helium 4, Plenum Press, N.Y. (1969).

Koehler, T.R., Phys. Rev. Lett. 17, 89 (1966).

Koehler, T.R., Phys. Rev. Lett. 18, 654 (1967).

Koehler, T.R., Phys. Rev. 165, 942 (1968).

Lipshultz, F.P., Minkiewicz, V.J., Kitchens, T.A., Shirani, G., Nathans, R., Phys. Rev. Lett. 19, 1307 (1967).

Mason, W.P. (edit), Physical Acoustics, Academic Press, N.Y. (1965).

McSkimin, H.J., Journal of Acoust. Soc. of Am. 33, 12 (1961).

Meuller, K.H., Jr., and Fairbank, H.A., To be published (LT13-1973).

Minkiewicz, V.J., Kitchens, T.A., Lipschultz, F.P., Nathans, R., Shirani, G., Phys. Rev. 174, 267 (1968).

Musgrave, M.J.P., Proc. Toy. Soc. A226, 339, 356 (1954).

Niklasson, G., and Sjölander, A., Ann. Phys. 49, 249-296 (1968).

Niklasson, G., Fortschr. Phys. 17, 235 (1965).

Niklasson, G., Ann. Phys. 59, 263 (1970).

Niklasson, G., Phys. Kondens. Materie 14, 138 (1972).

Nosanow, L.H., Phys. Lett. 13, 270 (1964).

Nosanow, L.H. Phys. Rev. 146, 120 (1966).

Nye, J.F., Physical Properties of Crystals, Clarendon Press, Oxford (1964).

Raninger, J., Phys. Rev. 140, A2031 (1965).

Reese, R.A., Sinha, S.K., Brun, T.O., Tilford, C.R., Phys. Rev. A3, 1688 (1971).

Seki, H., Granote, A., Trull, R., Journal of Acoust. Soc. of Am. 28, (1956).

Skillig, H.H., , Electronic Transmission Lines, McGraw-Hill, N.Y. (1951).

Trickey, S.B., Kirk, W.P., Adams, E.D., Rev. of Mod. Phys. 44, 668 (1972).

Van Dael, W., and Van Itterbeek, A., Physics of High Pressures and the Condensed Phase, (A. Van Itterbeek editor), Chapt. 7, 1965, John Wiley and Sons. N.Y.

Vignos, J.H., Fairbank, H.A., Phys. Rev. 147, 183 (1966).

Walker, E.J., Rev. Sci. Instr. 30, 834 (1959).

Wanner, R., Thesis, University of Alberta (1970).

Werthamer, N.R., Am. Jour. of Phys. 37, 763 (1969).

Whitney, W.M. and Chase, C.E., Phys. Rev. 158, 200 (1967).

Wilks, J., Properties of Liquid and Solid Helium, Clarendon Press, Oxford (1967).

Zener, C., Phys. Rev. 49, 122 (1936).

Ziman, J.M., Principles of the Theory of Solids, University Press, Cambridge (1965).

A1 Appendix for Derivation of Certain Thermodynamic Relations

$$ds = \left(\frac{\partial s}{\partial T}\right)_V dT + \left(\frac{\partial s}{\partial V}\right)_T dV$$

$$= \frac{c_V}{T}\, dT + \left(\frac{\partial s}{\partial V}\right)_T dV \quad .$$

From this

$$\left(\frac{\partial s}{\partial T}\right)_P = \frac{c_V}{T} + \left(\frac{\partial s}{\partial V}\right)_T \left(\frac{\partial V}{\partial T}\right)_P \quad .$$

But on the other hand

$$\left(\frac{\partial s}{\partial T}\right)_P = \frac{c_P}{T}$$

giving

$$c_P - c_V = T\left(\frac{\partial s}{\partial V}\right)_T \cdot \left(\frac{\partial V}{\partial T}\right)_P$$

and with the Maxwell relations

$$\left(\frac{\partial s}{\partial V}\right)_T = \left(\frac{\partial P}{\partial T}\right)_V$$

$$c_P - c_V = T \cdot \left(\frac{\partial P}{\partial T}\right)_V \left(\frac{\partial V}{\partial T}\right)_P \quad .$$

A2 Niklasson Theory as Applied to Hexagonal Crystals

Sound waves do not propagate perpendicular to the transducer in a hexagonal solid except at certain symmetry points. Therefore, the phonon drift velocity in the crystal will in generral be at some angle $\delta(\theta)$, a function of orientation θ, to the externally applied field.

Thus, if we excite a crystal at orientation θ, frequency Ω and wave vector Q, we will internally develop a phonon drift velocity at some angle $\theta+\delta(\theta)$, with individual phonons of wave vectors and frequencies ω, q.

Assuming linear dispersion

$$\Omega = \vec{c}_j(\theta)\cdot\vec{Q}(\theta)$$

where $\vec{c}_j(\theta)$ is the velocity (phase and group velocity are identical here) of sound mode j at orientation θ, as c_j and Q are colinear

$$\omega = c_j(\theta')q(\theta') \quad .$$

We will be performing averages over the internal variables θ', ϕ'

$$\langle f,g\rangle = \sum_j \int_{cell} \frac{dq}{v} \int_{-\infty}^{\infty} \frac{d\omega}{2\Pi} A_j(q,\omega)n(\omega)[1+n(\omega)\ f^*g] \quad .$$

where v is the volume of the unit cell

$A_j(q,\omega)$ is the generalized spectral fit

$h(\omega) = \frac{1}{e^{h\omega/kT} - 1}$ the bose occupation number.

If we assume harmonic phonons

$$A_j(q,\omega) \sim A_j^H(q,\omega) = \tfrac{1}{2}[\delta\{\omega+\omega_j(q)\}+\delta\{\omega-\omega_j(q)\}]$$

where $\omega_j(q) = c_j(\theta)q$ the harmonic phonon frequencies.

We will be calculating averages over real quantities which depend only on q, $c_j(\theta')$, and θ'.

$$<f,g> = \sum_j \int_{cell} \frac{d}{v} \int_{-\infty}^{\infty} \frac{d\omega}{2\Pi} A_j^H(q,\omega) n(\omega)[n(\omega)+1] d\omega fg$$

$$= \sum_j \frac{1}{v} \int n(\omega_j)[n(\omega_j)+1] fgdq \quad .$$

Now we will use a Debye like approximation so that

$$<f,g> = \frac{V}{8\Pi^3} \sum_j \int_0^{\Pi} \int_0^{\omega_j^D} f(\omega_j,\theta')g(\omega_j,\theta') \frac{\sin\theta' d\theta'}{c_j^3(\theta')} \frac{e^{h\omega_j/kT}}{[e^{h\omega_j/kT} - 1]} d\omega_j$$

where

$$\omega_j^D = \{\frac{24\Pi^3 N}{V}\}^{1/3} \{\int_0^{\Pi} \frac{\sin\theta' d\theta'}{c_j^3(\ ')}\}^{1/3}$$

thus $<\omega,\omega> = \frac{c_v kT^2 V}{h^2}$ where C_v is the heat capacity at constant volume per unit volume.

Section 2.7 gives an introduction to the theory by Niklasson wherein the integrals are calculated assuming an isotopic or cubic medium.

Now let $\tau(\theta') = \left(\frac{1}{\tau_u(\theta')} + \frac{1}{\tau_N} + \frac{1}{\tau_B}\right)^{-1}$ be our total relaxation time where τ_u, τ_N and τ_B are the umpklapp, normal and boundary relaxation times, respectively. Only τ_u depends on orientation (assumed).

As there is no dependence on Azimuthal orientation we can choose $\phi = \frac{\pi}{2}$ and thus only x and z components will contribute.

If we define

$$\vec{\theta} = \begin{pmatrix} \sin\theta \\ 0 \\ \cos\theta \end{pmatrix}$$

and

$$\bar{\bar{\Theta}} = \begin{matrix} \sin^2\theta' & 0 & 0 \\ 0 & \sin^2\theta' & 0 \\ 0 & 0 & 2\cos^2\theta' \end{matrix}$$

then we can write the solution to the Pieirls-Boltzmann equation (using the notation of section 2.7) as

$$N^{oo} = \Omega A + i D^{oo}$$

$$A = \langle\omega|\omega\rangle$$

$$D^{oo} = \Omega^2(\theta)\cos^2\delta(\theta)\ \vec{\theta}\cdot\bar{\bar{E}}^{oo}\cdot\vec{\theta}$$

$$\bar{\bar{E}}^{oo} = \langle\tau(\theta')c_j^2(\theta')\omega^2\bar{\bar{\Theta}}\rangle - \frac{\langle\tau(\theta')\omega^2\bar{\bar{\Theta}}\rangle^2\left\langle\dfrac{\bar{\bar{\Theta}}\ \omega^2}{\tau(\theta')\ c_j^2(\theta')}\right\rangle}{\left\langle\dfrac{\bar{\bar{\Theta}}\ \omega^2}{c_j^2\theta')}\right\rangle}$$

$$\vec{N}^{01} = -Q(\theta)\ \vec{\theta}\cdot\ \overline{\overline{B}}$$

$$\overline{\overline{B}} = <\omega^2\ \overline{\overline{\theta}}> \cos\ \delta(\theta)\quad .$$

$$\vec{F}^0 = \frac{ih\gamma}{kT}\ \Omega\vec{Q}(\theta)A$$ if γ is isotopic gruneisen parameter.

$$\overline{\overline{F}}' = \xi\ \frac{h\gamma}{kT}\ \Omega\overline{\overline{D}}"$$

ξ is a parameter that brings the quantum nature of He^4 to this picture.

$$\overline{\overline{D}}" = Q^2(\theta)\ \vec{\theta}\cdot\tilde{\tilde{E}}\cdot\vec{\theta}$$

$$\tilde{E} = <\tau(\theta')\tilde{\theta}> - \{<\tau(\theta')\overline{\overline{\theta}}> \otimes <\tau(\theta')\overline{\overline{\theta}}>\}\ \frac{<\tau(\theta')>}{A}$$

where $\tilde{\theta} = \overline{\overline{\theta}} \otimes \overline{\overline{\theta}}$ and $\otimes$ means outer product.

$\tilde{\tilde{E}}$ is a fourth rank tensor.

$$\overline{\overline{N}}" = \Omega\ \overline{\overline{Y}} + i(\overline{\overline{L}} + \overline{\overline{D}}")$$

$$\overline{\overline{Y}} = <\frac{\omega^2\ \overline{\overline{\theta}}}{c_j^2(\theta')}>$$

$$\overline{\overline{L}} = <\frac{\omega^2\ \overline{\overline{\theta}}}{\tau_u(\theta')c_j^2}>$$

Now, the generalized thermal conductivity $\overline{\overline{K}}$ is

$$\vec{Q}\cdot\overline{\overline{K}}\cdot\vec{Q} = i\ C_v\ \{\Omega - \frac{N^{oo}-N^{01}\cdot[\overline{\overline{N}}"]^{-1}\cdot\vec{N}^{10}}{A}\}$$

or

$$\overline{\overline{K}} = \frac{C_v}{A}\ \{\overline{\overline{E}}^{oo} + i\ \overline{\overline{B}}\cdot[\ \overline{\overline{Y}} + i(\overline{\overline{L}}+\overline{\overline{D}}")]^{-1}\cdot\overline{\overline{B}}\}$$

where $C_v = \frac{2\pi\rho h^2}{M\ kT^2}\ A$

for steady state

$$\bar{\bar{K}}_o = \frac{C_v}{A}\{\bar{\bar{E}}^{oo} + \bar{\bar{B}}\cdot\bar{\bar{L}}\cdot\bar{\bar{B}}\}$$

These calculations are in Q space. To convert to "r" space one uses

$\vec{Q}\ \bar{\bar{K}}_o\ \vec{Q}$ in q space is equivalent to

$$\{\frac{1}{K_{o_z}} \sin^2\theta + \frac{1}{K_{o_x}}\cos^2\theta\}^{-1}$$

in real space.

Now if we assume that coupling to lattice deformation adds only second order terms to the calculation of second sound, we can derive second sound by the following arguments.

$$[-i\Omega C_v + \vec{Q}\cdot\bar{\bar{K}}\cdot\vec{Q}]\bar{T}(Q,\Omega) = \text{lattice contributions}$$

where $\bar{T}(Q,\Omega)$ is the temperature gradient,

or

$$-i\Omega C_v + \vec{Q}\cdot\bar{\bar{K}}\cdot\vec{Q} = 0$$

or

$$\Omega^2 + i\vec{\theta}\cdot\{\bar{\bar{\theta}}\bar{\bar{B}}^{-1}(\bar{\bar{L}}+\bar{\bar{D}})\bar{\bar{Y}}^{-1}\bar{\bar{B}} + \frac{Q^2(\theta)}{A}\bar{\bar{E}}^{oo}\}$$

$$-\frac{Q^2(\theta)}{A}\vec{\theta}\cdot\{\bar{\bar{B}}\bar{\bar{Y}}^{-1}\bar{\bar{B}}+\bar{\bar{E}}^{oo}\bar{\bar{B}}^{-1}(\bar{\bar{L}}+\bar{\bar{O}})\bar{\bar{Y}}^{-1}\bar{\bar{B}}\}\cdot\vec{\theta} = 0$$

which is in the form

$$\Omega^2 + 2i\Gamma_2^o(\theta) - [Q^2(\theta)C_{II}^2(\theta)] = 0$$

where

$$C_{\text{II}}^2(\theta) = \frac{\vec{\theta}}{A} \cdot \{\bar{\bar{B}}\bar{\bar{Y}}^{-1}\bar{\bar{B}} + \bar{\bar{E}}^{oo}\bar{\bar{B}}^{-1}(\bar{\bar{L}}+\bar{\bar{D}})\bar{\bar{Y}}^{-1}\bar{\bar{B}}\} \cdot \vec{\theta}$$

$$\Gamma_2^o(\theta) = \frac{1}{2}\,\vec{\theta} \cdot \{\bar{\bar{\Theta}}\bar{\bar{B}}^{-1}(\bar{\bar{L}}+\bar{\bar{D}})\bar{\bar{Y}}^{-1}\bar{\bar{B}} + \frac{Q^2(\theta)}{A}\,\bar{\bar{E}}^{oo}\}$$

where C_{II} and Γ_2^o are the speed and attenuation of second sound respectively.

In the normal region where second sound propagates

$$\omega\tau_N << 1 << \omega\tau_u$$

or

$$\{C_{\text{II}}(\theta)\}_{\text{real}} = \{AB_{xx}^{-1}(\theta)Y_{xx}B_{xx}^{-1}(\theta)\cos^2\theta$$
$$+AB_{zz}^{-1}(\theta)Y_{zz}B_{zz}^{-1}(\theta)\sin^2\theta\}^{-\frac{1}{2}}$$

where θ is the orientation of the crystal in real space.

Define the generalized viscosity

$$\tilde{\eta} = \frac{2\Pi\rho h^2\gamma^2}{MkT}\,\tilde{E}$$

Further, let the coupling between the temperature field and the lattice (which is proportional to $\vec{Q}\cdot\bar{\bar{W}}$) be non-zero.

$$\vec{Q}\cdot\bar{\bar{W}} = -\frac{2\Pi ih}{NT}\{\vec{F}^o - N^o \cdot [N'']^{-1} \cdot F'\}$$

$$\vec{Q}\cdot\bar{\bar{W}} = \frac{2\Pi h^2\gamma\Omega}{MkT^2}\,Q(\theta)\,\{A\vec{\theta}+i\vec{\theta}\cdot\bar{\bar{B}}\cdot[\Omega\bar{\bar{Y}}+i(\bar{\bar{L}}+\bar{\bar{D}}'')]^{-1}\xi\bar{\bar{D}}''\} .$$

We will now calculate the propagation of first sound with coupling to the local temperature deformation.

We must solve the simultaneous equations

$$\Omega^2\langle\vec{u}\rangle - \frac{1}{\rho}\,\overline{\overline{\mu}}\cdot\langle\vec{u}\rangle + \frac{i\Omega}{\rho}\,\overline{\overline{\eta}}\cdot\langle\vec{u}\rangle = -\frac{1}{\mu}\,\vec{j} + i\overline{\overline{W}}\cdot Q\overline{\overline{T}}(Q,\Omega)$$

$$[-i\Omega C_v + Q\cdot\overline{\overline{K}}\cdot Q]\overline{T}(Q,\Omega) = -\rho T\Omega Q\cdot\overline{\overline{W}}\langle\vec{u}\rangle$$

where

$$\mu = \sum_{\beta\gamma} C^{(is)}_{\alpha\beta\gamma\delta}\, Q_\beta Q_\gamma$$

$C^{(is)}_{\alpha\beta\gamma\delta}$ are the isothermal elastic constants

$$\overline{\overline{\eta}} = \sum_{\beta\gamma} \tilde{\eta}\ \alpha\beta\gamma\delta Q_\beta Q_\gamma$$

j = is the heat current

$\overline{\overline{W}}$ is roughly the thermal expansion.

Solve the lower equation for $\overline{T}(Q,\Omega)$

$$\overline{T}(Q,\Omega) = \frac{-\rho T\Omega\vec{Q}\cdot\overline{\overline{Q}}\cdot\langle\vec{u}\rangle}{\langle -i\Omega C_v + \vec{Q}\cdot\overline{\overline{K}}\cdot\vec{Q}\rangle}$$

and put this value into the upper equation

$$\Omega^2\langle u\rangle - \frac{1}{\rho}\,\overline{\overline{\mu}}\cdot\langle u\rangle + \frac{i\Omega}{\rho}\,\overline{\overline{\eta}}\langle u\rangle = -\frac{1}{\mu}\,\vec{j}\ \frac{-i\rho T\{(\vec{Q}\cdot W)\otimes(Q\cdot W)\}\langle u\rangle}{\Omega\ [-i\Omega C_v + \vec{Q}\cdot\overline{\overline{K}}\cdot\vec{Q}]}$$

let

$$\overline{\overline{R}} = \frac{i\{\vec{Q}\cdot\overline{\overline{W}}\otimes\overline{\overline{W}}\cdot\vec{Q}\}\rho T}{[-i\Omega C_v + \vec{Q}\cdot\overline{\overline{K}}\cdot\vec{Q}]\Omega} \quad \text{and} \quad \overline{\overline{R}} = \frac{\overline{\overline{\mu}}}{\Omega\rho} + i\,\frac{\overline{\overline{\lambda}}}{\rho}$$

then

$$\Omega^2\langle u\rangle - \frac{1}{\rho}(\overline{\overline{\mu}}+\overline{\gamma})\langle\overline{\overline{u}}\rangle + \frac{i\Omega}{\rho}\,(\overline{\overline{\eta}} + \overline{\overline{\mu}})\langle u\rangle = -\frac{1}{\mu}\,\vec{j} \quad .$$

Thus $\overline{\overline{\lambda}}$ is the change in velocity and $\overline{\overline{\mu}}$ the change

in attenuation for first sound.

$$\bar{\bar{\lambda}} = \frac{\rho^2 T}{\Omega} \quad \text{Im} \left\{ \frac{(\vec{Q}\cdot\bar{\bar{W}}) \otimes (\bar{\bar{W}}\cdot\vec{Q})}{[-i\Omega C_V + \vec{Q}\cdot\bar{\bar{K}}\cdot\vec{Q}]} \right\}$$

$$\bar{\bar{\mu}} = \rho^2 T \ \text{Re} \left\{ \frac{(\vec{Q}\cdot\bar{\bar{W}}) \otimes (\bar{\bar{W}}\cdot\vec{Q})}{[-i\Omega C_V + \vec{Q}\cdot\bar{\bar{K}}\cdot\vec{Q}]} \right\} .$$

Projecting onto polarization vectors $e^j(Q)$ and neglecting polization mixing

$$\frac{C^2(Q,\Omega)}{C_T^2(Q,\Omega)} = 1 + \frac{K_T}{\rho[C_T(Q)]^2} \left(\frac{C_p}{C_V} - 1\right) N(Q,\Omega)$$

$$N(Q,\Omega) = \frac{\sum_{\alpha\beta} e_\alpha^j \lambda_{\alpha\beta} e_\beta^j}{\frac{K_T}{\rho \ C_T^2} \left(\frac{C_p}{C_V} - 1\right)}$$

$$K_T = \frac{C_{33} + 2C_{13}}{3} = \frac{C_{11} + C_{12} + C_{13}}{3}$$

if the linear coefficient of compression is isotropic (Wanner (1970))

$$\gamma^2 = \frac{K_T V}{C_V T} \left(\frac{C_p}{C_V} - 1\right) .$$

A3 A Method for Scaling Elastic Constants in hcp He^4

We have, at present, the elastic constants at four molar volumes from the work of Crepeau et al (1971) at 20.97 cc/mole, Greywall et al (1970) at 20.5 cc/mole and Franck et al (1970) at 20.32 and 19.28 cc/mole.

These elastic constants were primarily determined from acoustic measurements. There was great variety in the method of determining the orientation, and some of the authors used various assumptions to calculate all the elastic contants.

We would wish to calculate the elastic constants at any density, the following being a plausible way of doing this.

First, Franck et al (1970) proved that as a result of the c/a ratio remaining constant in hcp He^4 to very high densities

$$C_{11} + C_{12} = C_{13} + C_{33} \quad . \tag{A3-1}$$

Using this equation one can simplify the expression for the compressibility to

$$K_T = \frac{3}{C_{11}+C_{12}+C_{13}} = \frac{3}{C_{33}+2C_{13}} \quad . \tag{A3-2}$$

The compressibility has been measured from $(\frac{\partial P}{\partial T})_V$ by Jarvis et al (1968) from 17.77 to 20.72 cc/mole.

Recalling that the Debye Theta has also been measured by Ahlers (1970) at a wide range of molar

volume, one can use these data to scale the elastic constants.

First we must modify the data of Crepeau et al (1970) to fit condition (A3-1). This can be done within their experimental error.

Then at all four molar volumes

$$\frac{C_{33}}{C_{11}} = 1.3 \pm .01 \quad . \tag{A3-3}$$

It should also be noted that in this form systematic errors in the measurements (such as distance calibration error, or time scale calibration error) are negated. Also C_{33} and C_{11} are probably the simpliest elastic constants to find as they are simply related to the longitudinal velocity along the 'C' axis and in the basal plane respectively (see section 2.3).

Recall, also, that

$$\theta_D = \frac{\text{const}}{V^{1/3}} v_D$$

$$v_D = \text{cost x } \{\int_o^{\Pi} \sin \theta d\theta \, (\frac{1}{v_e^3} + \frac{1}{v_{t_1}^3} + \frac{1}{v_{t_2}}) \}^{-/3}$$

For He^4, $v_e >> v_{t_1}, v_{t_2}$ thus

$$v_D \sim v_t$$

or the transverse velocities are directly proportional to the Debye Theta.

Further let

$$\alpha = C_{11} - C_{12}$$

$$\beta = C_{11}+C_{12}+C_{13} = C_{33}+2C_{13} \quad .$$

We will further assume that the ratios of the transverse velocities σ remain constant at all densities

$$\sigma = \frac{2\,C_{44}}{C_{11}-C_{12}} \quad .$$

We can finally write

$$C_{44} = \frac{\Delta\ \theta_D^2}{V^{1/3}}$$

$$C_{11}-C_{12} = \quad = \frac{\Delta}{\sigma}\,\frac{\theta_D^2}{V^{1/3}}$$

$$\beta = \frac{3}{K_T(V)}$$

and

$$C_{44} = \frac{\Delta\ \theta_D^2}{V^{1/3}}$$

$$C_{11}-C_{12} = \frac{\Delta}{\sigma}\,\frac{\theta_D^2}{V^{1/3}}$$

$$C_{11}+C_{12}+C_{13} = \frac{3}{K_T(V)}$$

$$C_{33} = 1.3 \times C_{11}$$

$$C_{13} = C_{12} - .3 \times C_{11} \quad .$$

Finally

$$C_{11} = \frac{1}{2.7}\left[\frac{3}{K_T(V)} + 2\,\frac{\Delta}{\sigma}\,\frac{\theta_D^2}{V^{1/3}}\right]$$

$$C_{12} = \frac{1}{2.7}\left[\frac{3}{K_T(V)} - 0.7\,\frac{\Delta}{\sigma}\,\frac{\theta_D^2}{V^{1/3}}\right]$$

$$C_{13} = \frac{1}{2.7}\left[\frac{2.1}{K_T(V)} - 1.3\,\frac{\Delta}{\sigma}\,\frac{\theta_D^2}{V^{1/3}}\right] \qquad \text{(A3-4)}$$

$$C_{33} = \frac{1.3}{2.7}\left[\frac{3}{K_T(V)} + 2\,\frac{\Delta}{\sigma}\,\frac{\theta_D^2}{V^{1/3}}\right]$$

$$C_{44} = \frac{\Delta\theta_D^2}{V^{1/3}}$$

From experiment σ is in the range 1 to 2. If one chooses a value of σ and then calculates Δ to give the correct θ_D, one can get reasonable fits. The final fit is surprisingly insensitive to the size of σ.

In extrapolations of elastic constants for comparison with theories, I have used

$$\Delta = 7.876 \times 10^5$$

$$\sigma = 1.266$$

and

$$K_T(V) = \sum_{j=o}^{3} \{a_j \times 10^{-9} \times V^{-j}\}$$

$$a_0 = 122.6$$

$$a_1 = -18.29$$

$$a_2 = .8861$$

$$a_3 = -.01354$$

and

$$\theta_D = 68.56 \left\{\frac{V}{14.208}\right\}^{-1.02} e^{-0.83(V-14.208)} .$$

This gives K_T to 1% and θ_0 to 1%.

This scaling gives results within experimental error, except for the data of Crepeau et al (1970) which appear about 2% low. Also, this scaling gives results consistent with the velocities I have measured at 120 bar and 86 bar.

A4 Computer Programs

This appendix gives some of the computer programs used during the completion of this work.

TEMP is the function that converts resistance to temperature. COTEMP and COXTEMP are the coefficients used for the main region of fit and for extrapolation respectively. LL and LU define the main region of fit.

PO fits a number X to a polynomial with coefficients C.

VPLOT calculates and plots the velocity versus temperature from the raw experimental data.

VSS is used to give the printout in the next appendix. It fits the velocities from VPLOT to the theories of Bhatia or Niklasson.

CODEX arranges the raw data. SCALE calculates the elastic constants at a given pressure. THETAV calculates the Debye theta for a given volume, while KTVM calculates the compressibility. DEBH calculates the Debye theta from the elastic constants for hexagonal crystals. BHAT is the theory of Bhatia , while VEL gives the theory of Niklasson. SDFIT, FIT, WFITL, and LINEAR are functions that calculate the least square coefficients. REL calculates the relaxation times. UMKLAPP calculates Umklapp relaxation times. CV calculates the heat capacity. ORVL calculates the orientation. PVDEG produces a polynomial of fractional or negative powers.

HEXA gives the velocities and related quantities for

hexagonal crystals. DELL gives the deviation from a pure mode. DELTAL, DELTAT1, DELTAT2 give the deviation from wave normal. VL, VT1, and VT2 give the velocities. PH is a subroutine.

VEL2,INSET, and INFUN are functions to calculate the orientation dependence of the velocity of second sound.

Finally, DEBC, VCUB, CUDEF, and RCR are used to calculate the Debye theta of cubic materials. RCR is a functions that gives the three real solutions of a cubic equation if they exist.

```
                 ∇TEMP[⎕]∇
    ∇ TT←TEMP R;T;TX;A
[1]   T←(A-COTEMP[ρCOTEMP])÷COTEMP[ι(ρCOTEMP)-1] PO A←
      10⍟S←(~R∊(SU←((R>LU)/R)),(SL←((R<LL)/R)))/R
[2]   TX←(A-COXTEMP[4])÷COXTEMP[ι3] PO A←10⍟SU,SL
[3]   TT←TX[(ρSU)+ι(ρSL)],T,TX[ιρSU]
    ∇
      COTEMP
1304.5  ¯2614.8  1765.6  ¯239.66  ¯221.09  72.702
      10.475  ¯4.4611  ¯1.5037  0.67755  ¯0.067433
      ¯7.9399
      COXTEMP
4.5628  ¯4.2941  1.059  0.92388
      LL,LU
135  849

                 ∇PO[⎕]∇
    ∇ Y←C PO X
[1]   Y←(X∘.*¯1+ι1ρρC)+.×C
    ∇

      ∇VPLOT[⎕]∇
    ∇ VL←VELT VPLOT DISV;A;S;SD;T
[1]   SD←S SDFITιρS←ASCALE×VELT
[2]   A←DIST÷A[2]
[3]   VL←VL,VACT←⍉(2,E)ρ(T←TEMP R),VACT←÷VL[E←ρVL]÷VL←A÷1+
      DISV×BSCALE÷DELAY×ASCALE
[4]   CODE
[5]   '                  PLOT OF ΔV VS TEMP'
[6]   ''
[7]   '                  VELOCITY AT 0 K  IS ';VL[E;1];' + OR
      - ';VL[E;1]×SD×A÷DIST;' M/S'
[8]   50 PLOT VACT
[9]   '          TEMPERATURE (KELVIN)'
[10]  ''
[11]  'VELOCITIES'
[12]  VL
    ∇
```

```
              ∇VSS[⎕]∇
    ∇ VR←MODE VSS NAME;VDEG;VD;WEIGHT;DEL;CL;CT;Z;Z1;V;GAM;
      VT;ETA;ATT;ATTEN;TAU1
[1]   7 1 ρLS
[2]   CODEX NAME
[3]   2 1 ρLS
[4]   BLAH← 2 11 ρ'(NIKLASSON)(BHATIA)   '
[5]   SCALE PRESS
[6]   T←T,T1+0×A←ρT←0.2+0.1×⍳(⌈10×⌈/T1)-2
[7]   →(MODE≠ 5 10)/E0
[8]   →(V=V←BHAT OMEGA÷○2)/E1
[9]  E0:V←VEL OMEGA
[10]  WEIGHT←(~WEIGHT)+COWT×WEIGHT←T1<1
[11] E1:E←(V1÷V[A+⍳ρT1]) WFITL T1+0×+/VDEG←0,CTP
[12]  VR←(VT←V×E PVDEG T)÷E[1]
[13]  SD←((+/((VT[A+⍳ρT1]-V1)*2)+.×WEIGHT)÷ρT1)*
      0.5
[14]  'ISOTHERMAL VELOCITY = A+B×T*N'
[15]  'A=';E[1];' +/- ';VE×E[1];' M/S';'     B=';E[
      2];'      N=';CTP
[16]  'DEBYE Θ=';THETA;'      MOLAR VOLUME=';VM;' CC/M'
[17]  'SECOND SOUND=';C2;' M/S';'      FREQUENCY=';OMEGA÷○
      2;' HZ'
[18]  'STANDARD DEVIATION FOR FIT IS  ';SD
[19]  'RELAXATION FACTORS ';TNCH;'×TN,';TUCH;'×TU,';TAU1CH;'
      ×TAU1'
[20]  →((ρB←ORVL VE)=4)/E2+0×V0←E[1]
[21]  'ORIENTATION IS BETWEEN ';B[1];' AND ';B[2]
[22] E2:→((ρB)=2)/E3
[23]  'ORIENT. IS BTWN. ';B[1];' AND ';B[2];' OR ';B[
      3];' AND ';B[4]
[24] E3:LS
[25]  'THEORETICAL CALCULATIONS';BLAH[(1++/MODE=5);]
[26]  'TEMP      V[T]÷V[0]     ATTEN     NIKFAC'
[27]  4 1 13 5 11 3 11 3 DFT VR[⍳A] AND(ATTEN[⍳A]÷
      100×V0) AND Z[⍳A] VS T[⍳A]
[28]  Z←(-1-(V1÷E PVDEG T1)*2)÷DEL×GAM[A+⍳ρT1]
[29]  7 2 ρ⎕
[30]  'EXPERIMENTAL DATA FOR CRYSTAL ';NAME
[31]  ' TEMP        V[T]       V[T]÷V[0]       NIKFAC'
[32]  5 3 12 2 13 5 13 3 DFT V1 AND(V1÷E[1]) AND Z VS T1
    ∇
```

```
              ∇CODEX[⎕]∇
    ∇ CODEX Y
      Y←(2ρY)×.=⍉ 13 2 ρ'03A8C2D3D4D5E2F2F3G1H2I2DS'
      T1←((,Y/TDAT)>0)/,Y/TDAT
      V1←((,Y/VDAT)>0)/,Y/VDAT
      ,Y/CODEDAT
      PRESS←Y/PDAT
      VE←Y/VEDAT
    ∇
              ∇SCALE[⎕]∇
    ∇ SCALE PRESS;A;B;C
      A←DELTA×(VM*÷¯3)×(THETAV VM←VOLPR PRESS)*2
      B←3÷KTVM VM
      C44←SIGMA×A
      C33←1.3×C11←(B+2×A)÷2.7
      C12←(B-A-0.3×C11)÷3
      C13←C12-0.3×C11
      THETA←DEBH 4
      BS←÷KT←3÷C11+C12+C13
      VD←VDEB THETA
    ∇
              ∇THETAV[⎕]∇
    ∇ THETA←THETAV VM
      THETA←2340×(VM*¯0.8114)×*¯0.0969×VM
    ∇
              ∇KTVM[⎕]∇
    ∇ KT←KTVM VM
      KT←1E¯9×COKT PO VM
    ∇
              ∇DEBH[⎕]∇
    ∇ Z←DEBH D;A;B
      B←(Z←3×D+1)ρA←0,○(0.5÷D)×⍳D←2×D
      Z←Zρ1,((D-1)ρ 4 2),1
      Z←+/Z×(1○B)÷((VL A),(VT1 A),VT2 A)*3
      Z←0.004499465×(D÷VM×Z)*÷3
    ∇
              ∇VDEB[⎕]∇
    ∇ V←VDEB THETA
      V←3.98×THETA×VM*÷3
    ∇
```

```
                ∇BHAT[⎕]∇
     ∇ V←BHAT FREQ;ALPHA;FX;K0;K90;TU0;T90;CVT
[1]    CTP←5.556488427-0.0466713171×THETA
[2]    UMKLAPP
[3]    TU←300×TU0×TU90÷TU90+2×TU0
[4]    →(MODE=10)/E10
[5]    →D10
[6]   E10:'TU CHANGE IS'
[7]    TU←⎕×TU
[8]   D10:KAP←(CVT←CV THETA)×(÷VM×1E¯6)×(TU⌊DIST÷C2)×C2×C2←
       0.3×CL←0.01×(C11÷RHO)*0.5
[9]    FX←CVT×C11÷KAP×RHO×○2
[10]   ALPHA←(GAM←GAMMA THETA)×DEL←(C11+2×C12)÷3×C11
[11]   V←(1+ALPHA×Z←FX×FX÷(FX×FX)+(1+ALPHA)×FREQ×FREQ)*
       0.5
[12]   ATTEN←(ALPHA÷1+ALPHA)×FREQ×FX÷(FX×FX)+(FREQ÷1+ALPHA)*
       2
     ∇
                ∇VEL[⎕]∇
     ∇ V←VEL OMEGA;CT;TAU;S;T00;TR;TN;TU;T11
[1]    CL←0.01×(C11÷RHO)*0.5
[2]    CT←0.01×((C11-C12)÷2×RHO)*0.5
[3]    →(MODE=1)/E1
[4]    →(DEL=DEL←(0.0001×(C11+2×C12)÷3)÷RHO×CL×CL)/D1
[5]   E1:'ADIABATIC COEFFICIENT IS'
[6]    DEL←⎕
[7]   D1:→(MODE=2)/E2
[8]    →(S=S←C2÷CL)/D2
[9]   E2:'SECOND SOUND RATIO IS'
[10]   S←⎕
[11]  D2:→(MODE=3)/E3
[12]   →(CTP=CTP←5.556488427-0.0466713171×THETA)/D3
[13]  E3:'POWER OF FIT IS'
[14]   CTP←⎕
[15]  D3:TAU←REL
[16]   S←S÷B←(1+T00÷TR)*0.5
[17]   G20←0.5×(÷TR)+OMEGA×OMEGA×S×S×(÷B×B)×T00+T11
[18]   G00←0.5×(÷TR)+OMEGA×OMEGA×S×S×(÷B×B)×T11-2×TAU1
[19]   V←(OMEGA×OMEGA×(1-S×S)*2)+4×G20×G20
[20]   ETA←3000×((1.02+0.083×VM)*2)×CVT×T×TAU×OMEGA×OMEGA÷CL
       ×CL×AW
[21]   ATTEN←ETA-ATT←DEL×(GAM←GAMMA THETA)×((OMEGA×OMEGA×(1-
       S×S)×G00)-OMEGA×OMEGA×G20)÷V
[22]   V←1+DEL×GAM×Z←((OMEGA×OMEGA×(1-S×S))+4×G00×G20)÷V
[23]   V←V*0.5
     ∇
```

```
                ∇SDFIT[⎕]∇
    ∇ SD←Y SDFIT X
[1]   DIFF←Y-POL←(X∘.*VDEG)+.×A←Y FIT X
[2]   SD←((÷⍴X)×+/DIFF*2)*0.5
[3]   'POWER FIT      ';VDEG
[4]   'COEFFICIENTS      ';A
[5]   'VARIATIONS'
[6]   DIFF
[7]   'STANDARD DEVIATION      ';SD
    ∇
                ∇FIT[⎕]∇
    ∇ Z←Y FIT X;WEIGHT
[1]   WEIGHT←1
[2]   Z←Y WFITL X
    ∇
                ∇WFITL[⎕]∇
    ∇ Z←Y WFITL X
[1]   Z←(WEIGHT+.×X∘.*VDEG∘.+VDEG) LINEAR(WEIGHT×Y)+.×X∘.*
      VDEG
    ∇
                ∇LINEAR[⎕]∇
    ∇ R←M LINEAR A;N;K;I;V;B
[1]   M←(((N←(⍴M)[K←1])⍴1),0)\M
[2]   M[;N+1]←A
[3]   A←⍳N
[4]   M[I,K;]←M[K,I←(K-1)+V⍳B←⌈/V←|M[(K-1)+⍳N+1-K;K];]
[5]   →0×⍳CRITERION>B
[6]   M←M-(V\(V←K≠A)/M[;K])∘.×M[K;]←M[K;]÷M[K;K]
[7]   →4×⍳N≥K←K+1
[8]   R←M[;N+1]
    ∇
```

```
              ∇REL[⎕]∇
    ∇ TAU←REL;TU;TU0;TU90;K0;K90;A
[1]   C2←CL×CT×(((CT*3)+2×CL*3)÷3×(CT*5)+2×CL*5)*
      0.5
[2]   UMKLAPP
[3]   TU←TUCH×((C2÷S×CL)*2)×300×TU0×TU90÷TU90+2×TU0
[4]  D6:TR←DIST×TU÷DIST+TU×C2
[5]   A←((VD÷S×CL)*2)÷3
[6]   TN←TNCH×A×2.1E¯12×(THETA÷T)*3
[7]  D7:TAU←TN×TR÷TN+TR
[8]   T00←TAU×2×CL×CT×(((CL×CL)-CT×CT)*2)÷((CT×CT×CT)+
      2×CL×CL×CL)*2
[9]   T11←0.8×TAU
[10]  TAU1←TAU1CH×0.8×TAU
    ∇
              ∇UMKLAPP[⎕]∇
    ∇ UMKLAPP;A
[1]   K0←(C0KAP PO PRESS)×*THETA÷B0×T
[2]   K90←(C90KAP PO PRESS)×*THETA÷B90×T
[3]   TU0←K0×A←1E¯6×VM÷(CVT←CV THETA)×C2×C2
[4]   TU90←A×K90
    ∇
              ∇CV[⎕]∇
    ∇ CVT←CV THETA
[1]   CVT←1940×(T÷THETA)*3
    ∇
     C0KAP
¯2.133E¯5  2.851E¯6
      C90KAP
¯2.877E¯6  1.373E¯7
      B0,B90
4.67  2.49
              ∇ORVL[⎕]∇
    ∇ ΔW←ORVL VE;S;E
[1]   V←0.01×VL○(W←0,5×⍳18)÷180+0×E←
      0.03×V0
[2]  A1:S←(V>V0+E)+V<V0-E
[3]   ΔW←((~((⌊/V)=V)+(⌈/V)=V)×1=S+0,18⍴S)/W
[4]   →(0=S[1],S[19])/A2,A3
[5]   →A1×(0=⍴ΔW),E←E+0.01×V0×0=⍴ΔW
[6]  A2:→0×+/ΔW←0,ΔW
[7]  A3:→0×+/ΔW←ΔW,90
    ∇
              ∇PVDEG[⎕]∇
    ∇ Z←C PVDEG X
[1]   Z←(X∘.*VDEG)+.×C
    ∇
```

```
              ∇HEXA[⎕]∇
    ∇ Z←HEXA D
[1]   Z←0,(DELTAL D), 0 0 ,(DELTAT1 D), 0 0 ,(DELTAT2 D), 0
      0 ,(DELL(D←(○(⍳(90÷D)-1)×D)÷180)),0
[2]   Z←⍉(8,⍴D)⍴Z←(D←D×180÷○1),(100×VL D),(100×VT1 D),(
      100×VT2 D←0,D,○÷2),Z
    ∇
              ∇DELL[⎕]∇
    ∇ Z←DELL A
[1]   Z←(RHO×(VL A)*2)-C44
[2]   Z←¯3○(Z-(C33-C44)×N*2)÷(M←1○A)×(N←2○A)×C13+C44
[3]   Z←(¯2○((1○Z)×M)+(2○Z)×N)×180÷○1
    ∇
              ∇DELTAL[⎕]∇
    ∇ Z←DELTAL A;B;H
[1]   H←(Z←RHO×(VL A)*2)-C44
[2]   B←(H-(C33-C44)×N*2)÷(N←2○A)×(M←1○A)×C13+C44
[3]   B←¯2○÷((((1○¯3○B)*4)÷M*2)+(((2○¯3○B)*4)÷N*2))*
      0.5
[4]   Z←(¯3○((H×3○B)÷Z))×180÷○1
    ∇
              ∇DELTAT1[⎕]∇
    ∇ Z←DELTAT1 A
[1]   Z←(¯3○((Z-C44)×3○¯2○1○A)÷(Z←RHO×(VT1 A)*2))×
      180÷○1
    ∇
              ∇DELTAT2[⎕]∇
    ∇ Z←DELTAT2 A;B;H;M;N
[1]   H←(Z←RHO×(VT2 A)*2)-C44
[2]   B←(H-(C33-C44)×N*2)÷(N←2○A)×(M←1○A)×C13+C44
[3]   B←¯2○÷((((1○¯3○B)*4)÷M*2)+(((2○¯3○B)*4)÷N*2))*
      0.5
[4]   Z←(¯3○((H×3○B)÷Z))×180÷○1
    ∇
```

```
              ∇VEL2[⎕]∇
    ∇ V←D VEL2 E;BX;BZ;YX;YZ;A
[1]   D INSET E←○E÷180
[2]   INFUN
[3]   B←YZ×A÷BZ×BZ
[4]   C←YX×A÷BX×BX
[5]   V←((B×(1○E)*2)+C×(2○E)*2)*¯0.5
    ∇
              ∇INSET[⎕]∇
    ∇ D INSET E;V1;V2;V3
[1]   C←(3×D+1)⍴(1,((D-1)⍴ 4 2),1)+0×D←2×D
[2]   B1←(3×D+1)⍴B←0,(⍳D)×○÷D
[3]   C←C×(1○B1)÷((V1←0.01×VL B),(V2←
      0.01×VT1 B),V3←0.01×VT2 B)*3
[4]   V←÷V1,V2,V3
[5]   DEL←2○⍉(3,⍴E)⍴(DELTAL E),(DELTAT1 E),DELTAT2 E
    ∇
              ∇INFUN[⎕]∇
    ∇ INFUN
[1]   BX←+/DEL+.×(3,1+2×D)⍴C×(1○B1)*2
[2]   BZ←2×+/DEL+.×(3,1+2×D)⍴C×(2○B1)*2
[3]   YX←+/C×(V×1○B1)*2
[4]   YZ←2×+/C×(V×2○B1)*2
[5]   A←2×+/C
    ∇
              ∇VL[⎕]∇
    ∇ Z←VL A
[1]   Z←(((((C11+C44)×(1○A)*2)+(C44+C33)×(2○A)*2)+PH A)×VM÷
      8.006)*0.5
    ∇
              ∇VT1[⎕]∇
    ∇ Z←VT1 A
[1]   Z←(((0.5×(C11-C12)×(1○A)*2)+C44×(2○A)*2)×VM÷
      4.003)*0.5
    ∇
              ∇VT2[⎕]∇
    ∇ Z←VT2 A
[1]   Z←((((C11+C44)×(1○A)*2)+((C33+C44)×(2○A)*2)-PH A)×VM÷
      8.006)*0.5
    ∇
              ∇PH[⎕]∇
    ∇ PHI←PH A
[1]   PHI←(((C11-C44)×(1○A)*2)*2)+((C33-C44)×(2○A)*
      2)*2
[2]   PHI←(PHI+(2×((1○A)×(2○A))*2)×((C11-C44)×C44-C33)+
      2×(C13+C44)*2)*0.5
    ∇
```

```
                ∇DEBC[⎕]∇
    ∇ Z←DEBC D;M;N
[1]   M←(((2×D×D)ρ 0 1)\(D×D)ρ(-○÷8×D)+(ιD)×○÷4×D)ρ 1 0)\N←
      ,⍉(D,D)ρ(-○÷4×D)+(ιD)×○÷2×D
[2]   Z←0.36261948×(CRHO×2×D×D÷○CAW×(+/(1○(D×D)ρ,N)×(+/(
      VCUB M)*¯3)))*÷3
    ∇
                ∇VCUB[⎕]∇
    ∇ Z←VCUB A
[1]   C←CUBDEF A
[2]   Z←RCR C
[3]   Z←100×(Z÷CRHO)*0.5
    ∇
                ∇CUBDEF[⎕]∇
    ∇ C←CUBDEF A;L1;L2;L3;D11;D12;D13;D23;D22;D33;Z
[1]   D13←(1○A[¯1+Z])×2○A[Z←2×ι(ρ(A←,A))÷2
[2]   D23←(1○A[¯1+Z])×1○A[Z]
[3]   A←2○A[¯1+Z]
[4]   D11←CC44+(C←CC11-CC44)×D13×D13
[5]   D22←CC44+C×D23×D23
[6]   D33←CC44+C×A×A
[7]   D12←(C←CC12+CC44)×D23×D13
[8]   D13←C×A×D13
[9]   D23←(A←0)+C×A×D23
[10]  C←(D22×D13×D13)+(D11×D23×D23)+(D33×D12×D12)-(D11×D22×
      D33)+2×D12×D13×D23
[11]  C←(-D11+D22+D33+D12←D13←D23←0),((D11×D33)+(D22×D33)+(
      D11×D22)-(D12×D12)+(D13×D13)+(D23×D23)),C
[12]  C←((Z←(ρC)÷3)ρ1+D11←D22←D33←0),C
[13]  C←(4,Z)ρC
    ∇
                ∇RCR[⎕]∇
    ∇ Z←RCR C;A;D;DET;P
[1]   →(((ρρC)>2),((ρρC)=2),((ρρC)=0))/E1,E2,E3
[2]   →((ρC)≠4)/E4
[3]   C←(4 1)ρC
[4]  E2:→((ρC)[1]≠4)/E3
[5]   C←(((3×C[3;])-P*2)÷3),((2×P*3)+(¯9×(P←C[2;])×C[
      3;]+27×(C←C÷(ρC)ρC[1;])[4;])÷27
[6]   C←(C[ιA]÷3),C[A+ιA←(ρC)÷2]÷2
[7]   →((+/((DET←(C[A+ιA]*2)+C[ιA]*3)>CRITERION))>
      11)/E6
[8]   PHI←¯2○(PHI×0≤1-|PHI)+(×PHI)×0>1-|PHI←-C[A+ιD+DET←0]÷
      (-C[ιD←ρDET]*3)*0.5
[9]   Z←⍉(3,D)ρ(C[ιD]×2○(C[A+ιD]-○2÷3)),(C[ιD]×2○(C[A+ιD]+○
      2÷3)),(C[ιD]←2×(-C[ιD])*0.5)×2○(C[A+ιD]←PHI÷
      3)
[10]  Z←Z-⍉(3,P←ρP)ρP÷3+PHI←0
[11]  →0
[12] E1:→0=ρ⎕←'RANK OF ARGUMENT MUST BE MATRIX OR VECTOR'
[13] E4:→0=ρ⎕←'RANK OF VECTOR MUST BE TWO OR FOUR'
[14] E6:→0=ρ⎕←'POLYNOMIAL HAS COMPLEX ROOTS'
[15] E3:'ARGUMENT MUST HAVE FOUR ROWS'
    ∇
```

A5 Experimental Data

This appendix gives the output of function VSS. It is a compilation of the experimental data on twelve crystals and the fits to these crystals fron the theory of Niklasson.

The headings give the temperature, normalized velocity, attenuation, and N(T) factor respectively for the theoretical fit. The next page gives the experimental data for the same crystal. The headings give the temperature, absolute velocity, normalized velocity, and N(T) factor respectively for the experimental data.

CRYSTAL 03 ;125.0 BAR ;14/07/70

ISOTHERMAL VELOCITY = A+B×T*N
A=772.9 +/- 18.32 M/S   B= 0.1567   N=3.561
DEBYE Θ=42.76   MOLAR VOLUME=17.41 CC/M
SECOND SOUND=206.1 M/S   FREQUENCY=5E6 HZ
STANDARD DEVIATION FOR FIT IS 0.1231
RELAXATION FACTORS 1×TN,1×TU,1×TAU1
ORIENT. IS BTWN. 35 AND 50 OR 70 AND 90

THEORETICAL CALCULATIONS(NIKLASSON)

TEMP	V[T]+V[0]	ATTEN	NIKFAC
0.3	1.00000	0.168	-0.855
0.4	0.99999	0.237	-0.833
0.5	0.99998	0.303	-0.767
0.6	0.99996	0.369	-0.612
0.7	0.99994	0.436	-0.340
0.8	0.99991	0.503	0.010
0.9	0.99988	0.570	0.350
1.0	0.99984	0.631	0.615
1.1	0.99980	0.682	0.796
1.2	0.99974	0.717	0.908
1.3	0.99967	0.731	0.971
1.4	0.99957	0.719	1.002
1.5	0.99946	0.682	1.012
1.6	0.99932	0.622	1.010
1.7	0.99915	0.549	1.003
1.8	0.99896	0.470	0.999
1.9	0.99873	0.394	0.998
2.0	0.99848	0.327	0.998
2.1	0.99819	0.269	0.999
2.2	0.99787	0.222	1.000
2.3	0.99750	0.184	1.000
2.4	0.99709	0.153	1.000
2.5	0.99663	0.128	1.000
2.6	0.99612	0.108	1.000
2.7	0.99556	0.092	1.000
2.8	0.99495	0.079	1.000
2.9	0.99427	0.069	1.000
3.0	0.99353	0.060	1.000
3.1	0.99272	0.053	1.000
3.2	0.99185	0.047	1.000
3.3	0.99089	0.042	1.000
3.4	0.98986	0.038	1.000
3.5	0.98874	0.034	1.000
3.6	0.98754	0.031	1.000
3.7	0.98625	0.028	1.000
3.8	0.98485	0.026	1.000

EXPERIMENTAL DATA FOR CRYSTAL 03

TEMP	V[T]	V[T]÷V[0]	NIVFAC
3.755	761.72	0.98555	1.007
3.750	761.95	0.98585	1.036
3.709	762.18	0.98615	1.003
3.620	762.88	0.98706	0.967
3.544	763.57	0.98795	0.958
3.470	764.45	0.98908	0.998
3.394	765.20	0.99005	1.023
3.332	765.61	0.99059	1.002
3.210	766.60	0.99187	1.024
3.102	767.07	0.99248	0.945
2.992	767.89	0.99353	0.983
2.911	768.48	0.99430	1.032
2.740	769.12	0.99513	0.925
2.664	769.65	0.99581	1.017
2.531	770.36	0.99673	1.126
2.384	770.59	0.99703	0.924
2.218	771.30	0.99795	1.119
2.085	771.48	0.99819	0.950

CRYSTAL A8 ;120.8 BAR ;30/08/71

ISOTHERMAL VELOCITY = A+B×T⋆N
A=756.8 +/- 32.84 M/S   B=¯0.1119   N=3.585
DEBYE Θ=42.25   MOLAR VOLUME=17.49 CC/M
SECOND SOUND=203.4 M/S   FREQUENCY=5E6 HZ
STANDARD DEVIATION FOR FIT IS 0.08358
RELAXATION FACTORS 1.5×TN,3.7×TU,6×TAU1
ORIENTATION IS BETWEEN 40 AND 90

THEORETICAL CALCULATIONS(NIKLASSON)

TEMP	V[T]÷V[0]	ATTEN	NIKFAC
0.3	0.99999	0.250	¯9.443
0.4	0.99997	0.360	¯9.387
0.5	0.99993	0.466	¯9.207
0.6	0.99987	0.575	¯8.762
0.7	0.99978	0.693	¯7.884
0.8	0.99970	0.825	¯6.511
0.9	0.99964	0.967	¯4.818
1.0	0.99960	1.110	¯3.149
1.1	0.99959	1.242	¯1.772
1.2	0.99960	1.352	¯0.769
1.3	0.99960	1.432	¯0.097
1.4	0.99959	1.477	0.324
1.5	0.99956	1.480	0.567
1.6	0.99950	1.440	0.692
1.7	0.99940	1.356	0.744
1.8	0.99928	1.236	0.763
1.9	0.99914	1.088	0.784
2.0	0.99901	0.930	0.830
2.1	0.99889	0.785	0.890
2.2	0.99875	0.662	0.938
2.3	0.99858	0.561	0.967
2.4	0.99838	0.478	0.983
2.5	0.99814	0.409	0.991
2.6	0.99787	0.352	0.995
2.7	0.99756	0.304	0.998
2.8	0.99722	0.265	0.999
2.9	0.99685	0.232	0.999
3.0	0.99644	0.204	1.000
3.1	0.99599	0.181	1.000
3.2	0.99550	0.161	1.000
3.3	0.99497	0.145	1.000
3.4	0.99439	0.131	1.000
3.5	0.99376	0.118	1.000
3.6	0.99308	0.108	1.000

EXPERIMENTAL DATA FOR CRYSTAL A8

TEMP	*V[T]*	*V[T]÷V[0]*	*NIKFAC*
3.530	751.97	0.99363	1.009
3.464	752.25	0.99399	1.001
3.386	752.68	0.99456	1.015
3.233	752.92	0.99488	0.914
3.243	753.26	0.99533	1.010
3.183	753.48	0.99562	1.006
3.099	753.76	0.99600	1.001
2.982	754.19	0.99656	1.012
2.896	754.45	0.99691	1.011
2.804	754.73	0.99728	1.020
2.708	754.98	0.99760	1.023
2.561	755.31	0.99804	1.021
2.318	755.73	0.99859	0.997
2.210	755.83	0.99872	0.931
2.096	755.96	0.99890	0.887
1.774	756.22	0.99924	0.635
1.609	756.35	0.99941	0.513
1.419	756.46	0.99955	0.262
1.262	756.53	0.99965	¯0.067
0.841	756.64	0.99979	¯3.023
0.784	756.69	0.99986	¯2.427

CRYSTAL C2 ;119.5 BAR ;01/11/71

ISOTHERMAL VELOCITY = A+B×T*N
A=738 +/- 43.18 M/S   B= ¯0.1185   N=3.592
DEBYE θ=42.09   MOLAR VOLUME=17.52 CC/M
SECOND SOUND=202.5 M/S   FREQUENCY=5E6 HZ
STANDARD DEVIATION FOR FIT IS 0.04629
RELAXATION FACTORS 1.5×TN,5.4×TU,51×TAU1
ORIENTATION IS BETWEEN 45 AND 90

THEORETICAL CALCULATIONS(BHATIA)

TEMP	V[T]+V[0]	ATTEN	NIKFAC
0.3	0.99991	0.266	¯86.714
0.4	0.99973	0.388	¯86.230
0.5	0.99942	0.526	¯84.692
0.6	0.99893	0.713	¯80.893
0.7	0.99831	0.997	¯73.423
0.8	0.99768	1.409	¯61.809
0.9	0.99725	1.926	¯47.627
1.0	0.99710	2.473	¯33.785
1.1	0.99721	2.970	¯22.479
1.2	0.99746	3.372	¯14.300
1.3	0.99776	3.660	¯8.818
1.4	0.99802	3.829	¯5.333
1.5	0.99819	3.873	¯3.237
1.6	0.99822	3.791	¯2.079
1.7	0.99809	3.581	¯1.531
1.8	0.99779	3.242	¯1.324
1.9	0.99741	2.772	¯1.207
2.0	0.99714	2.201	¯0.949
2.1	0.99714	1.634	¯0.473
2.2	0.99735	1.192	0.058
2.3	0.99755	0.903	0.463
2.4	0.99760	0.722	0.711
2.5	0.99751	0.600	0.846
2.6	0.99731	0.511	0.917
2.7	0.99703	0.441	0.955
2.8	0.99667	0.384	0.975
2.9	0.99626	0.338	0.985
3.0	0.99580	0.299	0.991
3.1	0.99528	0.266	0.995
3.2	0.99472	0.238	0.997
3.3	0.99410	0.214	0.998
3.4	0.99342	0.193	0.999
3.5	0.99269	0.176	0.999
3.6	0.99190	0.161	0.999

EXPERIMENTAL DATA FOR CRYSTAL C2

TEMP	V[T]	V[T]÷V[0]	NIKFAC
3.577	732.24	0.99215	1.008
3.553	732.33	0.99227	0.998
3.505	732.61	0.99265	0.999
3.456	732.87	0.99300	0.936
3.393	733.23	0.99349	1.002
3.309	733.60	0.99399	0.990
3.244	733.90	0.99440	0.988
3.149	734.28	0.99491	0.975
3.059	734.71	0.99549	0.992
2.981	734.99	0.99587	0.987
2.888	735.33	0.99633	0.990
2.794	735.71	0.99685	1.022
2.688	735.95	0.99717	0.991
2.552	736.12	0.99741	0.882
2.363	736.23	0.99755	0.610
1.836	736.26	0.99759	¯1.369

CRYSTAL D3 ;119.2 BAR ;19/11/71

ISOTHERMAL VELOCITY = A+B×T*N
A=758.2 +/- 22.75 M/S   B= ¯0.1025   N=3.594
DEBYE Θ=42.06   MOLAR VOLUME=17.52 CC/M
SECOND SOUND=202.3 M/S   FREQUENCY=5E6 HZ
STANDARD DEVIATION FOR FIT IS 0.153
RELAXATION FACTORS 1.5×TN,6.8×TU,45×TAU1
ORIENT. IS BTWN. 40 AND 55 OR 65 AND 90

THEORETICAL CALCULATIONS(NIKLASSON)

TEMP	V[T]÷V[0]	ATTEN	NIKFAC
0.3	0.99992	0.260	¯76.410
0.4	0.99977	0.380	¯75.980
0.5	0.99949	0.512	¯74.614
0.6	0.99906	0.686	¯71.241
0.7	0.99850	0.943	¯64.617
0.8	0.99796	1.311	¯54.334
0.9	0.99758	1.770	¯41.810
1.0	0.99746	2.254	¯29.627
1.1	0.99755	2.697	¯19.708
1.2	0.99778	3.062	¯12.548
1.3	0.99804	3.335	¯7.743
1.4	0.99828	3.514	¯4.669
1.5	0.99845	3.595	¯2.787
1.6	0.99852	3.573	¯1.712
1.7	0.99845	3.446	¯1.171
1.8	0.99824	3.208	¯0.957
1.9	0.99792	2.856	¯0.884
2.0	0.99762	2.395	¯0.766
2.1	0.99751	1.878	¯0.470
2.2	0.99764	1.414	¯0.041
2.3	0.99788	1.077	0.359
2.4	0.99806	0.857	0.637
2.5	0.99810	0.711	0.801
2.6	0.99804	0.605	0.891
2.7	0.99789	0.524	0.940
2.8	0.99768	0.459	0.966
2.9	0.99742	0.404	0.980
3.0	0.99712	0.359	0.988
3.1	0.99677	0.320	0.993
3.2	0.99639	0.287	0.996
3.3	0.99597	0.259	0.997
3.4	0.99551	0.235	0.998
3.5	0.99501	0.214	0.999
3.6	0.99446	0.196	0.999
3.7	0.99388	0.180	0.999

EXPERIMENTAL DATA FOR CRYSTAL D3

TEMP	V[T]	V[T]÷V[0]	NIKFAC
3.619	753.94	0.99440	1.004
3.568	754.09	0.99459	0.993
3.484	754.27	0.99483	0.962
3.414	754.67	0.99536	0.986
3.361	754.96	0.99574	1.006
3.257	755.29	0.99618	1.002
3.151	755.57	0.99655	0.989
3.060	755.85	0.99691	0.990
2.951	756.20	0.99737	1.011
2.846	756.55	0.99783	1.051
2.840	756.63	0.99794	1.077
2.692	756.63	0.99794	0.948
2.549	756.63	0.99794	0.790
2.308	756.63	0.99794	0.410
1.668	756.63	0.99794	¯2.373
1.185	756.63	0.99794	¯12.103

CRYSTAL D4 ;119.6 BAR ;26/11/71

ISOTHERMAL VELOCITY = A+B×T*N
A=754.1 +/- 4.223 M/S B=¯0.1161 N=3.591
DEBYE Θ=42.1 MOLAR VOLUME=17.52 CC/M
SECOND SOUND=202.6 M/S FREQUENCY=5E6 HZ
STANDARD DEVIATION FOR FIT IS 0.04922
RELAXATION FACTORS 1.5×TN,2×TU,30×TAU1
ORIENTATION IS BETWEEN 40 AND 90

THEORETICAL CALCULATIONS(NIKLASSON)

TEMP	V[T]÷V[0]	ATTEN	NIKFAC
0.3	0.99994	0.261	¯50.654
0.4	0.99984	0.379	¯50.369
0.5	0.99966	0.502	¯49.462
0.6	0.99937	0.653	¯47.224
0.7	0.99900	0.859	¯42.820
0.8	0.99863	1.137	¯35.956
0.9	0.99837	1.474	¯27.521
1.0	0.99830	1.821	¯19.199
1.1	0.99838	2.120	¯12.326
1.2	0.99856	2.329	¯7.350
1.3	0.99876	2.426	¯4.098
1.4	0.99890	2.401	¯2.178
1.5	0.99893	2.261	¯1.183
1.6	0.99884	2.022	¯0.746
1.7	0.99867	1.701	¯0.543
1.8	0.99853	1.329	¯0.303
1.9	0.99852	0.973	0.084
2.0	0.99861	0.709	0.476
2.1	0.99864	0.539	0.737
2.2	0.99858	0.429	0.874
2.3	0.99844	0.350	0.940
2.4	0.99824	0.290	0.971
2.5	0.99799	0.244	0.985
2.6	0.99770	0.207	0.992
2.7	0.99737	0.177	0.996
2.8	0.99701	0.152	0.998
2.9	0.99661	0.132	0.999
3.0	0.99617	0.116	0.999
3.1	0.99568	0.102	1.000
3.2	0.99515	0.091	1.000
3.3	0.99458	0.081	1.000
3.4	0.99396	0.073	1.000
3.5	0.99328	0.066	1.000
3.6	0.99255	0.060	1.000
3.7	0.99176	0.055	1.000

EXPERIMENTAL DATA FOR CRYSTAL D4

TEMP	V[T]	V[T]÷V[0]	NIKFAC
3.651	748.10	0.99205	0.987
3.623	748.33	0.99236	0.998
3.567	748.61	0.99272	0.990
3.495	749.03	0.99329	0.996
3.419	749.45	0.99384	1.001
3.358	749.79	0.99429	1.011
3.262	750.26	0.99492	1.022
3.212	750.44	0.99515	1.012
3.070	750.93	0.99581	0.995
2.988	751.29	0.99628	1.013
2.831	751.74	0.99688	0.997
2.721	752.07	0.99731	1.001
2.580	752.43	0.99780	1.006
2.406	752.72	0.99818	0.951
2.164	753.12	0.99871	0.910
1.571	753.16	0.99876	¯1.122
1.366	753.18	0.99879	¯2.987
0.763	753.21	0.99883	¯36.490

CRYSTAL D5 ;119.6 BAR ;30/11/71

ISOTHERMAL VELOCITY = A+B×T*N
A=757.9 +/- 13.49 M/S B=¯0.1147 N=3.591
DEBYE θ=42.1 MOLAR VOLUME=17.52 CC/M
SECOND SOUND=202.6 M/S FREQUENCY=5E6 HZ
STANDARD DEVIATION FOR FIT IS 0.0421
RELAXATION FACTORS 1.5×TN,1.5×TU,33×TAU1
ORIENT. IS BTWN. 40 AND 55 OR 65 AND 90

THEORETICAL CALCULATIONS(NIKLASSON)

TEMP	V[T]÷V[0]	ATTEN	NIKFAC
0.3	0.99994	0.260	¯55.806
0.4	0.99983	0.378	¯55.492
0.5	0.99962	0.502	¯54.495
0.6	0.99931	0.657	¯52.033
0.7	0.99890	0.872	¯47.190
0.8	0.99850	1.166	¯39.630
0.9	0.99822	1.524	¯30.307
1.0	0.99815	1.890	¯21.062
1.1	0.99826	2.195	¯13.392
1.2	0.99849	2.389	¯7.853
1.3	0.99872	2.444	¯4.300
1.4	0.99887	2.357	¯2.292
1.5	0.99889	2.146	¯1.322
1.6	0.99878	1.838	¯0.915
1.7	0.99863	1.460	¯0.653
1.8	0.99858	1.066	¯0.257
1.9	0.99867	0.747	0.237
2.0	0.99877	0.541	0.614
2.1	0.99877	0.415	0.820
2.2	0.99868	0.330	0.917
2.3	0.99853	0.269	0.961
2.4	0.99832	0.223	0.981
2.5	0.99807	0.186	0.991
2.6	0.99779	0.157	0.995
2.7	0.99747	0.134	0.997
2.8	0.99712	0.115	0.999
2.9	0.99673	0.100	0.999
3.0	0.99631	0.087	1.000
3.1	0.99584	0.077	1.000
3.2	0.99533	0.068	1.000
3.3	0.99478	0.061	1.000
3.4	0.99418	0.055	1.000
3.5	0.99353	0.050	1.000
3.6	0.99282	0.045	1.000
3.7	0.99206	0.041	1.000

EXPERIMENTAL DATA FOR CRYSTAL D5

TEMP	V[T]	V[T]÷V[0]	NIKFAC
3.638	752.20	0.99253	0.999
3.600	752.39	0.99279	0.995
3.553	752.66	0.99314	0.998
3.487	753.00	0.99358	0.996
3.423	753.33	0.99402	0.998
3.350	753.68	0.99449	1.001
3.278	754.04	0.99497	1.011
3.194	754.38	0.99540	1.007
3.106	754.71	0.99584	1.006
3.010	755.04	0.99628	1.004
2.895	755.39	0.99675	0.997
2.749	755.81	0.99729	0.994
2.607	756.18	0.99778	1.001
2.459	756.46	0.99816	0.978
2.403	756.57	0.99830	0.976
2.230	756.86	0.99868	0.956
2.109	756.89	0.99871	0.785
1.817	756.91	0.99874	0.048
1.370	756.90	0.99873	¯3.215
0.662	756.90	0.99873	¯67.525

CRYSTAL E2 ;117.8 BAR ;27/12/71

ISOTHERMAL VELOCITY = A+B×T*N
A=742.1 +/- 13.28 M/S B=¯0.1162 N=3.602
DEBYE Θ=41.88 MOLAR VOLUME=17.55 CC/M
SECOND SOUND=201.4 M/S FREQUENCY=5E6 HZ
STANDARD DEVIATION FOR FIT IS 0.04584
RELAXATION FACTORS 1.5×TN,1.5×TU,27×TAU1
ORIENTATION IS BETWEEN 40 AND 90

THEORETICAL CALCULATIONS(NIKLASSON)

TEMP	V[T]÷V[0]	ATTEN	NIKFAC
0.3	0.99995	0.270	¯45.499
0.4	0.99986	0.391	¯45.234
0.5	0.99968	0.517	¯44.394
0.6	0.99942	0.668	¯42.322
0.7	0.99908	0.871	¯38.259
0.8	0.99874	1.142	¯31.959
0.9	0.99851	1.466	¯24.255
1.0	0.99846	1.792	¯16.684
1.1	0.99855	2.061	¯10.460
1.2	0.99874	2.228	¯6.003
1.3	0.99892	2.269	¯3.174
1.4	0.99903	2.181	¯1.596
1.5	0.99902	1.982	¯0.848
1.6	0.99891	1.695	¯0.536
1.7	0.99876	1.348	¯0.319
1.8	0.99871	0.994	0.019
1.9	0.99877	0.711	0.420
2.0	0.99882	0.528	0.711
2.1	0.99877	0.410	0.867
2.2	0.99865	0.329	0.939
2.3	0.99847	0.269	0.971
2.4	0.99825	0.223	0.986
2.5	0.99798	0.186	0.993
2.6	0.99768	0.157	0.996
2.7	0.99735	0.134	0.998
2.8	0.99697	0.115	0.999
2.9	0.99656	0.100	0.999
3.0	0.99611	0.088	1.000
3.1	0.99562	0.077	1.000
3.2	0.99508	0.069	1.000
3.3	0.99450	0.061	1.000
3.4	0.99386	0.055	1.000
3.5	0.99317	0.050	1.000
3.6	0.99243	0.046	1.000
3.7	0.99162	0.042	1.000
3.8	0.99076	0.038	1.000

EXPERIMENTAL DATA FOR CRYSTAL E2

TEMP	V[T]	V[T]÷V[0]	NIKFAC
3.726	735.72	0.99135	0.995
3.692	735.93	0.99163	0.993
3.653	736.18	0.99197	0.995
3.594	736.54	0.99246	0.999
3.492	737.11	0.99323	1.000
3.433	737.44	0.99368	1.005
3.329	737.96	0.99438	1.009
3.254	738.30	0.99482	1.009
3.174	738.63	0.99527	1.009
3.066	739.07	0.99587	1.016
2.971	739.38	0.99629	1.009
2.838	739.79	0.99684	1.005
2.696	740.17	0.99734	0.992
2.585	740.43	0.99770	0.985
2.444	740.70	0.99807	0.959
2.277	740.99	0.99845	0.925
1.975	741.22	0.99877	0.609
1.773	741.29	0.99886	0.141
1.615	741.33	0.99891	¯0.443
1.368	741.33	0.99891	¯2.340
0.641	741.33	0.99891	¯63.089

CRYSTAL F2 ;119.0 BAR ;01/02/72

ISOTHERMAL VELOCITY = A+B×T*N
A=718.4 +/- 19.11 M/S   B=¯0.1013   N=3.595
DEBYE Θ=42.03   MOLAR VOLUME=17.53 CC/M
SECOND SOUND=202.2 M/S   FREQUENCY=5E6 HZ
STANDARD DEVIATION FOR FIT IS 0.04307
RELAXATION FACTORS 1.5×TN,0.3×TU,17×TAU1
ORIENTATION IS BETWEEN 50 AND 70

THEORETICAL CALCULATIONS(NIKLASSON)

TEMP	V[T]+V[0]	ATTEN	NIKFAC
0.3	0.99997	0.275	¯28.331
0.4	0.99991	0.397	¯28.167
0.5	0.99980	0.520	¯27.646
0.6	0.99964	0.658	¯26.361
0.7	0.99942	0.826	¯23.822
0.8	0.99921	1.034	¯19.783
0.9	0.99909	1.261	¯14.565
1.0	0.99912	1.443	¯9.085
1.1	0.99928	1.498	¯4.567
1.2	0.99944	1.391	¯1.810
1.3	0.99951	1.167	¯0.589
1.4	0.99949	0.896	¯0.135
1.5	0.99946	0.631	0.182
1.6	0.99948	0.422	0.551
1.7	0.99949	0.292	0.812
1.8	0.99946	0.213	0.929
1.9	0.99938	0.160	0.973
2.0	0.99927	0.123	0.990
2.1	0.99913	0.096	0.996
2.2	0.99898	0.076	0.998
2.3	0.99880	0.061	0.999
2.4	0.99861	0.050	1.000
2.5	0.99838	0.041	1.000
2.6	0.99814	0.035	1.000
2.7	0.99786	0.029	1.000
2.8	0.99756	0.025	1.000
2.9	0.99723	0.022	1.000
3.0	0.99687	0.019	1.000
3.1	0.99647	0.016	1.000
3.2	0.99604	0.015	1.000
3.3	0.99557	0.013	1.000
3.4	0.99506	0.012	1.000
3.5	0.99450	0.011	1.000
3.6	0.99390	0.010	1.000
3.7	0.99325	0.009	1.000

EXPERIMENTAL DATA FOR CRYSTAL F2

TEMP	V[T]	V[T]÷V[0]	NIKFAC
3.637	713.83	0.99363	0.996
3.621	713.93	0.99377	1.000
3.561	714.13	0.99405	0.988
3.558	714.33	0.99433	1.022
3.429	714.72	0.99487	0.996
3.336	715.09	0.99539	1.000
3.225	715.45	0.99589	0.994
3.166	715.72	0.99627	1.015
3.022	716.06	0.99674	0.989
2.945	716.27	0.99703	0.989
2.687	716.88	0.99788	0.994
2.539	717.17	0.99829	0.999
2.273	717.53	0.99879	0.958
2.054	717.84	0.99922	1.014
1.868	718.04	0.99949	1.066
1.418	718.04	0.99949	¯0.063
0.640	718.04	0.99949	¯29.706

CRYSTAL F3 ;119.2 BAR ;13/02/72

ISOTHERMAL VELOCITY = A+B×T*N
A=732.4 +/- 11.72 M/S B=¯0.1046 N=3.594
DEBYE θ=42.06 MOLAR VOLUME=17.52 CC/M
SECOND SOUND=202.3 M/S FREQUENCY=5E6 HZ
STANDARD DEVIATION FOR FIT IS 0.05129
RELAXATION FACTORS 1.5×TN,0.7×TU,23×TAU1
ORIENTATION IS BETWEEN 45 AND 85

THEORETICAL CALCULATIONS(NIKLASSON)

TEMP	V[T]+V[0]	ATTEN	NIKFAC
0.3	0.99996	0.269	¯38.633
0.4	0.99988	0.390	¯38.413
0.5	0.99973	0.514	¯37.713
0.6	0.99951	0.658	¯35.983
0.7	0.99923	0.846	¯32.578
0.8	0.99894	1.090	¯27.238
0.9	0.99876	1.374	¯20.567
1.0	0.99873	1.646	¯13.820
1.1	0.99886	1.837	¯8.169
1.2	0.99906	1.891	¯4.219
1.3	0.99923	1.796	¯1.945
1.4	0.99928	1.582	¯0.884
1.5	0.99923	1.295	¯0.455
1.6	0.99915	0.976	¯0.165
1.7	0.99916	0.683	0.229
1.8	0.99923	0.476	0.606
1.9	0.99924	0.349	0.828
2.0	0.99918	0.268	0.928
2.1	0.99907	0.210	0.970
2.2	0.99893	0.168	0.987
2.3	0.99876	0.136	0.994
2.4	0.99855	0.112	0.997
2.5	0.99833	0.093	0.999
2.6	0.99807	0.078	0.999
2.7	0.99779	0.066	1.000
2.8	0.99748	0.057	1.000
2.9	0.99714	0.049	1.000
3.0	0.99677	0.043	1.000
3.1	0.99636	0.038	1.000
3.2	0.99591	0.033	1.000
3.3	0.99542	0.030	1.000
3.4	0.99489	0.027	1.000
3.5	0.99432	0.024	1.000
3.6	0.99370	0.022	1.000

EXPERIMENTAL DATA FOR CRYSTAL F3

TEMP	*V[T]*	*V[T]÷V[0]*	*DIVFAC*
3.594	727.85	0.99378	1.005
3.538	728.10	0.99413	1.005
3.431	728.55	0.99473	1.001
3.231	729.28	0.99573	0.994
3.114	729.69	0.99629	0.999
3.002	730.05	0.99678	1.004
2.940	730.20	0.99699	0.939
2.781	730.48	0.99736	0.943
2.693	730.85	0.99787	1.020
2.470	731.15	0.99829	0.945
2.308	731.43	0.99866	0.946
2.173	731.78	0.99914	1.113
1.948	731.87	0.99926	0.934
1.807	731.87	0.99926	0.678
1.360	731.87	0.99926	¯1.245
1.349	731.87	0.99926	¯1.333
1.313	731.87	0.99926	¯1.650
0.716	731.87	0.99926	¯28.324
0.655	731.87	0.99926	¯39.770

CRYSTAL G1 ; 86.2 BAR ;15/04/72

ISOTHERMAL VELOCITY = A+B×T*N
A=754 +/- 13.04 M/S B=¯0.1625 N=3.807
DEBYE Θ=37.48 MOLAR VOLUME=18.34 CC/M
SECOND SOUND=178.9 M/S FREQUENCY=5E6 HZ
STANDARD DEVIATION FOR FIT IS 0.0142
RELAXATION FACTORS 1.5×TN,1×TU,4×TAU1
ORIENTATION IS BETWEEN 10 AND 30

THEORETICAL CALCULATIONS(NIKLASSON)

TEMP	V[T]÷V[0]	ATTEN	NIKFAC
0.3	0.99999	0.384	¯6.001
0.4	0.99997	0.540	¯5.932
0.5	0.99992	0.692	¯5.713
0.6	0.99986	0.850	¯5.192
0.7	0.99978	1.019	¯4.254
0.8	0.99971	1.196	¯2.981
0.9	0.99969	1.358	¯1.653
1.0	0.99970	1.470	¯0.554
1.1	0.99973	1.497	0.184
1.2	0.99975	1.424	0.583
1.3	0.99972	1.266	0.750
1.4	0.99967	1.057	0.810
1.5	0.99960	0.835	0.855
1.6	0.99954	0.638	0.916
1.7	0.99947	0.486	0.963
1.8	0.99938	0.374	0.985
1.9	0.99925	0.291	0.994
2.0	0.99909	0.229	0.998
2.1	0.99891	0.183	0.999
2.2	0.99870	0.148	1.000
2.3	0.99845	0.121	1.000
2.4	0.99817	0.100	1.000
2.5	0.99786	0.084	1.000
2.6	0.99751	0.072	1.000
2.7	0.99711	0.062	1.000
2.8	0.99667	0.053	1.000
2.9	0.99617	0.047	1.000
3.0	0.99562	0.041	1.000
3.1	0.99501	0.037	1.000

EXPERIMENTAL DATA FOR CRYSTAL G1

TEMP	V[T]	V[T]÷V[0]	NIKFAC
3.047	750.45	0.99531	0.996
3.012	750.63	0.99554	0.998
2.974	750.80	0.99577	0.999
2.914	751.07	0.99613	1.003
2.840	751.35	0.99649	1.001
2.753	751.66	0.99690	1.002
2.649	751.99	0.99734	1.004
2.543	752.29	0.99774	1.005
2.420	752.57	0.99812	1.001
2.242	752.93	0.99860	0.999
2.092	753.18	0.99893	1.000
1.910	753.41	0.99922	0.989
1.776	753.53	0.99939	0.971
1.677	753.62	0.99950	0.967
1.523	753.68	0.99959	0.874
1.339	753.74	0.99967	0.706
1.190	753.81	0.99975	0.580
0.657	753.81	0.99975	¯6.649

CRYSTAL H2 ; 86.6 BAR ;04/05/72

ISOTHERMAL VELOCITY = A+B×T*N
A=674.7 +/- 6.207 M/S B=¯0.1557 N=3.804
DEBYE Θ=37.54 MOLAR VOLUME=18.32 CC/M
SECOND SOUND=179.2 M/S FREQUENCY=5E6 HZ
STANDARD DEVIATION FOR FIT IS 0.06896
RELAXATION FACTORS 1.5×TN,1×TU,1×TAU1
ORIENTATION IS BETWEEN 40 AND 90

THEORETICAL CALCULATIONS(NIKLASSON)

TEMP	V[T]÷V[0]	ATTEN	NIKFAC
0.3	1.00000	0.427	¯0.855
0.4	0.99999	0.599	¯0.836
0.5	0.99998	0.764	¯0.777
0.6	0.99995	0.928	¯0.636
0.7	0.99993	1.093	¯0.381
0.8	0.99990	1.253	¯0.035
0.9	0.99988	1.393	0.328
1.0	0.99986	1.485	0.628
1.1	0.99985	1.503	0.829
1.2	0.99982	1.432	0.938
1.3	0.99977	1.282	0.982
1.4	0.99971	1.086	0.993
1.5	0.99962	0.880	0.993
1.6	0.99951	0.693	0.994
1.7	0.99939	0.539	0.997
1.8	0.99924	0.418	0.999
1.9	0.99907	0.326	0.999
2.0	0.99887	0.257	1.000
2.1	0.99863	0.205	1.000
2.2	0.99837	0.166	1.000
2.3	0.99806	0.136	1.000
2.4	0.99771	0.113	1.000
2.5	0.99732	0.095	1.000
2.6	0.99688	0.081	1.000
2.7	0.99639	0.069	1.000
2.8	0.99584	0.060	1.000
2.9	0.99523	0.053	1.000
3.0	0.99455	0.047	1.000

EXPERIMENTAL DATA FOR CRYSTAL H2

TEMP	V[T]	V[T]+V[0]	NIKFAC
2.969	671.16	0.99482	1.006
2.965	671.19	0.99487	1.008
2.940	671.28	0.99500	1.004
2.894	671.46	0.99526	0.999
2.847	671.65	0.99554	0.998
2.808	671.82	0.99581	1.001
2.771	671.96	0.99601	1.001
2.749	672.05	0.99614	1.002
2.686	672.26	0.99645	0.998
2.562	672.65	0.99703	0.994
2.551	672.68	0.99707	0.993
2.526	672.73	0.99714	0.986
2.486	672.86	0.99733	0.990
2.395	673.04	0.99761	0.971
2.315	673.27	0.99795	0.983
2.252	673.39	0.99813	0.975
2.214	673.48	0.99826	0.979
2.181	673.54	0.99835	0.976
2.116	673.66	0.99853	0.974
2.064	673.74	0.99864	0.967
1.986	673.87	0.99883	0.970
1.941	673.92	0.99891	0.956
1.909	673.96	0.99897	0.951
1.864	674.02	0.99905	0.950
1.995	674.10	0.99917	1.143
1.961	674.12	0.99920	1.130
1.930	674.15	0.99925	1.128
1.850	674.21	0.99935	1.122
1.586	674.24	0.99939	0.837
1.704	674.29	0.99947	1.071
1.515	674.42	0.99966	1.068
1.411	674.45	0.99970	1.001
1.225	674.50	0.99978	0.846
1.175	674.50	0.99978	0.725
0.647	674.50	0.99978	-6.292

CRYSTAL I2 ; 86.4 BAR ;31/05/72

ISOTHERMAL VELOCITY = A+B×T*N
A=667.4 +/- 26.56 M/S   B=¯0.1612   N=3.806
DEBYE Θ=37.51   MOLAR VOLUME=18.33 CC/M
SECOND SOUND=179.1 M/S   FREQUENCY=5E6 HZ
STANDARD DEVIATION FOR FIT IS 0.05547
RELAXATION FACTORS 1.5×TN,0.2×TU,8×TAU1
ORIENTATION IS BETWEEN 45 AND 90

THEORETICAL CALCULATIONS(NIKLASSON)

TEMP	V[T]÷V[0]	ATTEN	NIKFAC
0.3	0.99998	0.433	¯12.862
0.4	0.99993	0.610	¯12.727
0.5	0.99985	0.787	¯12.296
0.6	0.99972	0.979	¯11.269
0.7	0.99957	1.192	¯9.362
0.8	0.99947	1.399	¯6.553
0.9	0.99950	1.510	¯3.361
1.0	0.99962	1.421	¯0.946
1.1	0.99968	1.158	0.135
1.2	0.99966	0.844	0.468
1.3	0.99962	0.565	0.666
1.4	0.99960	0.369	0.859
1.5	0.99954	0.251	0.955
1.6	0.99944	0.177	0.986
1.7	0.99931	0.128	0.996
1.8	0.99914	0.095	0.998
1.9	0.99895	0.072	0.999
2.0	0.99872	0.055	1.000
2.1	0.99846	0.043	1.000
2.2	0.99816	0.035	1.000
2.3	0.99782	0.028	1.000
2.4	0.99743	0.023	1.000
2.5	0.99699	0.019	1.000
2.6	0.99649	0.016	1.000
2.7	0.99594	0.014	1.000
2.8	0.99532	0.012	1.000
2.9	0.99463	0.011	1.000
3.0	0.99387	0.009	1.000

EXPERIMENTAL DATA FOR CRYSTAL I2

TEMP	V[T]	V[T]÷V[0]	NIKFAC
2.966	663.50	0.99421	1.008
2.955	663.55	0.99429	1.008
2.930	663.64	0.99442	1.002
2.897	663.80	0.99466	1.001
2.867	663.94	0.99487	1.001
2.811	664.18	0.99523	0.998
2.766	664.39	0.99554	1.000
2.724	664.56	0.99580	1.001
2.699	664.70	0.99601	1.010
2.664	664.78	0.99613	0.998
2.635	664.89	0.99629	0.998
2.604	664.99	0.99644	0.995
2.580	665.08	0.99658	0.998
2.552	665.17	0.99670	0.994
2.522	665.26	0.99684	0.992
2.480	665.39	0.99703	0.991
2.434	665.52	0.99723	0.988
2.366	665.70	0.99751	0.985
2.279	665.91	0.99782	0.981
2.237	666.00	0.99796	0.976
2.189	666.11	0.99812	0.975
2.147	666.20	0.99826	0.975
2.103	666.28	0.99837	0.967
2.061	666.33	0.99845	0.951
1.983	666.46	0.99864	0.937
1.934	666.54	0.99876	0.937
1.879	666.61	0.99886	0.921
1.988	666.70	0.99901	1.125
1.935	666.76	0.99909	1.116
1.896	666.79	0.99913	1.100
1.867	666.81	0.99917	1.095
1.756	666.90	0.99930	1.056
1.665	666.97	0.99940	1.032
1.596	666.99	0.99944	0.977
1.525	667.03	0.99950	0.941
1.449	667.06	0.99954	0.866
1.373	667.09	0.99959	0.780
1.264	667.12	0.99963	0.588
1.201	667.13	0.99965	0.437
1.088	667.16	0.99969	0.103
1.008	667.16	0.99969	¯0.397
0.926	667.16	0.99969	¯1.162
0.648	667.16	0.99969	¯9.160